

ANALYZING EFFECTIVE CONNECTIVITY OF BRAIN USING FMRI DATA: DCM AND PPI

A THESIS SUBMITTED TO  
THE GRADUATE SCHOOL OF NATURAL AND APPLIED SCIENCES  
OF  
MIDDLE EAST TECHNICAL UNIVERSITY

BY

SINA MOJTAHEDI

IN PARTIAL FULFILLMENT OF THE REQUIREMENTS  
FOR  
THE DEGREE OF MASTER OF SCIENCE  
IN  
BIOMEDICAL ENGINEERING

JANUARY 2013



Approval of the thesis:

**ANALYZING EFFECTIVE CONNECTIVITY OF BRAIN USING FMRI DATA: DCM AND  
PPI**

Submitted by **SINA MOJTAHEDI** in partial fulfillment of the requirements for the degree of **Master of Science in Biomedical Engineering Department, Middle East Technical University** by,

Prof. Dr. Canan Özgen -----  
Dean, Graduate School of **Natural and Applied Sciences**

Prof. Dr. Semra Kocabıyık -----  
Head of Department, **Biomedical Engineering**

Prof. Dr. Uğur Halıcı -----  
Supervisor, **Electrical and Electronics Engineering Dept., METU**

Prof. Dr. Metehan Çiçek -----  
Co-Supervisor, **Physiology Dept., Ankara University**

**Examining Committee Members:**

Prof. Dr. Nevzat Güneri Gençer -----  
Electrical and Electronics Engineering Dept., METU

Prof. Dr. Uğur Halıcı -----  
Electrical and Electronics Engineering Dept., METU

Asst. Prof. Dr. Ilkay Ulusoy -----  
Electrical and Electronics Engineering Dept., METU

Prof. Dr. Gerhard Wilhelm Weber -----  
Institute of Applied Mathematics Dept., METU

Prof. Dr. Metehan Çiçek -----  
Physiology Dept., Faculty of Medicine, Ankara University

Date: \_\_\_\_\_

**I hereby declare that all information in this document has been obtained and presented in accordance with academic rules and ethical conduct. I also declare that, as required by these rules and conduct, I have fully cited and referenced all material and results that are not original to this work.**

Name, Last name: Sina Mojtahedi

Signature:

## ABSTRACT

### ANALYZING EFFECTIVE CONNECTIVITY OF BRAIN USING FMRI DATA: DCM AND PPI

Mojtahedi, Sina

M.Sc., Department of Biomedical Engineering

Supervisor: Prof. Dr. Ugur HALICI

Co-Supervisor: Prof. Dr. Metehan CICEK

January 2013 , 110 pages

In neuroscience and biomedical engineering fields, one of the most important issues nowadays is finding a relationship between different brain regions when it is stimulated. Connectivity is an important research area in neuroscience which tries to determine the relationship between different brain region when the brain is stimulated externally or internally. Three main type of connectivity are discussed in this field: Anatomical, Functional and Effective connectivity. Importance of effective connectivity is its ability to detect brain disorders in early stages. Some brain disorders are Schizophrenia, MS and Major Depression disease. Comparing the effective connectivity between a healthy and unhealthy brain will help to diagnose brain disorder. In this master study, two methods named Dynamic Causal Modeling (DCM) and Psychophysiological Interaction (PPI) are used to compare effective connectivity and neuronal activity between different regions of brain when there are three different stimulations. Since the neural activity is latent in fMRI data, there is a need to a model which is able to transfer data from neuronal level to a visible data like Blood-Oxygen level dependent (BOLD) signal. DCM uses a haemodynamic balloon model (HD) to represent this data transfer. The hemodynamic model must be so that the parameters of neural and BOLD signal be the same. It should be noted that what is looked for is not the BOLD signal but the neuronal activity. In this study, as the first step, we did preprocessing of MR images and after ROI's are created using the program MARSBAR. Ten ROIs, which are thought to have connections between them are selected by considering the stimulations used in the experiments in obtaining the data used in this thesis. The data used contains fMRI images of 11 healthy subjects. Stimulations of experiment are applied to images got from group analysis of 11 healthy subjects. These Stimulations are then used in preparing the design matrix and the parameters related to DCM. These parameters are the values related to connection matrices defining bilinear dynamic model on ROI. Bayesian method is used to select best model between all these models.

Another method of PPI is also applied to analyze effective connectivity between 10 ROIs. This method considers two issues of physiological and psychological effects. Like DCM, the preprocessing steps and ROI selection is done for PPI and hemodynamic model is designed for this method. Neural and hemodynamic responses of ROIs are compared using this method.

**Keywords:** Functional MRI, Effective connectivity, Dynamic Causal Modeling, Psychophysiological Interaction, Haemodynamic Model.

## ÖZ

### FMRI VERİLERİ KULLANILARAK BEYİNDEKİ ETKİLİ KONNEKTIVİTE ANALİZİ: DCM VE PPI

Mojtahedi, Sina

Yüksek Lisans, Biyomedikal Mühendisliği Anabilim Dalı

Tez Yöneticisi: Prof. Dr. Uğur Halıcı

Ortak Tez Yöneticisi: Prof. Dr. Metehan Çiçek

Ocak 2013 , 110 sayfa

Son günlerde sinirbilim ve biyomedikal mühendisliği alanında dışarıdan uygulanan bir uyarının etkisi altında beynin farklı bölgeleri arasındaki ilişkinin bulunması önem kazanmıştır. Konnektivite sinirbilim çalışmalarında dış ya da iç uyarımlarla uyarılan beynin değişik bölgeleri arasındaki ilişkisini ortaya konması açısından önemlidir. Bu alanda üç tür konnektivite ön plana çıkmaktadır: Anatomik, işlevsel ve efektif konnektivite. Efektif konnektivitenin önemi ruh ve sinir hastalıklarında erken tanı imkanı sağlayabilmesidir. Bu hastalıkların bazıları şizofreni, multiple sklerosis ve major depresyondur. Hasta ve sağlıklı beyinlerin efektif konnektivitelerinin karşılaştırılması bozukluğun teşhisinde faydalı olacaktır. Bu çalışmada, değişik uyarımların varlığında beynin bölgelerinin efektif konnektivitelerinin karşılaştırılması için Psiko fizyolojik Etkileşim (PPE) ve Dinamik Nedensel Modelleme (DNM) isimli yöntemler kullanılmıştır. İşlevsel Manyetik Rezonans görüntüleme (fMRI) da nöral aktivite gizli olduğu için BOLD sinyali gibi görülebilen bir sinyal elde edebilmek için bir modele ihtiyaç vardır. DNM veriyi dönüştürmek için hemodinamik balon modeli kullanılmaktadır. Hemodinamik model öyle bir seçilmelidir ki nöral sinyalin ve BOLD'un parametreleri aynı olmalıdır. Burada dikkat edilmesi gereken nokta aranılanın BOLD sinyali değil nöronal aktivite olmasıdır. Bu çalışmada ilk aşamada MR görüntülerinde ön işlemler yapıldıktan sonra MARSBAR ile ilgilenilen bölgeler seçildi. İlişkinin olabileceği on bölge seçildi. Daha sonra 11 sağlıklı deneğe grup analizi yapıldı ve deneyin uyarımlarıyla beraber model oluşturuldu. Uyarımlar dizayn matrisine uygulandı ve parametreler DNM ile bulundu. Modeller içinden en iyisi Bayesçi yaklaşımla seçildi. On bölge arasındaki efektif konnektivite ayrıca PPE ile de bulundu. Bu yöntem fizyolojik ve psikolojik etkileri de dikkate alır. DNM gibi, veri önışlemeden geçer, ilgilenilen bölgeler seçilir ve hemodinamik model tasarlanır. Bölgelerin nöronal ve hemodinamik yanıtları bu yöntem ile karşılaştırılır.

**Anahtar Kelimeler:** işlevsel MRG, Efektif konnektivite, Dinamik Nedensel Modelleme, Psikofizyolojik Etkileşim, Haemodynamic Model.

*To My Family,*

## **ACKNOWLEDGMENTS**

I would like to express my sincere gratitude and appreciation to my supervisor Prof. Dr. Ugur HALICI for her endless support throughout this research. She was always an advisor, professor, and friend for me during my master's period.

I would like to offer my sincere thanks for my co-advisor Prof. Dr. Metehan ÇIÇEK, Ankara University, who gave me invaluable suggestions about my thesis.

We thank to Assist. Prof. Dr. Didem Gokcay, Informatics Institute METU, for fMRI data she provided. The fMRI data used in this thesis was collected at in the UMRAM center by the team led by Didem Gokcay under TUBITAK 109E081 Project support. The ethical committee approval for the healthy subjects were provided by Ankara University.

I would like to thank all my friends specially Emre Kale and Yousef Rezayitabar for their kind suggestions and encouragement during my study.

Finally, I would like to express my special thanks to my parents, my brother and my fiancé Sevil for their love and support during my education.

## TABLE OF CONTENTS

ABSTRACT .....	v
ÖZ.....	vi
ACKNOWLEDGMENTS.....	vii
TABLE OF CONTENTS.....	viii
LIST OF TABLES .....	ix
LIST OF FIGURES .....	x
CHAPTERS	
1. INTRODUCTION.....	1
1.1. Motivation of the Thesis.....	1
1.2. Scope of the Thesis .....	1
1.3. Thesis Outline.....	2
2. THEORETICAL BACKGROUND.....	3
2.1. Effective Connectivity.....	3
2.2. Dynamic System Model.....	3
2.2.1 Bilinear Dynamic Model .....	4
2.2.2 Nonlinear Dynamic I Model .....	5
2.3. Haemodynamic Model.....	5
2.4. Dynamic Causal Modeling.....	7
2.4.1 Bayesian Model Selection.....	8
2.5 Psychophysiological Interactions.....	9
2.5.1. Regression Analysis.....	9
2.5.2. Factorial Design and Physiological Interaction.....	10
2.5.3. Psychophysiological Interaction.....	12
3. MATERIALS AND MODELS.....	15
3.1. Data Description.....	15
3.2. Applying Methods on Data.....	16
3.2.1. Preprocessing Steps.....	16
3.2.1.1. DICOM Transformation.....	17
3.2.1.2. Design Matrix and Contrasts .....	19
3.2.1.3 First Level General Linear Model .....	20
3.2.1.4 ROI Creation.....	21
3.3. Dynamic Causal Modeling.....	22
3.4. Psychophysiological Interactions.....	26
4. EXPERIMENTAL RESULTS.....	29
4.1. Dynamic Causal Modeling Results.....	29
4.2. Psychophysiological Interactions Results.....	42
5. CONCLUSIONS.....	47
5.1. Conclusions.....	47
5.2. Future Work.....	48
REFERENCES.....	49
APPENDICES.....	53

A. T-TEST.....	53
B. STATISTICAL REGRESSION ANALYSIS AND GENERAL LINEAR MODEL.....	57
C. DCM RESULTS.....	61
D. PPI RESULTS.....	101

## LIST OF TABLES

### TABLES

Table 3.1 Data description: Functional scans.....	15
Table 3.2 Data description: Structural scans.....	15
Table 3.3 Stimulations.....	19
Table 3.4 Name and MNI coordinates of ROI's for each condition.....	21
Table 4.1 Probability of error for all modes.....	42

## LIST OF FIGURES

### FIGURES

Figure 2.1. Schematic form of the DCM .....	4
Figure 2.2. Schematic summary of the conceptual basis of DCM.....	6
Figure 2.3. Regression of activity.....	11
Figure 2.4. Regression of activity.....	11
Figure 2.5.a. Activity and attentional effects in PPI.....	12
Figure 2.5.b. Interaction effects in PPI.....	12
Figure 2.6. Psychophysiological Interaction example .....	13
Figure 3.1. Graphics of stimulations.....	16
Figure 3.2. Example of reoriented anatomical image.....	18
Figure 3.3 Example of realignment step.....	18
Figure 3.4. Example of design matrix.....	20
Figure 3.5.a. Sample ROI in brain.....	22
Figure 3.5.b. Sample ROI in brain.....	22
Figure 3.6. General model for DCM.....	23
Figure 3.7. Example of ROI's and stimuli cong.....	24
Figure 4.1.a. Intrinsic connectivity between ROI's of DorsalACC and LeftInsula.....	30
Figure 4.1.b. Responses and predictions of two ROI's of DorsalACC and LeftInsula.....	30
Figure 4.2.a. Intrinsic connectivity between ROI's of RostralACC and VentralACC.....	31
Figure 4.2.b. Responses and predictions of two ROI's of RostralACC and VentralACC.....	31
Figure 4.3.a. Intrinsic connectivity between ROI's of DorsalACC and LeftDLPFC.....	32
Figure 4.3.b. Responses and predictions of two ROI's of DorsalACC and LeftDLPFC.....	32
Figure 4.4.a. Intrinsic connectivity between ROI's of DorsalACC and RightDLPFC.....	33
Figure 4.4.b. Responses and predictions of two ROI's of DorsalACC and RightDLPFC.....	33
Figure 4.5.a. Intrinsic connectivity between ROI's of VentralACC and RightInsula.....	34
Figure 4.5.b. Responses and predictions of two ROI's of VentralACC and RightInsula.....	34
Figure 4.6.a. Intrinsic connectivity between ROI's of DorsalACC and VentralACC.....	35
Figure 4.6.b. Responses and predictions of two ROI's of DorsalACC and VentralACC.....	35
Figure 4.7. Best model of condition congruency:DorsalACC and LeftInsula.....	37
Figure 4.8. Best Model of condition cong*val: RostralACC and VentralACC.....	38
Figure 4.9. Best Model of condition valance:DorsalACC and LeftDLPFC.....	39
Figure 4.10. Best Model of condition valance: DorsalACC and RightDLPFC.....	40
Figure 4.11. Best Model of condition valance: VentralACC and RightInsula.....	40
Figure 4.12. Best Model of condition valance: DorsalACC and VentralACC.....	41
Figure 4.13. PPI of DorsalACC activity and LeftInsula response .....	43
Figure 4.14. PPI of DorsalACC activity and DLPFC response.....	44
Figure 4.15. PPI of RostralACC activity and DLPFC response.....	44
Figure 4.16. PPI of LeftInsula activity and DLPFC response.....	45
Figure C1. Model 1.....	61
Figure C2. Model 2.....	62
Figure C3. Model 3.....	63
Figure C4. Model 4.....	64
Figure C5. Model 5.....	65
Figure C6. Model 6.....	65
Figure C7. Model 7.....	66
Figure C8. Model 8.....	67
Figure C9. Model 9.....	67
Figure C10. Model 1.....	68
Figure C11. Model 2.....	69
Figure C12. Model 3.....	70
Figure C13. Model 4.....	71

Figure C14. Model 5.....	71
Figure C15. Model 6.....	72
Figure C16. Model 7.....	73
Figure C17. Model 8.....	73
Figure C18. Model 9.....	74
Figure C19. Model 1.....	75
Figure C20. Model 2.....	75
Figure C21. Model 3.....	76
Figure C22. Model 4.....	77
Figure C23. Model 5.....	78
Figure C24. Model 6.....	79
Figure C25. Model 7.....	79
Figure C26. Model 8.....	80
Figure C27. Model 9.....	81
Figure C28. Model 1.....	81
Figure C29. Model 2.....	82
Figure C30. Model 3.....	83
Figure C31. Model 4.....	84
Figure C32. Model 5.....	84
Figure C33. Model 6.....	85
Figure C34. Model 7.....	86
Figure C35. Model 8.....	86
Figure C36. Model 9.....	87
Figure C37. Model 1.....	88
Figure C38. Model 2.....	89
Figure C39. Model 3.....	89
Figure C40. Model 4.....	90
Figure C41. Model 5.....	91
Figure C42. Model 6.....	91
Figure C43. Model 7.....	92
Figure C44. Model 8.....	93
Figure C45. Model 9.....	94
Figure C46. Model 1.....	95
Figure C47. Model 2.....	95
Figure C48. Model 3.....	96
Figure C49. Model 4.....	97
Figure C50. Model 5.....	97
Figure C51. Model 6.....	98
Figure C52. Model 7.....	99
Figure C53. Model 8.....	99
Figure C54. Model 9.....	100
Figure C55. Haemodynamic, Response and PPI model.....	102
Figure C56. Haemodynamic, Response and PPI model.....	103
Figure C57. Haemodynamic, Response and PPI model.....	104
Figure C58. Haemodynamic, Response and PPI model.....	105
Figure C59. Haemodynamic, Response and PPI model.....	106
Figure C60. Haemodynamic, Response and PPI model.....	107
Figure C61. Haemodynamic, Response and PPI model.....	108
Figure C62. Haemodynamic, Response and PPI model.....	109
Figure C63. Haemodynamic, Response and PPI model.....	110

# CHAPTER 1

## Introduction

### 1.1 Motivation of the study

In neuroscience field, the question of how brain works has great importance. Because of complexity in neural connections of brain, answering this question is not easy. To analyze brain behavior, there is a need to the methods which are able to deal with a huge number of neurons. Furthermore, these neurons differ in behavior while considering their connectivity. Analyzing the connectivity and finding a relationship among these neurons is done in three main levels:

- 1) Structural or Anatomical Connectivity describes the actual connectivity in brain. The connection between all neurons of brain is discussed in this connectivity.
- 2) Functional Connectivity describes the connectivity among group of neurons. The emphasize in this connectivity is on effect of one region of brain on all other regions.
- 3) Effective Connectivity gives the details of connection between regions or voxels of interest in brain. It considers the whole brain as it is divided into small regions as DorsalACC, VentralACC, LeftInsula, etc. and tries to find a relationship between these regions.

In field of neuroimaging, there are some usual techniques as Magnetic Resonance Imaging (MRI), Electroencephalography (EEG) and Magnetoencephalography (MEG). All these techniques can be used to identify the regions of brain that have special characteristics.

Main reason for analyzing the connectivity of brain is the importance of this analysis in detecting brain disorder diseases in early stages is the answer of the question. Analysis of effective connectivity gives important information about responding of brain to stimulations. Using this information, it will be possible to differentiate healthy and disease brain.

Effective connectivity can be analyzed using methods: Structural Equation Modeling (SEM), Granger Causality Modeling (GC), Psychophysiological Interaction Method (PPI) and Dynamic Causal Modeling (DCM). The main purpose in this thesis work is to find effective connectivity using fMRI data time-series by using two methods of Dynamic Causal Modeling and Psychophysiological Interactions. Between these models we eliminated SEM and GC methods because of some drawbacks of these two methods. SEM method has 3 main weak points. This method is depending on sample sizes to estimate model fit. To use this method one needs to know direction of connections. SEM does not support reciprocal models (in which the connections are symmetric).

In case of GC method, stability of hypothesis is decreased if there are many regions and this method needs short repetition times (TR) to extract time-series. The most important weakness of GC method is that it cannot give true estimation of directional effects in fMRI data time-series. For the case that data is acquired from a stimulated brain, the DCM is a suitable method. This method relates stimulation of brain, physiological interactions and effective connectivity to each other.

### 1.2 Scope of the study

Before analyzing fMRI data however, there is a need for preprocessing the data. During acquisition of MR images, the subject may move his head and data maybe noisy. Also the brain sizes differ in different people. To solve discussed problems, preprocessing is done. This step includes slice-timing correction, realignment, co-registration, normalization and smoothing. Then, design matrix and contrast matrices are determined and applied to data. At next step is ROI's are created. These ROI's are the active parts of brain after applying stimulation to the brain. In finding effective connectivity, the only important areas to be

analyzed are ROI's (region of interest. After these steps, as neural activity is latent in fMRI data, there is a need to a model which transfers latent data to visible format. This model is named hemodynamic model that turns neural activity to a visible BOLD (Blood-Oxygen Level Dependent) signal. In order to make a general decision on connectivity between different ROIs, group analysis is done. This analysis covers all subjects in the experiment. There are three parameters which bilinear DCM tries to find. These three parameters are in the shape of 3 matrices. First one is A matrix which gives intrinsic connectivity. Intrinsic Connectivity shows connection between brain regions without considering any stimulation on brain.

Second is B matrix which gives modulatory effects of stimulations on connection between brain regions.

The third is C matrix and shows the direct effect of stimulation directly on brain regions. The differences between these models are the place of applying stimulation. Stimulation applied directly to the regions or to the connections between regions. The application of stimulation to any place defines different models. In some cases there are more than 60 models. For each model, B and C matrices should be determined and then Bayesian method is used to compare models. After finding these three matrices, models are completed and best model can be chose by using Bayesian Factor. This is done by comparing model complexity and accuracy. The term "*log posterior*" is used for "*accuracy – complexity*". This means that the best model is selected among the most accurate and complex models. Bayesian Factor compares log-posteriors of models to give the best model as final step.

In addition to bilinear DCM, also PPI is considered in this study. Psychophysiological Interaction method (PPI) gives responses in one region of brain which is the result of affecting this region by another brain region or any stimulation. In this master thesis work only effect of stimulation is considered. Two important issues are discussed in this method as Psychological and physiological effects. Psychological effects refer to the stimulations in the experiment related to this thesis work.

### **1.3 Thesis outline**

This Thesis is organized as follows: In chapter one a survey of current studies in Effective connectivity is presented and then in second chapter DCM and PPI methods are explained in details. In the third chapter data description and the stimulations used are presented. Chapter four describes our methods and results. Finally, the overall conclusion of the research is given and the potential future works are described in chapter 5. APPENDICES A and B describe t-test and Statistical Regression analysis. The performance evaluation of the presented methods and all results including best models for DCM method are presented in APPENDIX C. PPI results including Neuronal and Haemodynamic responses and stimulations for all ROI's of subjects are included in APPENDIX D.

## CHAPTER 2

### Theoretical Background

#### 2.1 Effective Connectivity

The usage of Functional neuroimaging techniques in cognitive sciences to investigate the aspects of functional specialization and integration in human brain is inevitable. Functional integration could be characterized within Functional Connectivity and Effective Connectivity [1, 2, 3]. As functional connectivity is describing how data are dependent, effective connectivity concentrates on mechanistic models of causal effects which generated that data [4, 5].

In literature the term Effective Connectivity is defined in many ways. The most general one is that the effective connectivity is describing causal influences which neural units exert over another [1]. The simplest description of effective connectivity is the influence of one neuronal region on another. In details “Effective connectivity should be understood as the experiment-dependent and time-dependent simplest possible circuit diagram that would replicate the observed timing relationships between the recorded neurons”[6]. In both of definitions, the emphasize is on determining effective connectivity there is a need to a causal model of the interactions between the elements of the neural system.

#### 2.2 Dynamic System Model

Using general mathematical framework provided in dynamic system theory, brain is modeled as a dynamic system which is characterized by  $n$  variables which interact with each other. These variables are  $x_i$ , ( $1 < i < n$ ) time-varying state variables and progression of any of state variables depends on other state variables. As an example consider membrane potential which depends on number of ion channels which are open or opening the voltage-dependent ion channels directly depends on membrane voltage.

These kinds of functional dependencies could be expressed using differential equations and some parameters like  $\Theta$  determining form and strength of causal influences between variables.

In case of neuronal systems, parameters are time constants or synaptic strength in connections between elements. If the system is non-autonomous (a system with changing matter, energy and information with environment) inputs into the system like sensory information into brain must be considered.

In non-autonomous deterministic system with  $m$  vector function ( $m$  known inputs) one can define such a general equation:

$$\frac{dx}{dt} = F(x, u, \theta) \quad (\text{Eq. 2.1})$$

In the equation above,  $x$  are the neuronal states of system,  $u$  are inputs and  $\theta$  are the parameters of the desired model. The equation above easily describes how system structure can affect system dynamics as it describes two important issues: (i) time and region of external inputs to the system and (ii) changes happened in state of system. Let's integrate equation 1.1 considering initial state  $x(0)$ . This would be like

$$x(\tau) = x(0) + \int_0^\tau F(x, u, \theta) dt \quad (\text{Eq.2.2})$$

Equation 1.2 is a general form of models of effective connectivity for neural systems [6, 7].

As we want to work in continuous time we use time dependent equation. This situation is also true for discrete system as multivariate/vector autoregressive models (M/VAR) and static system (static systems are at equilibrium every single time).

This method has been applied to structural equation modeling also [8, 9, 10, 11].

The Psychophysiological Interactions (PPI) and Dynamic Causal Modeling (DCM) consider special cases of the Dynamic system model given here in order to find effective connectivity among brain regions represented by state variables. On the other hand, haemodynamic model is describing how the signal of neuronal state  $x(t)$  transfers to BOLD signal of  $y(t)$  included in 2.3 [12, 4, 5].

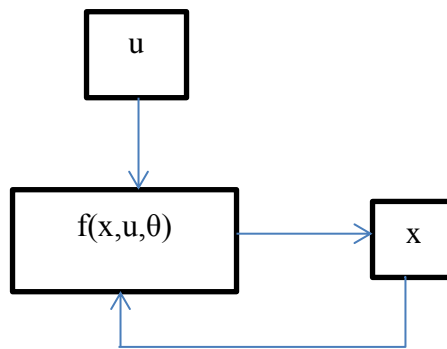


Figure 2.1. Schematic of a Dynamic system model.

Figure 2.1 is a graphical schematic of a dynamic model. In this figure  $u$  is inputs of system which have effect on the state of system. State of the system here is shown by  $x$ . The system is represented by a recurrent function of inputs ( $u$ ), system states ( $x$ ) and system parameters ( $\theta$ ).

Dynamic system model could be considered as Linear Dynamic system model as a special case. In linear dynamic model only simple form of Taylor series is considered. In next sections other special kinds of Dynamic model will be discussed in details. These special cases are bilinear and nonlinear dynamic models. In these two cases, Taylor series is expanded and this series is result in the equations of calculating dynamic causal modeling.

### 2.2.1 Bilinear Dynamic Model

In a system of  $n$  interacting brain regions, input-state-output model of neuronal dynamics could be represented by DCM. In order to show activity in each region there is a single variable which could change by experimentally controlled inputs  $u$ . DCM has the ability to model the temporal changes in neuronal vectors  $x$  whole the system is in resting state ( $x_0 = 0, u_0 = 0$ ). This could be possible using a bilinear Taylor series approximation to any nonlinear function  $f(x,u)$  [8].

$$f(x,u) = \frac{dx}{dt} \approx f(0,0) + \frac{\partial f}{\partial x}x + \frac{\partial f}{\partial u}u + \frac{\partial^2 f}{\partial x \partial u}xu \quad (\text{Eq.2.3})$$

This series is shortened in a way that it only includes bilinear (second-order) terms describing interactions between states and input  $n$ . For  $m$  known inputs the matrices will be like equation 2.3[8].

$$A = \frac{\partial f}{\partial x} \Big|_{u=0}, \quad B^{(i)} = \frac{\partial^2 f}{\partial x \partial u_i}, \quad C = \frac{\partial f}{\partial u} \Big|_{u=0} \quad (\text{Eq.2.4})$$

In this manner, the direct neurophysiological interpretation could be equation 2.5 [8].

$$f(x,u) = \frac{dx}{dt} = (A + \sum_{i=1}^m u_i B^{(i)})x + Cu \quad (\text{Eq.2.5})$$

There are three matrices in equation 2.5. Matrix A represents the fixed (endogenous) connections between regions. Matrix  $B^{(i)}$  represents the modulatory connections. When there is a change in inputs ( $u_i$ ) these matrices will change which is induced by the  $i^{th}$  input  $u_i$  as an additive change. These changes will be the result of learning or attention for example. Matrix C, gives the effect of exogenous or direct inputs to the system. These direct inputs are any given stimulation to the brain [8].

### 2.2.2 Nonlinear Dynamic Model

If one extend Taylor series in equation 2.13 to second state order, it will results in nonlinear interactions modeling for  $n$  states of system [12].

$$f(x,u) = \frac{dx}{dt} \approx f(0,0) + \frac{\partial f}{\partial x} x + \frac{\partial f}{\partial u} u + \frac{\partial^2 f}{\partial x \partial u} xu + \frac{\partial^2 f}{\partial x^2} \frac{x^2}{2} \quad (\text{Eq.2.6})$$

Setting  $D^{(j)} = \frac{1}{2} \frac{\partial^2 f}{\partial x_j^2} \Big|_{u=0}$  ( $1 \leq j \leq n$ ) will result in Eq.2.6:

$$f(x,u) = \frac{dx}{dt} = (A + \sum_{i=1}^m u_i B^{(i)} + \sum_{j=1}^n x_j D^{(j)})x + Cu \quad (\text{Eq.2.7})$$

Matrices  $D^{(j)}$  encrypt connections in the system, which are gated by regions. Specifically, any non-zero entry  $D_{kl}^{(j)}$  indicates that response of region  $k$  to inputs from region  $l$  depend on activity in region  $j$  [8].

Figure 2.4, simply depicts the difference between bilinear and nonlinear dynamic causal modeling method [8].

## 2.3 Haemodynamic Model

Reviewing literatures on cognitive neuroscience, one will come across with classical models of effective connectivity like SEM, VAR and PPI. All these methods operate at the level of measured signals but to identify causal structure of the system which lies under neuronal level, we come to an end with non-invasive methods. Considering fMRI data, all methods named above could be applied to time series which are the result of haemodynamic responses convolution with neuronal activity. There is a need to a forward model which link neuronal activity accuracy in the dynamic model to measured haemodynamic response signal to give a meaning for analysis of inter-regional connectivity, because different brain regions could be affected by different neurovascular stimulations [12].

Dynamic Causal Modeling combines neural dynamics with the experimentally confirmed haemodynamic model. This haemodynamic model shows transformation of neural activity to BOLD response. Haemodynamic model which is built on ‘‘Balloon Model’’[13] can be showed on a differential equations which shows that changes in neural activity can cause changes in vasodilatory signal, blood flow volume

and deoxyhemoglobin content [14]. The most recent version of haemodynamic model is shown in figure (2.3) which is completely described by *Stephan et al.* [15].

Measured BOLD signal will be able to estimate the set of neural and haemodynamic parameters as  $\Theta = \{\Theta^{(n)}, \Theta^{(h)}\}$ . For this purpose, among different methods, we choose Bayesian approach with empirical priors for haemodynamic and coupling parameters. More details on parameter estimation, Bayesian algorithm, Gaussian Estimation and expectation Maximization can be found in [4, 16, 17].

Neuronal and haemodynamic equations together, give a deterministic forward model with hidden states. Measured BOLD response which is shown with  $y$  could be modeled as a linear combination of predicted BOLD signal  $h(u, \Theta)$  and confounds signal drift which is shown by  $X\beta$  and Gaussian observation error  $e$  [8]:

$$y = h(u, \Theta) + X\beta + e \quad (\text{Eq.2.8})$$

Experimentally controlled input functions  $u$  evoke neural responses  $x$ , modeled by a bilinear differential state equation, which trigger a haemodynamic cascade, modeled by 4 state equations with 5 parameters. These haemodynamic parameters comprise the rate constant of the vasodilatory signal decay ( $k$ ), the rate constant for auto-regulatory feedback by blood flow ( $\gamma$ ), transit time ( $\tau$ ), Grubb's vessel stiffness exponent ( $\alpha$ ), and capillary resting net oxygen extraction ( $\rho$ ). The model consists of the two equations describing the dynamics of blood volume ( $v$ ) and deoxyhemoglobin content ( $q$ ). Integrating the state equations for a given set of inputs and parameters produces predicted time-series for  $v$  and  $q$  which enter a BOLD signal equation  $\lambda$  to give a predicted BOLD response.

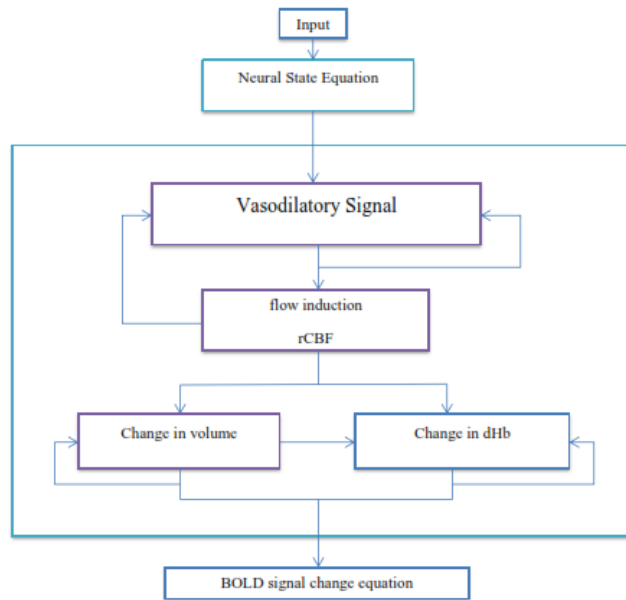


Figure 2.2. Schematic summary of the neural state equation and the haemodynamic forward model based on neuronal state equation explaining BOLD signals.

Vasodilatory signal is defined as :

$$ds/dt = x - ks - \gamma(f - 1) \quad (\text{Eq.2.9})$$

Flow induction is calculated as:

$$df/dt = s \quad (\text{Eq.2.10})$$

Using equation 2.8 gives us the change in volume:

$$\tau dv/dt = f - v^{1/a} \quad (\text{Eq.2.11})$$

Changes in deoxyhemoglobin level is defined as:

$$\tau dq/dt = f \frac{E(f,\rho)}{\rho} - v^{\frac{1}{a}} q/v \quad (\text{Eq.2.12})$$

Equation 2.8 gives us the information about changes in BOLD signal:

$$y = \lambda(v, q) \quad (\text{Eq.2.13})$$

## 2.4 Dynamic Causal Modeling (DCM)

In order to be able to infer on connectivity between neuronal regions, there must be models that are able to combine conceivable model of neural population dynamics in neurobiological manner with a forward model which is able to describe the transformation from neuronal activity form to measured signal form in a conceivable biophysical format [18, 19, 20]. Such a model then will fit predicted time-series similar to observed time-series.

Integrating the state equation gives predicted neural dynamics ( $x$ ) that enter a model of haemodynamic response ( $\lambda$ ) to give predicted BOLD responses ( $y$ ). The parameters at both neural and haemodynamic levels are adjusted such that the differences between predicted and measured BOLD series are minimized. Critically, the neural dynamics are determined by experimental manipulations. These enter the model in the form of external inputs. Driving inputs elicit local responses directly that is propagated through the system according to the intrinsic connections. The strength of these connections can be changed by modulatory inputs [21].

In classical form of DCM, the change of a neural vector  $x$  in time with each region which is being represented by a single variable, has been modeled. It's shown in Equation 2.9.

$$\frac{dx}{dt} = F(x, u, \theta) = (A + \sum_{i=1}^m u_i B^{(i)})x + Cu \quad (\text{Eq.2.14})$$

The given equation 2.9 is called the Bilinear model for DCM.

Considering equation 2.4, the neural parameters  $\theta = \{A, B, C\}$  can be expressed as partial derivatives of  $F$  as below [11]:

$$\begin{aligned} A &= \frac{\partial F}{\partial x} / u=0 \\ B^{(i)} &= \frac{\partial^2 F}{\partial x \partial u_i} \\ C &= \frac{\partial F}{\partial u} / x=0 \end{aligned} \quad (\text{Eq.2.15})$$

In equation 2.10 above, there are 3 matrices. Matrix  $A$  represents fixed or endogenous or intrinsic connectivity between regions in the absence of any input. Matrices  $B^{(i)}$  encode any change in connectivity

which is caused by any of inputs. Matrix  $C$  shows us direct or exogenous effect of inputs on neural activity.

### 2.4.1 Bayesian Model Selection (BMS)

The important part of DCM is selecting best fitted model for data. All preprocessing and processing steps are done and the data is prepared. The problem now is finding the best model.

The decision cannot be made just by comparing the relative fit of different models. The differences in complexity like number of parameters and the degree of inter-dependency are important issues. Notice that by increasing model complexity, there will be an increase in model fit but, in the same way, there will be an increase in noise either. Therefore, the problem changed from finding only optimal model to finding a model which is able to balance fit and complexity. Doing this will result in a model that maximizes model evidence [22, 23];

$$p(y|m) = \int p(y|\theta, m)p(\theta|m)d\theta \quad (\text{Eq2.16})$$

In equation 2.16, parameter  $y$  corresponds to changes in BOLD signal,  $m$  is the selected model and parameter  $\theta$  is parameters of model  $m$ . In this equation all parameters of determining interdependencies, including numbers of free parameters and functional form of generative model are subsumed by integration. As this integral cannot be solved analytically, there is an approximation to the log of the model evidence and this means that we apply logarithm to both sides of equation. This approximation is usually a free energy bound on the log evidence [17]. More detailed discussion on this issue could be found in [24, 25].

Given two models  $m_i$  and  $m_j$ , the difference in log evidence can be transformed into a *Bayes factor (BF)* as below:

$$BF_{ij} = \frac{p(y|m_i)}{p(y|m_j)} \quad (\text{Eq2.72})$$

BMS is applied to both single subjects and the whole groups. Random effects BMS could be used when variation of optimal model across subjects is expected. Also, variational Bayes [25] could be used in case of applying probability density on model themselves. Using all mentioned above with together, it's seen a specific model generated the data of a randomly chosen subject is similar to the increase probability of one model being more likely than any other model.

The most important role of BMS in DCM is that it is used to select most probable model than other estimations before considering any particular parameters. As an example BMS could be used to show effect of anatomical connection strength on effective connection strength [26].

BMS is also able to compare two or more portions of model space [25]. This is useful because model space reflects some important aspects like (i) including a specific connection in a model or not (ii) a particular connection is modulated by which condition (iii) special effects are linear or non-linear.

Ability of this method to consider large set of models together which allows one to be sure of selecting model structure and comparing different models with each other is its advantage.

## 2.5 Psychophysiological Interactions (PPI)

PPI is a method which is used to understand difference in correlation of activities between two different brain areas in different psychological situations. In a simple way this method shows relations between psychological condition and functional interaction between two regions in the brain.

As an example consider a task which activates both prefrontal cortex and hippocampus in brain. Here we must be able to explain two important matters. (i) both regions were activated independently (ii) both regions are working with each other interactively.

The first principle to look for regions which are interacting with each other is considering if the activity level in those areas will correlate in time. This means that any “in-synch” increase or decrease in activity between regions will result in a functional relation between them. There is a basic way: extracting time-series from some representative voxel in a region and then apply General Linear Model using the activity time-course of that region.

The most important issue here is change of interaction between areas in different conditions which will influence correlation between the time-course of those areas. Consider a task which your previous knowledge about the content of task may have an effect on it. So, in PPI, the areas of higher correlations with time-course in seed regions are considered and only relationships are considered which change during a task in an experiment. For example consider navigating around a labyrinth, some areas of your brain is active to find a way. We are interested in regions which interact during navigation not during passive travel.

In order to solve the problems mentioned above it's preferable to generate an interaction regressor instead of using explanatory variable in GLM [27, 28, 29, 30, 31, 32].

### 2.5.1 Regression Analysis

Changes in models in order to model the influences between regions will result in diversity in Effective Connectivity. In this part we want to focus on psychophysiological interactions. Consider a simple linear model and show regression analysis on this model.

Consider activity in  $i^{th}$  voxel to be modeled as;

$$x_i(t) = \sum C_{ij} \cdot x_j(t) \quad (\text{Eq.2.18})$$

with summation over  $j$ ; the activity of  $x_i(t)$  is sum of influences of  $C_{ij} \cdot x_j(t)$  from other regions. Notice that there is not any self-connection ( $C_{ij} = 0$ ). The  $C_{ij}$  corresponds to connection strength from  $j$  to  $i$ ; Note that  $C_{ij}$  is not equal to  $C_{ji}$ . In electrophysiology  $C_{ij}$  is known as *efficacy* and  $x_i(t)$  is postsynaptic response to presynaptic inputs  $x_j(t)$ . In such a simple model inputs sum with each other instead of interacting in time-courses. Also, connection strengths are fixed, preventing time-dependent changes [33]. These strong and unrealistic considerations are more robust than similar methods like Structural Equation Modeling [34, 35].

Consider a multiple linear regression equation in matrix format. This is given by equation 2.19.  $\mathbf{x}_i = [\mathbf{x}_1 \dots \mathbf{x}_k \dots \mathbf{x}_K][\beta_{i1} \dots \beta_{ik} \dots \beta_{iK}]^T + \mathbf{G} \cdot \beta_G + \mathbf{e}_i$  (Eq.2.19)

where T denotes transpose.  $\mathbf{x}_i$  is a column vector of response variables at each voxel  $i$ ;  $\mathbf{G}$  is a matrix whose columns contain a collection of unnecessary effects like global activity, time effects;  $\beta_{ik}$  and  $\beta_G$  are the parameter estimates and  $\mathbf{e}_i$  is a well-behaved error term. Estimated  $\beta_{ik}$  in this equation can be identified with  $C_{ik}$  as we include all regions from 1 ... K (in DCM case there were  $m$  selected regions) [38]. Response for only one region is given in equation 2.20 below:

$$\mathbf{x}_i = \mathbf{x}_k \beta_{ik} + \mathbf{G} \cdot \beta_G + \mathbf{e}_i \quad (\text{Eq.2.20})$$

If don't consider influence of other regions, the relation between  $\beta_{ik}$  and effective connectivity is fine here. It's logical to refer to  $\beta_{ik}$  as "contribution" to clarify that the slope of regression is not necessarily an estimate for effective connectivity. Regression significance test ( $\beta_{ik} = 0$ ) is also a correlation significance between  $\mathbf{x}_i$  and  $\mathbf{x}_k$  i.e. the functional connectivity. But there is no need to functional connectivity for this study work therefore, more and more areas must be included so that the contribution will approximate the effective connectivity [33]. This also means "contribution from voxel  $k$  to  $I$  as a regression just could be reached by showing activation in  $k$  as an explanatory variable and activation in  $i$  as a response" [33].

## 2.5.2 Factorial Design and Physiological Interactions

Factorial design means combining two or more facts in a task. This is done by combining the interactions between these factors or the effect of one factor on response of another one. In neuroimaging field, factorial design for the first time has been applied on interaction between motor activation [34]. It simply was the effect of time on activation which was resulted by motor performance. In general, interaction is different responses to any factor influenced by other factors or processes. As an example consider different brain responses when stimulation frequency is increasing and looking for a reasonable response like differential sensitivity, brain responses which are sensitive to stimulation, in brain.

In some of experiments [35], they gave auditory and visual stimulations and during stimuli application, they changed presentation ratio of stimuli. The subject had to pay attention to visual stimuli as well as motion. They used equation 2.18 to test differential sensitivity for increasing in rate of stimulation. Equation 2.20 will change to equation 2.21. in this situation [33].

$$\mathbf{x}_i = \mathbf{g}_r \times \mathbf{g}_a \cdot \beta_1 + [\mathbf{g}_r \mathbf{g}_a \mathbf{G}] \cdot \beta_G + \mathbf{e}_i \quad (\text{Eq.2.21})$$

In this equation  $\mathbf{g}_r$  and  $\mathbf{g}_a$  are explanatory variables of experimental conditions.  $\mathbf{g}_r$  gives a mean vector for the rate of presentation of the stimuli and  $\mathbf{g}_a$  is a variable which has a value 1 or -1 to indicate whether subject is pay attention to visual or motion stimulation. All these mentioned are the main effects in this experiment.  $\mathbf{g}_r \times \mathbf{g}_a$  shows interaction term which models differences in regression slope under different attentional sets. Notice that, this is an element by element matrix. At the end of experiment, interactions in thalamus were observed [35]. The important issue here is increasing in activation of thalamus happened in presence of auditory stimuli.

Explanation of regressor variables are shown by columns of a matrix named Design Matrix. *t-statistics* is able to detect positive and negative contribution of physiological interactions and it would treat main effects which are modeled by  $\mathbf{g}_r$  and  $\mathbf{g}_a$  as effects of interest.

$$\mathbf{x}_i = [\mathbf{g}_r \times \mathbf{g}_a \mathbf{g}_r \mathbf{g}_a] \cdot \beta_1 + \mathbf{G} \cdot \beta_G + \mathbf{e}_i \quad (\text{Eq.2.22})$$

Now, consider replacing the explanatory variables with measured physiological activity in two different brain regions and identify a significant interaction in a third brain area. If we do so, then third region will be explained as an activity in first area which will depend on activity in second area. This is what Physiological Interaction means.

As an example, consider experiment conducted by Buechel and Friston [36, 37] in which attention to visual motion was analyzed and the design was in a way that they could examine interactions among the three brain regions called: V5, PPC and PFC. The design was in a way that they could examine interactions among three regions of brain called V5, PPC and PFC (three regions in brain). Nonlinear structural equation modeling (SEM) also could modulate V5→PPC using PFC but this method don't show "How regionally specific was this modulation" Physiological interaction method answers this question easily. Modulation between V5→PPC as described above depends on PFC. Equation 2.23 gives the modulation:

$$[C_{PPC,PFC \times V5} \cdot X_{PFC}(t)] \cdot X_{V5}(t) \quad (\text{Eq.2.23})$$

where the *activity-dependent* efficacy from V5 to PPC (inside brackets of equation 2.23) incorporates the modulatory effects of  $X_{PFC}(t)$ . Considering the term  $C_{PPC,PFC \times V5}$  as *activity-independent* efficacy of interaction term equation 2.23 results in

$$[C_{PPC,PFC \times V5} \cdot X_{PFC}(t)] \cdot X_{V5}(t) = C_{PPC,PFC \times V5} \cdot [X_{PFC}(t) \cdot X_{V5}(t)] \quad (\text{Eq.2.24})$$

The statistical model by considering Eq.2.18 and Eq.2.19 will be as equation 2.25 below:

$$x_i = x_{PFC} \times x_{V5} \cdot \beta_i + [x_{PFC} x_{V5} G] \cdot \beta_G + e_i \quad (\text{Eq.2.25})$$

Product of  $x_{PFC} \times x_{V5}$  which is an element by element production of modulatory effects of regions PFC and V5, gives the activities in PFC and V5. Considering a regionally specific modulatory effect, we will have the contribution effect only in PPC. So, now we can apply this method to three different region of brain in any of subjects. Figure 2.5 illustrates that PPC is modulating V1→V5 connections. A *t-statistics* testing with null hypothesis  $\beta_i=0$  is considered and resulted in equation 2.26 as below:

$$x_i = x_{PPC} \times x_{V1} \cdot \beta_i + [x_{V1} x_{PPC} G] \cdot \beta_G + e_i \quad (\text{Eq.2.26})$$

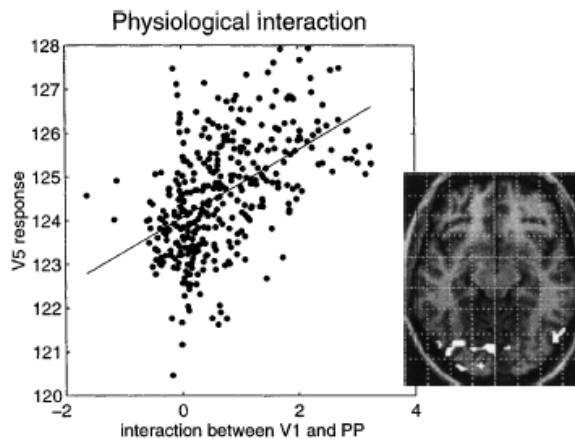


Figure 2.3. Regression of activity near right V5 on the product of activity in V1 and PPC. This regression shows the substantial contribution of the interaction effect to V5 response and can be interpreted as evidence for a positive modulation of V1→V5 [33].

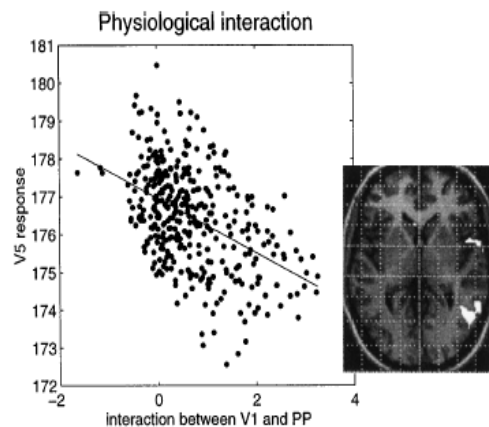


Figure 2.4. this figure is like fig.2.5. but for a voxel more anteriorly and superiorly. In this figure slope is negative suggesting a negative modulation of V1→V5 influences by PPC activity influences by PPC projections. This is an example of physiological interaction [33].

They chose a voxel in V1 with coordinates of (12, -81, -4) [38]. Another voxel from PPC with location of (21, -5, 60) has been chosen. They observed a regionally specific interaction near V5. Note that, effects of  $x_{V1}$  and  $x_{PPC}$  must be removed as it caused by contribution from V1 and PPC to V5, there will be a variance in  $x_i$  which could be explained by  $x_{PPC}$  and  $x_{V1}$ . Looking at two figures 2.3 and 2.4 above one may concern the meaning of positive and negative slopes. Positive slope means that, the amount of variation in V5 could be the result of positive interaction term. In this experiment they observed ( $Z=5.77$ ,  $P<0.001$ ,  $z$  is the rate of acceptability). Although, in figure 2.5 we can see some regions that have negative interactions either. Figure 2.6 illustrates this more clearly. Generally speaking, any positive or negative slope is considered as positive or negative interactions respectively. The modulatory interaction could be from V1 to V5 or vice versa.

### 2.5.3 Psychophysiological Interactions

Psychophysiological interactions explain that when there is an interaction between a sensorimotor or process with activity which happened in other part of brain. Equation 2.27 is the statistical model for psychophysiological interactions:

$$x_i = x_k \times g_p \cdot \beta_i + [x_k g_p G] \cdot \beta_G + e_i \quad (\text{Eq2.27})$$

Here, in this equation the term  $(x_k \times g_p \cdot \beta_i)$  is the psychophysiological interaction between the physiological activity in region  $k$  and another physiological parameter of the design  $g_p$  which is the result of conducting these two results. Just like previous part, we can examine any changes in contribution from V1, under the condition that there is attention to visual motion, to V5 [13]. This gives an opinion of the importance of this visual attention to motion in changing the contribution of between regions. In figure 2.5.a. V1 activity is showed in dotted line while the solid one is showing attentional effects. Figure 2.5.b. though illustrates conduction between these two elements. Remember equation 2.27 in which V1 activity resembles  $x_k$  and attentional effect or the solid line resembles  $g_p$  and therefore, figure 2.5.b. will give us the term  $x_k \times g_p$ .

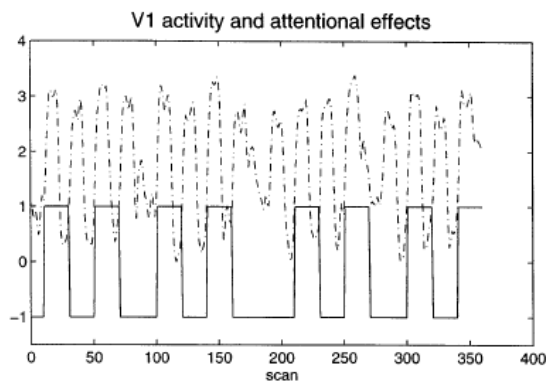


Figure (2.5.a) [33]

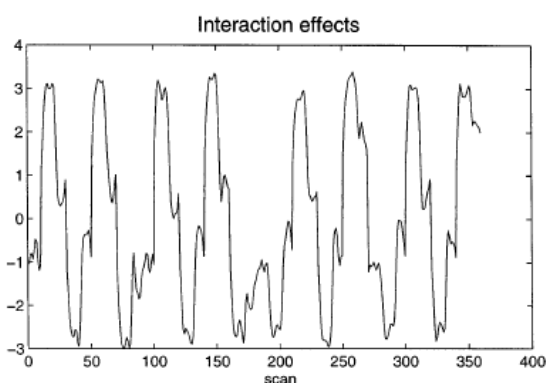


Figure (2.5.b) [33]

Remember that, any interaction could be written as modulation of one effect from any of factors at presence of other effects. For example, any response from V5 means that (i) there is a modulatory effect of attention on contribution from V1 or (ii) modulatory effects of inputs of V1 on attention responses. To

be generally speaking, one can consider psychophysiological interactions as (1) a change in contribution of one region to another region or (2) a contribution of one region which results in modulation of responses to a variable [33].

Figure 2.6 is the result of an experiment when two kinds of stimulations are considered at the same time.

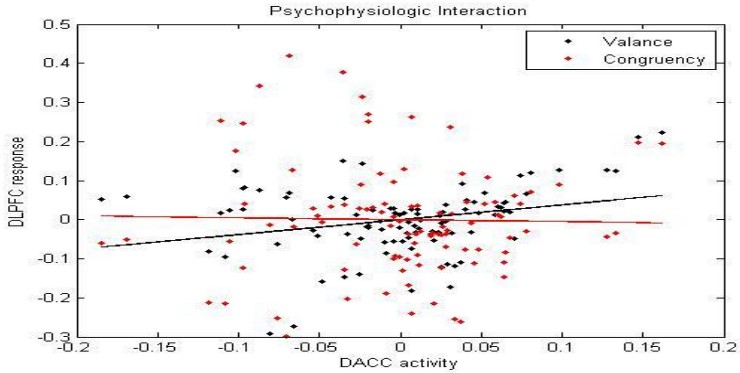


Figure2.6. Regression of DACC activity on DLPFC activity while the stimulation is valance and congruency.

Figure 2.6, shows the relation of activity in DACC to the responses DLPFC relatively in two stimulations of valance and congruency. Black line and dots shows the situation of stimulation being valance while red line and dots shows the situation of stimulations be congruency.



## CHAPTER 3

### Materials and Methods

This chapter includes four main sections. In section 3.1 data is described in details. Section 3.2 includes preprocessing steps, First level General Linear Model, Design and Contrast matrices, ROI creation and application of two methods DCM and PPI to data. In section 3.3, application of Dynamic Causal Modeling as our first method described in details. Section 3.4 includes Psychophysiological Interaction method application to data as second method.

#### 3.1 Data Description:

This part includes subjects and scanner, related to the data used in this thesis.

The fMRI data is provided by Assist. Prof. Dr. Didem Gokcay, Informatics Institute METU and my co-advisor Prof. Dr. Metehan Cicek, Ankara University. The fMRI data used in this thesis was collected in the UMRAM center by the team headed by Didem Gokcay under TUBITAK 109E081 project support. Design of experiments and programming is done by Didem Gokcay and her team also. The ethical committee approval for the healthy subjects was provided by Ankara University. This data includes 14 subjects but 3 of them have brain disorder or tumor and we couldn't use their data. There are 11 healthy subjects with no brain disorder or any brain tumor. Description of data in details is given in tables 3.1 and 3.2 below:

Table.3.1. Data description: Functional scans

fMRI	protocol	duration	slices	slice thickness	in-plane voxel resolution	TR	TE	samples per run
	echo planar	3.5 min each, 4 runs	34	4 mm	3X3 mm	2000	30	100

Table.3.2. Data description: Structural scans

mprage	protocol	duration	slices	slice thickness	in-plane voxel resolution	TR	TE	FOV
	sagittal	6 min	224	1 mm	1X1 mm	2500	3.3	256

Considered sequences for the experiment are: Resting state functional, DT1 (Diffusion Tensor Imaging), DT2, functional runs and structural scans.

There are four kinds of stimulations used in the experiment (see figure 3.1):

1. Congruency Positive: A situation in which two parts of stimulation are congruent and gives a positive feeling (as an example: showing an image in which a person is laughing and something written which gives a positive or happy feeling).
2. Congruency Negative: A situation in which two parts of stimulation are congruent and gives a negative feeling (as an example: showing an image in which a person is laughing and something written which gives a negative or unhappy feeling).
3. Incongruency Positive: A situation in which two parts of stimulation are not congruent and gives a positive feeling (as an example: showing an image in which a person is crying and something written which gives a positive or happy feeling).
4. Incongruency Negative: A situation in which two parts of stimulation are not congruent and gives a negative feeling (as an example: showing an image in which a person is laughing and something written which gives a negative or unhappy feeling).

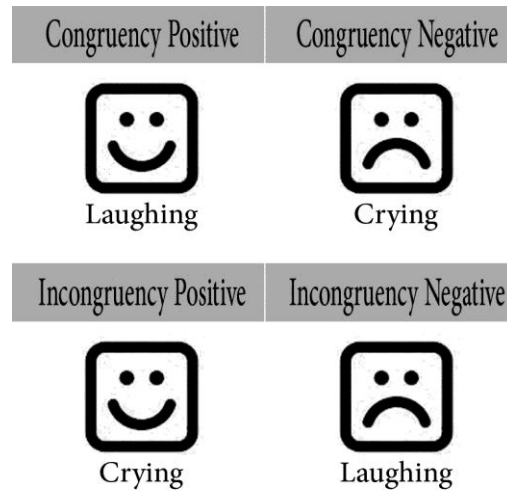


Figure 3.1. Graphical description of stimulations

### 3.2 Applying Methods on Data:

#### 3.2.1 Preprocessing Steps:

Before DCM and PPI are applied on the acquired data, in order to improve signal to noise (SNR) ratio and to be able to use data properly, we have to complete some preprocessing.

The preprocessing steps include: DICOM transformation, Slice-timing Correction, Realignment, Co-registration, Normalization and Smoothing. After preprocessing step is completed GLM analysis is done.

Then ROI's are created by using statistical group analysis. And finally DCM and PPI methods applied to fMRI data. Details of preprocessing step applied on fMRI data are as given below.

### 3.2.1.1 DICOM Transformation

As the first step of preprocessing we have DICOM transformation and Image Reconstruction. In this part we can use some software to make our data readable by computer. We use SPM8 program to produce an image file with a header which includes all the data related to that image. In fact the software does Fourier Transform on raw data. From now on we are able to see slices of brain using SPM8 review or any related programs. The details of preprocessing steps can be found in [39].

**Slice-timing Correction:** In functional MRI timing has an important rule. Generally, datasets are measured using an iterative two dimensional method which results in temporal offsets between slices of scans. Slice timing solves this problem.

**Realignment:** Main goal is to align a set of functional MRI images to a selected one of the images in a way that all images are in the standard coordinates. Because of movements of subjects during scanning session, functional images from time-series are not in same position. By realignment, it is provided that the source of the signal in any voxel is the same point within any of scans.

**Co-registration:** In this step we want to overlap functional and anatomical images over each other in order to be able to match activation regions to their real location on anatomical positions.

**Normalization:** Every person has different brain shape than others. If there is a single subject to be analyzed, there is no need to do Normalization. However in a group analysis, it is necessary to bring all brains in fMRI images to the same size and orientation. In this step, the images are warped to make homologous regions from different subjects close to each other. As it is obvious, there could not be exact overlap between function and structure images. Also, there is difference among anatomy of subjects.

**Smoothing:** This method mathematically means, convolving data with a Gaussian filter like Gaussian Kernel in order to reduce noise in the images and increase overlap of activation between subjects. Smoothing operation does not change the size of the number of pixels, however results in blurring in the images. This step is necessary because of the advantages listed below:

- (i) Increase in SNR: as the signal in a voxel from a smoothed image, influenced from both voxel itself and neighboring voxels, random noise is decreased.
- (ii) Increase in inter-subject overlap: there will be an increase between subjects in case of averaging signal in larger area.
- (iii) Increase in validity of analysis

Figure 3.1. illustrates reoriented anatomical brain image. We need this image to be able to specify our regions exactly on the brain.

Figure 3.2. gives the way to reach a realigned image. Complete description of realignment is given above.

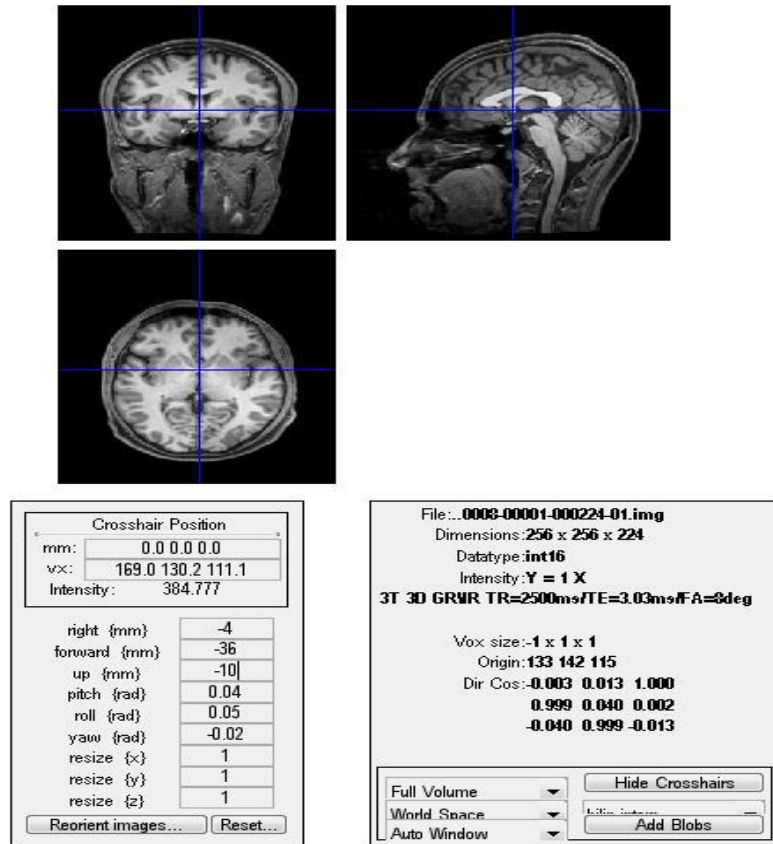


Figure 3.2. This Figure shows the reoriented anatomical images

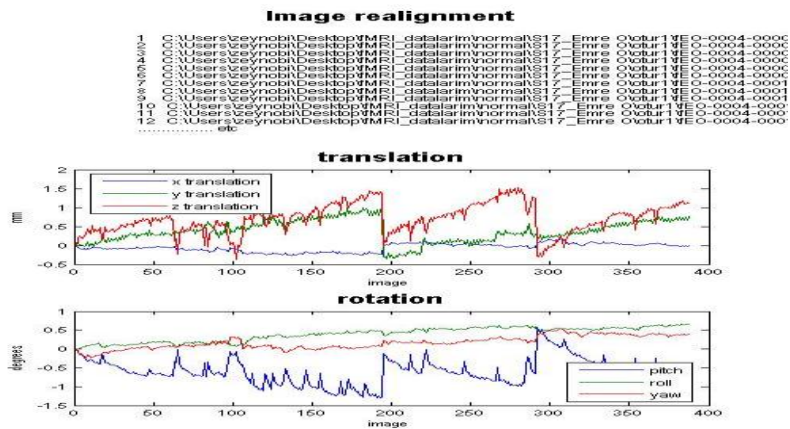


Figure3.3. This step which is done using SPM8 program, shows realignment step in image file.

**3.2.1.2 Design Matrix and Contrasts**

Design matrix is a matrix which includes preprocessed images, all regressors which in this case are stimulations and 6 parameters of head motions in this experiment. An example of applying design matrix is given in figure 3.3.

As discussed above we put stimulations in data as regressors and then high-pass filtered the data to remove unwanted parts. We consider 4 stimulations as below:

- Congruency Positive
- Congruency Negative
- Incongruency Positive
- Incongruency Negative

We produce a t-test design matrix for regressors above as we know the onsets for stimulations of data. We created a factorial design with two main effects and an interaction which is said to consider 3 different situation as: (i) Congruency (ii) Valance (iii) Congruency\*Valance

Table 3.3 below shows how to combine 4 stimulations to design 3 main stimuli.

Table.3.3. Stimulations

	CONGRUENCY	VALANCE	CONGRUENCY*VALANCE
Congruency Positive	1	1	1
Congruency Negative	1	-1	-1
Incongruency Positive	-1	1	-1
Incongruency Negative	-1	-1	1

The table above shows what is the exact meaning of Cong., Val and Cong\*Val.

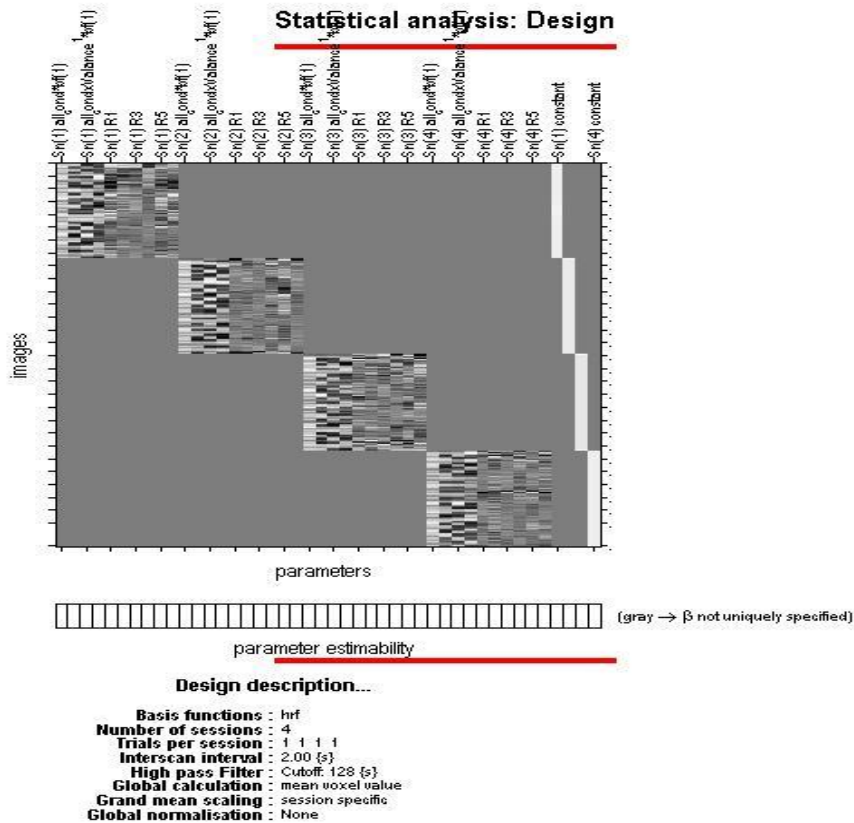


Figure 3.4. Shows applying design matrix and contrasts to data considering stimulation of congruency.

Figure 3.3. shows the image after applying design matrix. Description of design is seen under the image. Figure 3.4 gives active parts of brain after applying design matrix which are easily visible in figure and we can now create ROI's using this informations.

### 3.2.1.3 First Level General Linear Model

In GLM or statistical analysis we consider three steps:

- 1) Specifying a design matrix and filtering.
- 2) Estimating GLM parameters using Bayesian method.
- 3) Integrating results using contrast vectors.

Design matrix is our experimental design. This matrix consists of rows and columns which indicates scans and effect or explanatory variables respectively. Explanatory variables here are stimulus functions. Responses in our data are event-related designed. Mathematically, we model our responses by a box function to indicate the onsets of an event with a set of basic functions. These basic functions, model the

haemodynamic response of brain with inputs. Basic functions can be used to plot estimated responses to events [40, 41]. We can also use Bayesian functions to plot estimated response. First level GLM analysis is also used to implement a within subject analysis. This is an iterative method which we applied to 4 sessions of every single subject in our data. Note that, applying contrast to images from any subject gives the measure of brain response as we consider contrasts from our hypothesis and applied them to the images and now all that images are affected by contrast matrix. In another words, by GLM analysis we try to model our conditions and regressors into our images and apply a high-pass filter to that image. The reason of using high-pass filter here is to reduce the noise. Note that, signals with low frequencies will be emitted after filtering.

As discussed in previous part we applied our 4 different kinds of stimulations to data as regressors. Our main goal from entering these stimulations to images is to observe the influence of Congruency, Valance and Congruency\*Valance on connections between different ROI's.

Until now we have done preprocessing steps as slice-timing, realignment, smoothing. We also put our inputs which are stimulations as contrast matrix into data [42, 43]. Next step is creating ROI's from preprocessed data.

### 3.2.1.4 ROI Creation

After entering stimulations as contrasts to data, ROI's are created . In both methods ROI's will be used. There is a program named MARSBAR which creates ROI with a great details and we used this program. Here, it's so important to use MNI Atlas which is a brain atlas that maps brain parts. Considering active parts of brain and neurological information, we found 10 ROI's in brain which is significantly active ( $p < 0.05$ ). Before using marsbar program, we noted the coordination for each of ROI's and then created these regions considering three stimulations of Congruency, Valance and Congruency\*Valance.

Table 3.4. Name and MNI coordinates of ROI's for each condition.

<i>Congruency</i>	<i>Valance</i>	<i>Congruency*Valance</i>
<b>DorsalACC</b> (16,-2,34)	<b>DorsalACC</b> (-16,28,28)	<b>VentralACC</b> (-4,40,10)
<b>LeftInsula</b> (-44,0,6)	<b>VetralACC</b> (-4,40,-8)	<b>RostralACC</b> (-14,38,18)
	<b>LeftInsula</b> (-44,-2,-4)	
	<b>RightInsula</b> (44,8,-6)	
	<b>LeftDLPFC</b> (-22,22,46)	
	<b>RightDLPFC</b> (26,26,48)	

ACC is Anterior Cingulate Cortex and DLPFC is Dorsolateral Prefrontal Cortex.

As shown in table 3.4, now we have regions with coordinates of their center point. We choose the radius of 9 mm. and consider a sphere form for ROI's to be created.

Using marsbar and entering coordinates of ROI's and their radius we obtain what we were looking for.

Figures 3.5.a and 3.5.b are exmples of ROI creation.

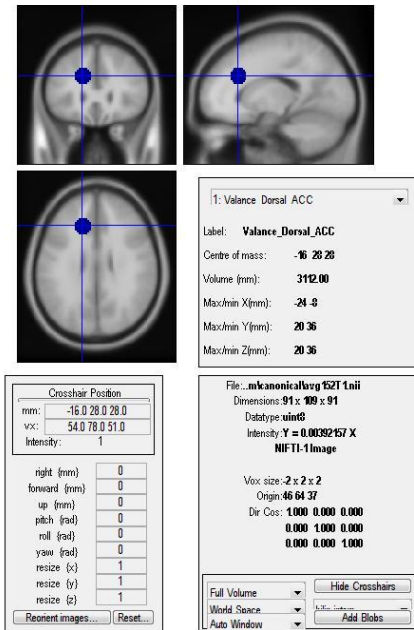


Figure 3.5.a. ROI DorsalACC when stimuli is valence

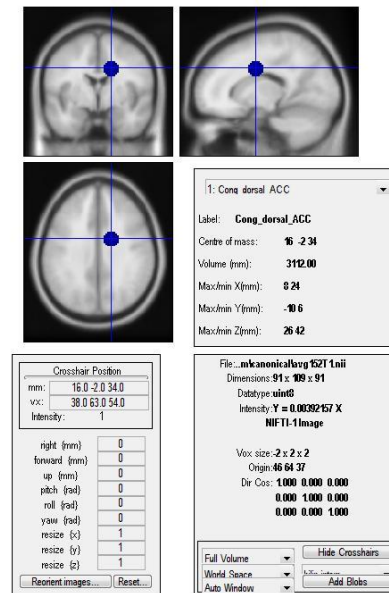


Figure 3.5.b. ROI DorsalACC when stimuli is congruency

Figure 3.5.a,b. shows two sample ROI's obtained as the results of group analysis. Figure 3.5.a shows the region of interest considering the effect of Valance in DorsalACC with center coordination of (-16,28,28) and figure 3.5.b. in the same way shows DorsalACC with center point of (16,-2,34) considering the effect of Congruency.

As we created these 10 ROI's from group analysis, we can use any of them instead of any of the subjects.

All the steps before applying methods of DCM and PPI are completed and from this step we can use data to analyze effective connectivity by applying two methods of DCM and PPI.

### 3.3 Dynamic Causal Modeling (DCM)

The main idea of DCM is to observe some changes in brain regions activity as a result of connectivity differences. By applying some changes in brain using inputs, changes in brain would be measured as responses of brain so that this enables us to give an idea about how states of brain could change. For example a bilinear approximation gives a reparametrization which could be considered as Effective Connectivity. This bilinear connectivity could be changed by model selection. This model selection will be done using Bayesian method.

The major difference between DCM and other methods like Structural Equation Modeling and Multivariate Autoregressivemethod is, in DCM the input enters as a known parameter not stochastically. Doing this, we can consider DCM as conventional method to analyze neuroimage time-series. This is because we enter causal parameters as known fixed variables.

Our generated model for DCM is described completely using figure 3.6.

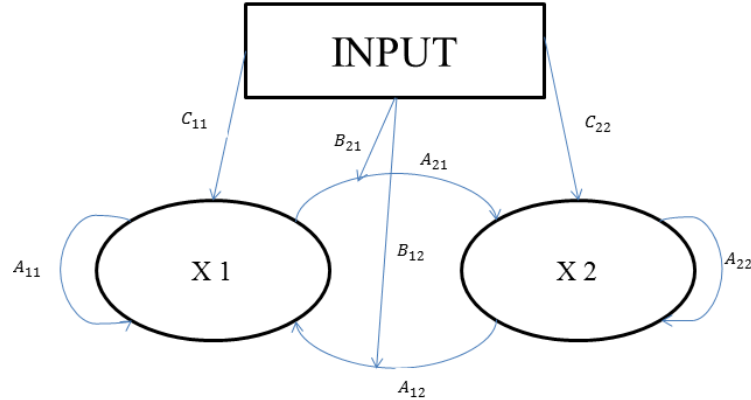


Figure 3.6. Generated model for DCM for this thesis work.

In figure 3.6. two inputs are shown by X1 and X2. If these inputs are considered to affect just ROI's, they are indicated by C and if they affect connection between ROI's they indicated by B. In the figure, intrinsic connectivities are shown by A matrices. For this special case input X1 affects ROI1 and input X2 affects ROI2. There is reciprocal connectivity between ROI1 and ROI2. Modulatory stimulation or B matrix only effects connection from ROI2 toward ROI1. In order to show all thses matrices which are the parameters of DCM we have:  $C = \begin{bmatrix} C_1 \\ C_2 \end{bmatrix}$   $B = \begin{bmatrix} 0 & B_{12} \\ B_{21} & 0 \end{bmatrix}$  and  $A = \begin{bmatrix} A_{11} & A_{12} \\ A_{21} & A_{22} \end{bmatrix}$ .

In this step, the theory that applied to data is described and then some sample models of our experiment will be given. Examples of all other models are included in Appendix C. Best models are included in this chapter.

The main purpose here is to find any changes in BOLD response . In the case of DCM, the terms of *priors* and *model likelihood* are very important. Bayes rule combines priors and likelihood which will result in formation of posterior distribution. To compute amount of posterior distribution, we use Expectation-Maximisation method iteratively. Second step however includes finding model evidence. Consider the term model evidence as choosing from accuracy and complexity. I will describe it later. Finally our best model will be choosen between models with highest evidence [44]. To make comparison between models, we use Bayes factors and model evidence ratios [39].

As it mentioned in chapter 2, DCM includes a bilinear model for neuronal responses and uses a Haemodynamic Balloon Model for haemodynamic responses[40]. Consider equation 2.3. Note that,  $t$  here shows continuity in time. We say this model is a bilinear model as  $\frac{dx}{dt}$  depends on both  $x(t)$  and  $u(t)$ . Term  $x(t)$  is the neuronal activity of brain which is a  $L \times I$  vector.  $L$  denotes regions and  $u(t)$  is also a vector which includes inputs of  $u_j(t)$  with  $j=1, \dots, M$ .

The term *effective connectivity* is known by three main matrices named A, B and C. Matrix A indicates intrinsic connectivity that shows which regions are connected. This matrix also shows whether these regions are connected in one or two directions, unidirectional or bidirectional. Matrix B shows which intrinsic connections could differ by applying which inputs or stimulations. Matrix C however, shows which stimulations are connected to which regions. These three matrices give an information of our model sturcture. We can define a connectivity vector as equation 3.1

$$\theta^n = \begin{bmatrix} \text{vec}(A) \\ \text{vec}(B) \\ \text{vec}(C) \end{bmatrix} = [A_{11}, A_{12}, A_{21}, A_{22}, B_{12}, B_{21}, C_1, C_2]^T \quad (\text{Eq.3.1.})$$

In equation 3.1  $\text{vec}(A)$ ,  $\text{vec}(B)$  and  $\text{vec}(C)$  are vectors. By changing the variables in matrices named above, model structure could change. Available connections and inputs will have a nonzero amount in matrices and only these nonzero variables will appear in connectivity vector. Number of entries for  $\theta^n$

will be the sum of all entries for matrices A, B and C.

Another important issue is parameter values  $\Theta$  as shown in equation 3.2 and includes neuronal and haemodynamic response parameters.

$$\Theta = \begin{bmatrix} \Theta^n \\ \Theta^h \end{bmatrix} \quad (\text{Eq.3.2.})$$

Whenever the parameters are determined, all parameters to estimate the DCM model are found. External stimulations or  $u$ , are known as we entered them in data and these are Congruency, Valance and CongValance. Estimating neuronal states results in predicting a model [41, 45].

For a data of  $n$  scans,  $N_s$ , the  $h(\Theta, u)$  will be a  $LN_s \times 1$  vector to cover all points in ROI's. Equation 3.3 gives observed data.

$$y = h(\Theta, u) + X\beta + e \quad (\text{Eq.3.3.})$$

In equation 3.3 above,  $e$  is also an  $LN_s \times 1$  vector and is error term. It has a zero mean and covariance of  $C_e$  which includes an  $L \times L$  matrix of error variance for any of ROI's.  $X$  in our condition, is the effect of resting states and it is in somehow irrelevant to our model.

Figure 3.7 is an example of our designed model. Consider *Congruency* as input. From neurological acknowledgment, we estimate there must be an intrinsic bidirectional connection between DorsalACC and LeftInsula regions. This means that there is an A matrix with nonzero parameters. We prefer to test the effect of *Congruency* on both ROI's and connections between ROI's.

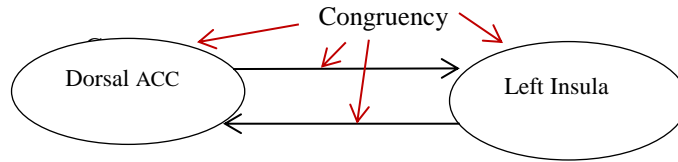


Figure 3.7. Example of ROI's and stimuli cong.

B and C matrices have nonzero parameters and will appear in model state equations. Consider this model as our first model. If we don't want to test the effects of congruency on for example one of ROI's or connections, we will put zero in its related matrix. Relatively, this will affect our neurodynamic equation and connectivity vector changes and the result will be changes in  $p$ -values vector and as a result we will observe differences in result of observed data  $y$ .

We know that priors that considered in two matrices A and B are different than priors and likelihood in matrix C [40]. The priors for matrix C are called "shrinkage-priors". In this case, prior mean is zero and posterior estimates shrink towards zero mean amount. Using equations 3.4 and 3.5, we can calculate priors of matrices A, B and C.

$$p(A_{ik}) = N(0, v_a) \text{ and } p(B_{ik}^j) = N(0, v_b) \quad (\text{Eq.3.4.})$$

$$p(C_{im}) = N(0, v_c) \quad (\text{Eq.3.5.})$$

In equations 3.4 and 3.5 above  $v_a$ ,  $v_b$  and  $v_c$  are vectors. We can use equations 3.6 and 3.7 to calculate initial prior.

$$p(\Theta^c) = N(\Theta_p^c, C_p^c) \quad (\text{Eq.3.6})$$

$$\Theta_p^c = [0_{N\Theta}]^T \text{ and } C_p^c = \text{diag} [v_a 1N_a, v_b 1N_b, v_c 1N_c] \quad (\text{Eq.3.7.})$$

$\Theta_p^c$  indicates priors and  $C_p^c$  shows covariances. For haemodynamic parameters in case of priors mean and covariance matrix which are showed by  $\Theta_p^h$  and  $C_p^h$ , we have to choose the parameters in a meaningful physiological ranges [43]. Finally, we are able to calculate total prior and covariance of our DCM model using equation 3.8 below:

$$\Theta_p = \begin{bmatrix} \Theta_p^c \\ \Theta_p^h \end{bmatrix} \text{ and } C_p = \begin{bmatrix} C_p^c & 0 \\ 0 & C_p^h \end{bmatrix} \quad (\text{Eq.3.8.})$$

From this moment, one is able to calculate the priors and likelihood respectively for any model named  $m$  using equations 3.9. and 3.10 below:

$$p(\Theta|m) = N(\Theta_p, C_p) \text{ and } p(y|\Theta, m) = N(h(\Theta, u) + X\beta + C_e) \quad (\text{Eq.3.9.})$$

$N(\Theta_p, C_p)$  is normal distribution with mean  $\Theta_p$  and covariance matrix  $C_p$ .

In case of expanding equation 3.9, result will be equation 3.10. as below:

$$p(\Theta|m) = (2\pi)^{-p/2} |C_p|^{-1/2} \exp\left(-\frac{1}{2} e(\Theta)^T C_p^{-1} e(\Theta)\right) \quad (\text{Eq.3.10})$$

and

$$p(y|\Theta, m) = (2\pi)^{-N_s/2} |C_e|^{-1/2} \exp\left(-\frac{1}{2} r(\Theta)^T C_e^{-1} r(\Theta)\right)$$

In equation 3.10,  $e(\Theta) = \Theta - \Theta_p$  term, gives parameter errors and  $r(\Theta) = y - h(\Theta, u) - X\beta$ , gives the prediction errors.

The main aim of calculating prior and likelihood is to find posterior distribution using Bayes formula as equation 3.11 below:

$$p(\Theta|y, m) = \frac{p(y|\Theta, m) p(\Theta|m)}{p(y|m)} \quad (\text{Eq.3.11.})$$

As equation 3.11 is not solvable in normal condition, taking logarithm of posterior distribution of equation 3.11 will give *log-posterior* as equation 3.12.

$$\mathbf{log}(\Theta|y, m) = \mathbf{log}(y|\Theta, m) + \mathbf{log}(\Theta|m) + \mathbf{log}(p(y|m)) \quad (\text{Eq.3.12.})$$

In case of fMRI data time-series which has large amount of data points, it would be logical to use Gaussian to approximate data proportion to regions [46]. So, using Gauss-Newton optimization method, we will find Maximum Posterior solution to make posterior probability maximum. Gaussian optimization will result in estimation of mean and covariance matrix. After estimating, the mean and covariance matrices could be calculated using Expectation-Maximization method [34]. There are two separate steps in EM method. First step is Expectation step and includes using Gaussian method to update posterior mean and covariance which we show them by  $\theta$  and  $\Sigma$ . Maximization step however, will update covariance matrix of noise. This method will iterate until finding proper posterior probability.

In this step we have the model  $m$ , but we are not sure if it is the best proper model or not. May be another hypothesis and its related model be better. So the question is which model best fits our parameters or which model is the best between different models. A mean to compare different models is called Model Evidence. Consider equations 3.13 to 3.15:

$$p(y|m) = \int p(y|\theta, m) p(\theta|m) d\theta \rightarrow \log p(y|m)_L = Accuracy(m) - Complexity(m) \quad (\text{Eq.3.13.})$$

$$Accuracy(m) = -1/2 \log |C_e| - 1/2 r(\theta_{MP})^T C_e^{-1} r(\theta_{MP}) \quad (\text{Eq.3.14.})$$

$$Complexity(m) = 1/2 \log |C_p| - 1/2 \log |\Sigma_{MP}| + 1/2 e(\theta_{MP})^T C_p^{-1} r(\theta_{MP}) \quad (\text{Eq.3.15.})$$

Here, just consider  $r(\theta_{MP})$  is observed error. In equation 3.13  $\log p(y|m)_L$  term gives the log-posterior probability considers the most accurate parameters for models.

Finally, proper models can be decided. The most important of all we discussed is finding the best model between all models. *Bayes factors* will give us the best model between all proper models. It will be so easy to calculate equation 3.16. below:

$$B_{ij} = \frac{p(y|m=i)}{p(y|m=j)} \quad (\text{Eq.3.16.})$$

In equation 3.16, if  $B_{ij} > 1$ , it means data is more fitted on model  $i$  and if  $B_{ij} < 1$ , it means data best fit model  $j$ .

### 3.4 Psychophysiological Interactions (PPI)

Between different methods for brain imaging, fMRI has different characteristics as it does filter neuronal activity by using haemodynamic responses function. In another word, neuronal response can be approximated by haemodynamic responses. In analyzing fMRI data, main challenge is to understand the time-series of data because these time-series are convolved neuronal and haemodynamic responses [44]. One way to analyze data is deconvolution of given BOLD signal with an assumed haemodynamic response [44].

As mentioned, interactions of brain happen in neuronal level but what is seen from fMRI data is in haemodynamic response form which is the result of that neuronal level response.

In this method main aim is to define suitable regressors for haemodynamic responses to enable modeling neuronal influences.

It would be possible to model haemodynamic response to neuronal activity using convolution with a finite impulse responses as equation 3.17 below:

$$y_t = \sum_{\tau} h_{\tau} x_{t-\tau} \quad (\text{Eq.3.17.})$$

Here,  $y_t$  is BOLD signal and  $h_{\tau}$  is haemodynamic response and  $x_{t-\tau}$  is neuronal response signal.

The equation 3.17 could be written in the matrix format as equation 3.18 below:

$$y = Hx \quad (\text{Eq.3.18.})$$

$H$  in Eq.3.18 is haemodynamic response frequency (HRF) [44]. Taking the product of BOLD signal from two regions A and B will not give us the proper signal for interaction because this signal is not convolved with HRF. If we want to say mathematically, we will introduce two equations 3.19 and 3.20 below:

$$y_A y_B = (Hx_A)(Hx_B) \neq H(x_A x_B) \quad (\text{Eq.3.19.})$$

$$HPy_A = (HP)(Hx_A) \neq H(Px_A) \quad (\text{Eq.3.20.})$$

BOLD signal ( $y$ ) is used to extract physiological-neuronal signal ( $x$ ). In order to do this, first of all we must expand  $x$  as a Fourier series in terms of temporal basis as equation 3.21 below:

$$x_A = X\beta \quad (\text{Eq.3.21.})$$

in which,  $\beta$  are variables that control the expression of various frequency parameters of  $x$ . We must consider noise here, also. We take a linear model with MLE (maximum likelihood estimations) as equations 3.22 and 3.23 below:

$$y_A = HX\beta + \varepsilon \quad (\text{Eq.3.22.})$$

$$\beta_{ML} = X^T H^T \Sigma^{-1} HX)^{-1} X^T H^T \Sigma^{-1} y_A \quad (\text{Eq.3.23.})$$

In these equations, consider  $\varepsilon \sim N(0, \sigma^2 \Sigma)$  a Gaussian and  $\sigma^2$  is error variance and  $\Sigma$  is the error correlation matrix.

Estimating  $\beta_{ML}$  extracts neuronal activity signal for any BOLD vector. Then we can calculate the required interaction terms using equation 3.20.

All discussed above is very inefficient in our case if we just consider coefficients in  $\beta$ , which is controlling high frequencies, where HRF diminishes high-frequency. We must use regular estimation. This is done using remaining high-frequency variables from main set. This would give us *least-squares maximum likelihood deconvolution*.

But, Bayesian estimation could be better alternative as it conforms neuronal signals to priors on its frequency. The advantage of using Bayesian formulation is its flexibility in specifying priors [32]. Mathematically saying, equation 3.24 would be given:

$$\beta_{MAP} = (X^T H^T \Sigma^{-1} HX + \sigma^2 C_\beta^{-1})^{-1} X^T H^T \Sigma^{-1} y_A \quad (\text{Eq.3.24.})$$

In equation 3.24, the term  $\beta_{MAP}$  is *maximum a posteriori* and  $C_\beta^{-1}$  is prior precision of  $\beta$ .

Considering all diagonal parameters of  $C_\beta$  be infinite (high-frequency),  $C_\beta^{-1}$  will be restricted to low-frequencies. Doing this means that, in equation 3.24 we get least-square deconvolution without having any high-frequency in  $x$ . Obviously for any parameter, if  $C_\beta^{-1}$  is infinite, it will give us a zero value and there won't be any change by entering  $X$  parameters into formulation [46].

In case of PPI, production of neuronal response and psychological variables will give psychophysiological interaction term.

$$y = (T_A - T_B) \beta_1 + (S_1 - S_2) \beta_2 + (T_A - T_B)(S_1 - S_2) \beta_3 + e \quad (\text{Eq.3.25})$$

In equation 3.25, term  $(T_A - T_B) \beta_1$  gives main effect of task. Term  $(S_1 - S_2) \beta_2$  gives main effect of stimulations and  $(T_A - T_B)(S_1 - S_2) \beta_3$  is the interaction term.  $e$  is error term.  $y$  gives the changes in slope of regression due to both psychological and physiological interaction terms and is the psychophysiological interaction term.

## CHAPTER 4

### Experimental Results

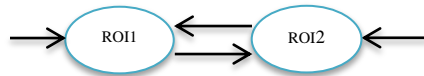
#### 4.1 Dynamic Causal Modeling Results

We apply DCM on our experiment. We considered ten separate basic models for any couple of ROI's which are explained in details. In this models, we tested the effect of *valance*, *Congruency* and *Congruency\*Valance* on selected pairs of ROI's and connections between regions. In the first step, we considered any of models without the effect of any stimuli. This step gives us intrinsic connectivity between ROI's and then considering any stimulation on any part of model will give us differences which appear by applying any of three stimulations above. ROI's and the related stimuli are the significant results of group analysis. For Valance, we restricted the couples to most probably connected regions according to the related cognitive studies. Six situations are considered. ROI pairs and stimulation related to any pairs are given below:

1. *Congruency* in between *DorsalACC* and *LeftInsula*
2. *Congruency\*Valance* in between *RostralACC* and *VentralACC*
3. *Valance* in between *DorsalACC* and *LeftDLPFC*
4. *Valance* in between *DorsalACC* and *RightDLPFC*
5. *Valance* in between *VentralACC* and *RightInsula*
6. *Valance* in between *DorsalACC* and *VentralACC*

For any stimuli and couple of ROI's as mentioned, we tested ten models. Among these models the only difference is the place of entering stimulus. These tested models are shown in graphs as follows:

*Model 1.*



In this model, we considered effect of *valance* on none of connections. This model will gives us only intrinsic connectivities. This model considered to show the intrinsic connectivities between ROI's for 6 situations discussed above.

- Intrinsic connectivity between DorsalACC and LeftInsula:

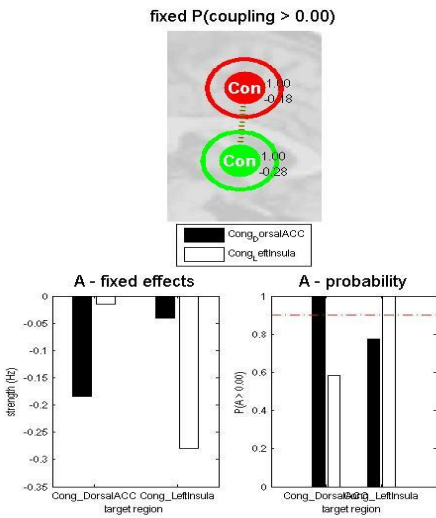


Figure 4.1.a

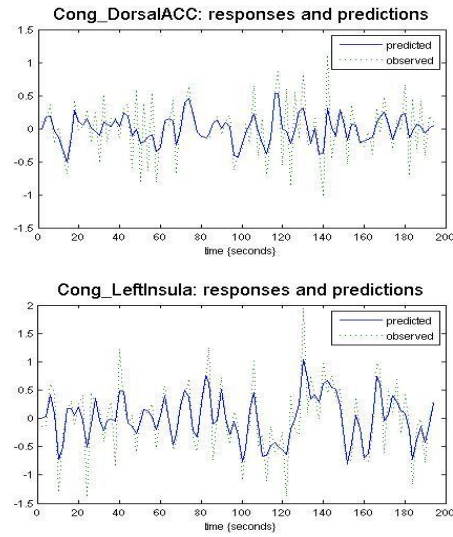


Figure 4.1.b

In figure 4.1.a it is seen that intrinsic connectivity between DorsalACC and LeftInsula is weak in its normal situation without applying any stimulation. In the figure 4.1.a only A matrix is available as  $A = \begin{bmatrix} a_{11} & a_{12} \\ a_{21} & a_{22} \end{bmatrix} = \begin{bmatrix} -0.18 & -0.02 \\ -0.05 & -0.28 \end{bmatrix}$ . Also, there is a negative activity on both regions and this means there is a negative effect of ROI's over each other. Probability of connection is also weak. Figure 4.1.b gives information on predicted and observed responses of ROI's DorsalACC and LeftInsula to the inputs of matrix A. Here, probability of connection from LeftInsula toward DorsalACC is stronger than the connection from DorsalACC to LeftInsula. Figure 4.1.b illustrates predicted and observed responses of regions to signals over each other. Matrix A is based on power of signal and because of that results for all three matrices are calculated in hertz.

- Intrinsic Connectivity between RostralACC and VentralACC:

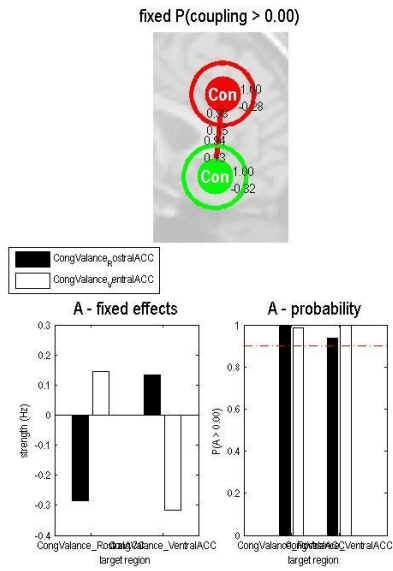


Figure 4.2.a

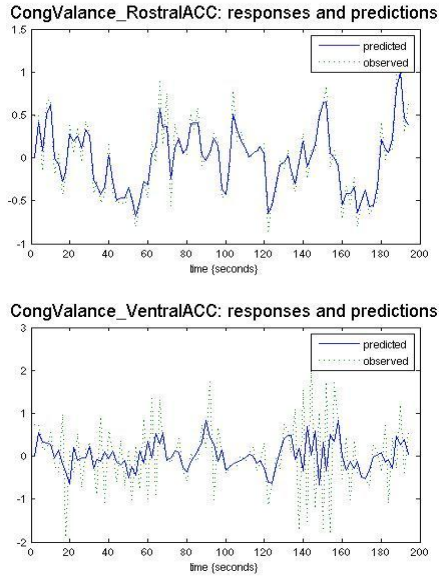


Figure 4.2.b

In figure 4.2.a above, we can see strong intrinsic connection between RostralACC and VentralACC without applying any stimuli. Here almost the probability of connection from RostralACC to VentralACC is 1. In figure 4.2.b we see differences between observed and predicted signals resulted from response of VentralACC. This could be from biological effects of other regions on VentralACC. A matrix for this condition is  $A = \begin{bmatrix} a_{11} & a_{12} \\ a_{21} & a_{22} \end{bmatrix} = \begin{bmatrix} -0.3 & 0.18 \\ 0.15 & -0.31 \end{bmatrix}$ .

- Intrinsic Connectivity between DorsalACC and LeftDLPFC:

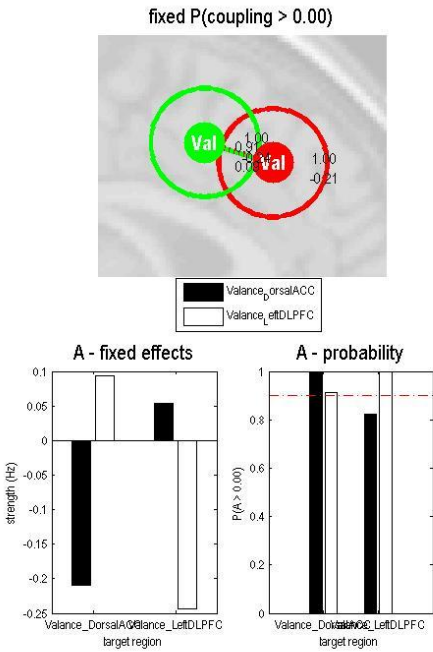


Figure 4.3.a

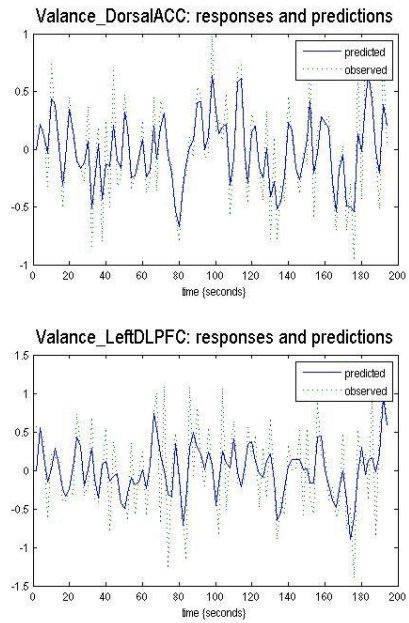


Figure 4.3.b

From figure 4.3.a, it's obvious that there is an strong intrinsic connectivity from DorsalACC toward LeftDLPFC. Observed and predicted response signals as shown in figure 4.3.b are similar and there is not so much differences between them. A matrix for this condition is  $A = \begin{bmatrix} a_{11} & a_{12} \\ a_{21} & a_{22} \end{bmatrix} = \begin{bmatrix} -0.2 & 0.1 \\ 0.06 & -0.24 \end{bmatrix}$ .

- Intrinsic Connectivity between DorsalACC and RightDLPFC:

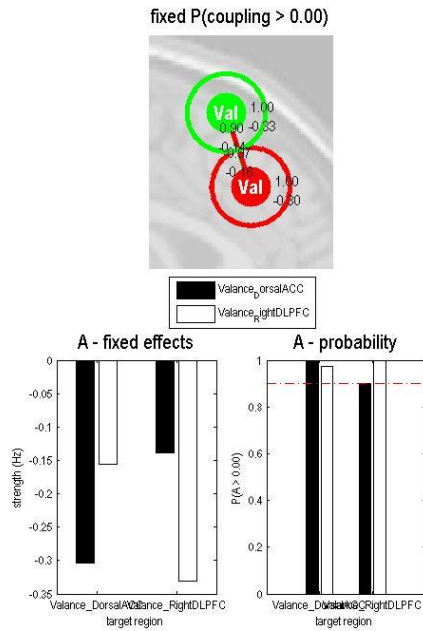


Figure 4.4.a

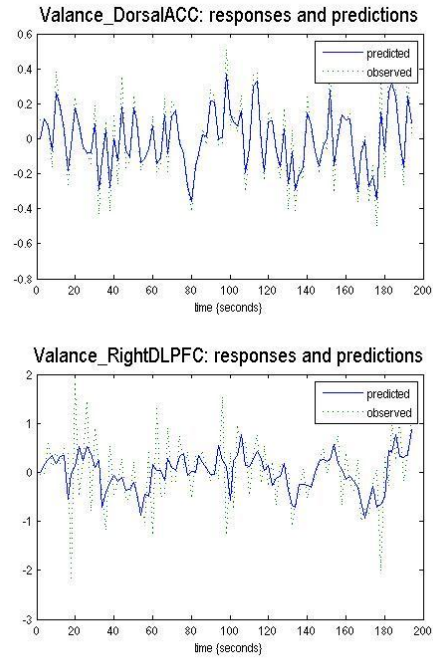


Figure 4.4.b

In figure 4.4.a, we can see an interesting result. These two regions have a negative effect on each other and this means that they reduce activity of each other. The intrinsic connection between these two ROI is strong in any direction. Here again, we see differences between observed and predicted response signals in RightDLPFC. A matrix for this condition is  $A = \begin{bmatrix} a_{11} & a_{12} \\ a_{21} & a_{22} \end{bmatrix} = \begin{bmatrix} -0.3 & -0.15 \\ -0.13 & -0.33 \end{bmatrix}$ .

- Intrinsic Connectivity between VentralACC and RightInsula:

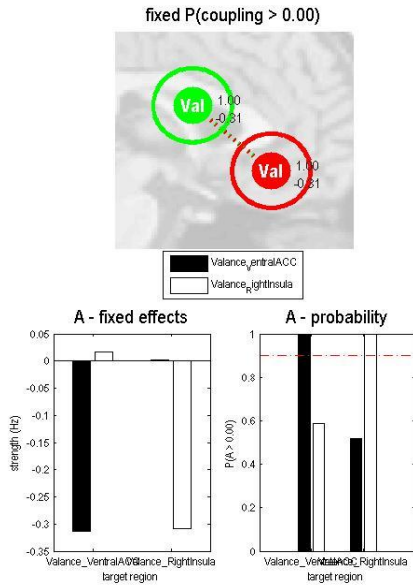


Figure 4.5.a

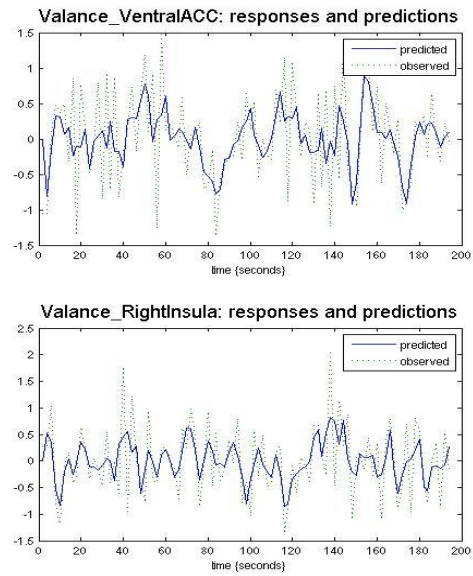


Figure 4.5.b

From figure 4.5.a, we can see that there is almost no intrinsic connection between VentralACC and RightInsula. Figure 4.5.b also gives us a same result as predicted and observed response signals in both of regions are different which shows the effect of other regions on these two ROI's. A matrix for this condition is

$$A = \begin{bmatrix} a_{11} & a_{12} \\ a_{21} & a_{22} \end{bmatrix} = \begin{bmatrix} -0.3 & 0.01 \\ 0 & -0.3 \end{bmatrix}$$

- Intrinsic Connectivity between DorsalACC and VentralACC:

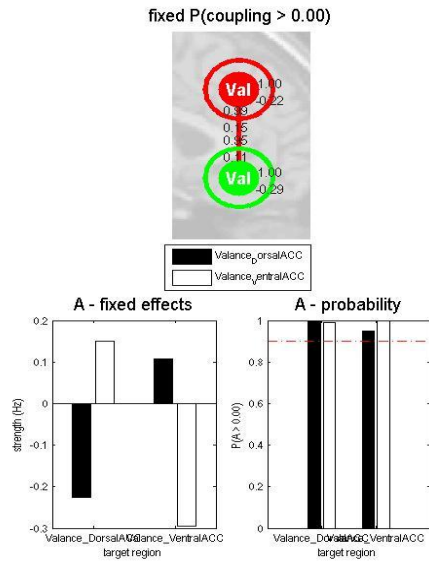


Figure 4.6.a

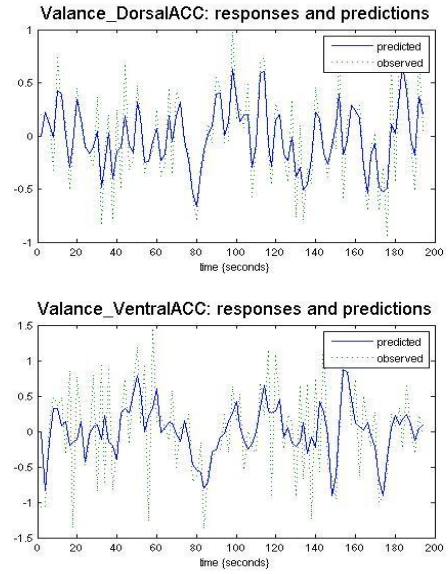


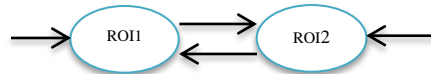
Figure 4.6.b

From figure 4.6.a, it's obvious there is strong connection between DorsalACC and VentralACC again in both directions. Probability of these connections is almost 1. Because of effect of other regions on VentralACC, we observe differences in observed and predicted response signals. A matrix for this condition is  $A = \begin{bmatrix} a_{11} & a_{12} \\ a_{21} & a_{22} \end{bmatrix} = \begin{bmatrix} -0.2 & 0.18 \\ 0.15 & -0.3 \end{bmatrix}$ .

In this step, we have some information about intrinsic connections between ROI's without applying any stimulations. After this step, I tested 9 other models by considering different stimulations in different affecting parts.

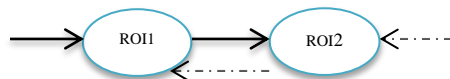
It would be useful to give my models and shows where the stimulations show their effect.

*Model 2:*



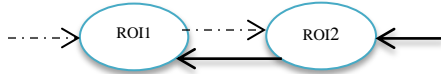
This model shows from which part we considered applying stimulation. In this model we have direct effect of stimuli on both of ROI's and in both connections between ROI's.

*Model 3:*



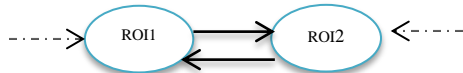
This model shows the applying of stimuli directly to ROI1 and connection from ROI1 to ROI2. Dashed lines shows that there is an intrinsic connectivity but no stimulation is affecting these connections.

*Model 4.:*



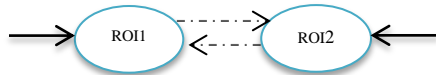
In this model we applied stimulations to ROI2 and connection from ROI2 to ROI1.

*Model 5:*



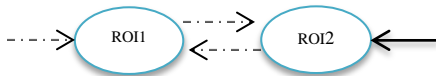
In model5 we considered stimuli only effects the connections between two ROI's. Here, we don't have any stimuli effecting regions of interest directly.

*Model 6:*



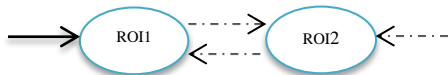
This model is just considered effects of stimulations on regions directly without considering this effect on connections between regions.

*Model 7:*



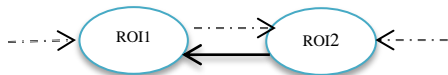
Another hypothesis could be considering effect of stimulations only on ROI2 without considering stimulation on any other region.

*Model 8:*



In our 8<sup>th</sup> model, we tried to observe effect of stimuli only on ROI1 without applying to any other region.

*Model 9:*



We thought that, it would be useful if we analyze a situation in which stimulation only affects connection between ROI2 to ROI1 without applying to other parts.

*Model 10:*

As the last model we considered that stimulation only affects connection from ROI1 to ROI2.

We considered all ten models for my 6 discussed situations. For example we considered stimulation to be Congruency and ROI1 and ROI2 be DorsalACC and LeftInsula, respectively. All the results will be showed in the rest of the work.

Results for remaining nine models of every six condition are in APPENDIX C.

Using model selection method, best model for each condition is selected and are depicted as figures 4.7 – 4.12 below.

For Congruency and considering two ROI's of DorsalACC and LeftInsula the best model is model2.

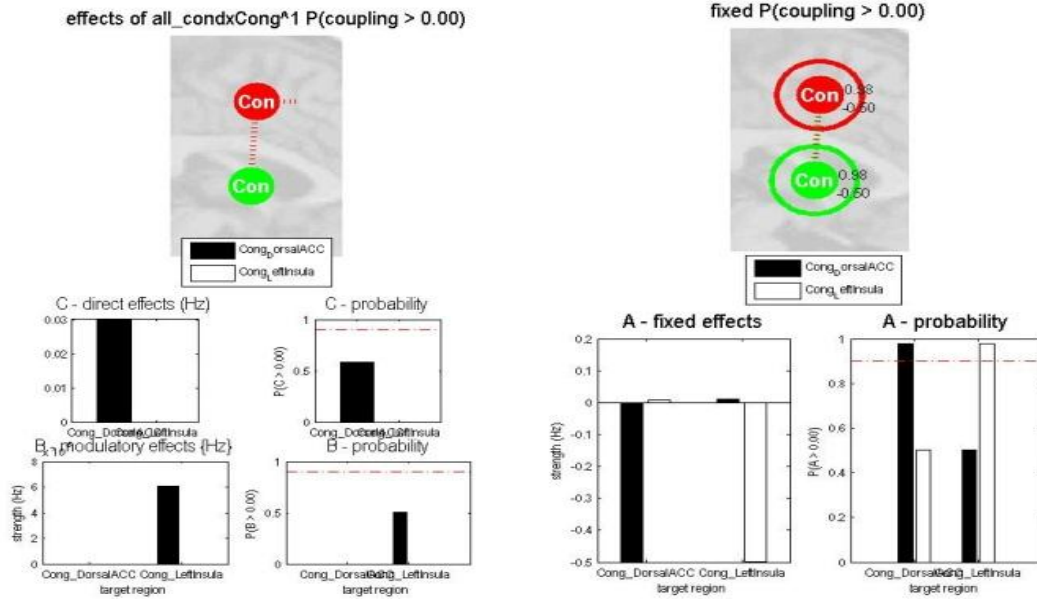


Figure 4.7. Best model of condition congruency: DorsalACC and LeftInsula

In this model, applying stimulation of congruency reduces almost intrinsic connectivity between two named regions of interest. Direct and modulatory effects of stimulation on regions and connection between regions are almost small. C matrix is in the form of  $C = \begin{bmatrix} C_1 \\ C_2 \end{bmatrix} = \begin{bmatrix} 0.03 \\ 0 \end{bmatrix}$  and for B matrix

its like  $B = \begin{bmatrix} B_{12} \\ B_{21} \end{bmatrix} = \begin{bmatrix} 0 \\ 6 * 10^{-8} \end{bmatrix}$  and A matrix is  $A = \begin{bmatrix} -0.5 & 0 \\ 0 & -0.5 \end{bmatrix}$ .

In case of congruency\*valance considering two regions of RostralACC and VentralACC the best model is model7.

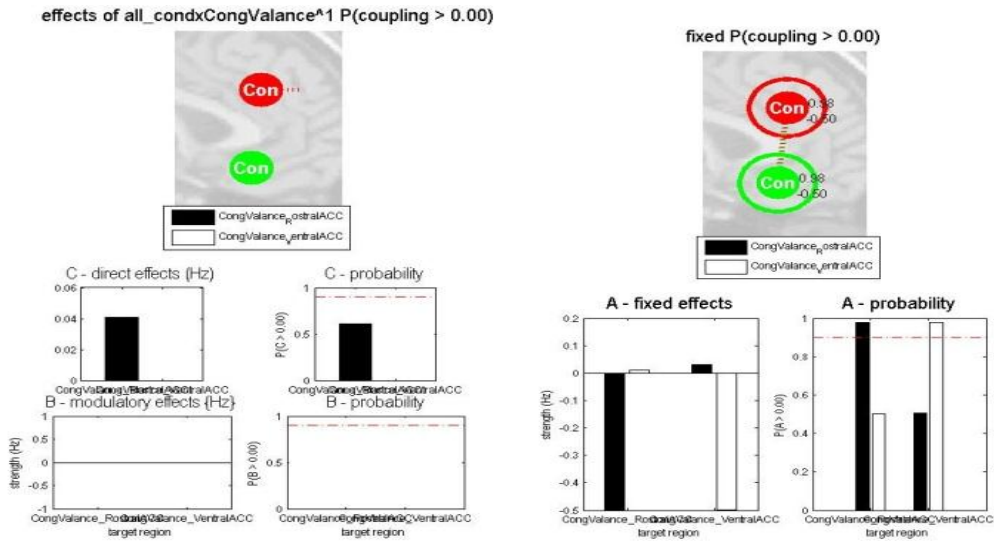


Figure 4.8. Best Model of condition cong\*val: RostralACC and VentralACC

In this selected model effect of stimuli, reduced connectivity between two regions. Here, this stimulation results in an stronger intrinsic connectivity, though.

For stimuli valance and regions of DorsalACC and LeftDLPFC, the best model is model7. C matrix is in the form of  $C = \begin{bmatrix} C_1 \\ C_2 \end{bmatrix} = \begin{bmatrix} 0.04 \\ 0 \end{bmatrix}$  and for B matrix its like  $B = \begin{bmatrix} B_{12} \\ B_{21} \end{bmatrix} = \begin{bmatrix} 0 \\ 0 \end{bmatrix}$  and A matrix is  $A = \begin{bmatrix} -0.5 & 0 \\ 0.02 & -0.5 \end{bmatrix}$ .



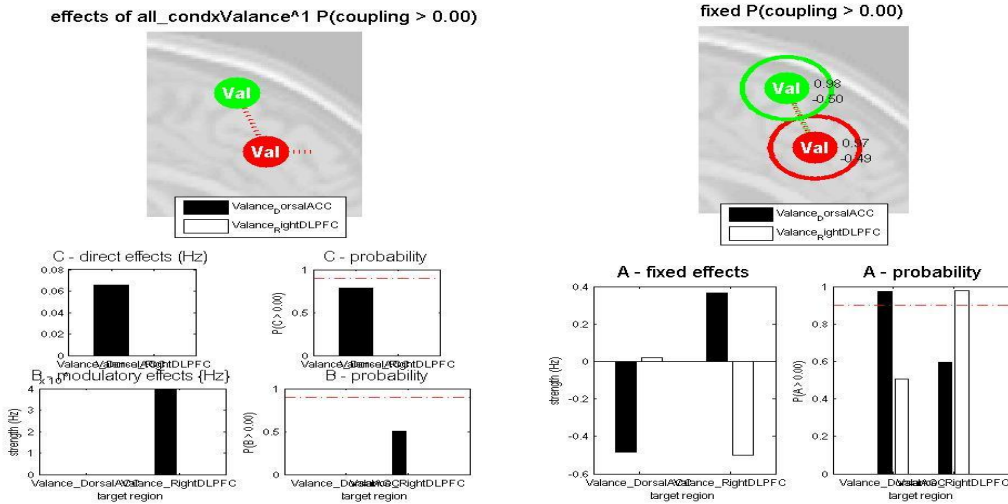


Figure 4.10. Best Model of condition valance: DorsalACC and RightDLPFC

Applying stimuli to DorsalACC and connection from DorsalACC toward RightDLPFC results in an increase in positive connectivity. There is decrease in intrinsic connectivity and an increase in effective connectivity between regions. The connectivity from RightDLPFC toward DorsalACC is also greater than the reverse connection.

Considering valance and two ROI's of VentralACC and RightInsula, the best model will be model5.

C matrix is in the form of  $C = \begin{bmatrix} C_1 \\ C_2 \end{bmatrix} = \begin{bmatrix} 0.06 \\ 0 \end{bmatrix}$  and for B matrix its like  $B = \begin{bmatrix} B_{12} \\ B_{21} \end{bmatrix} = \begin{bmatrix} 0 \\ 4 * 10^{-8} \end{bmatrix}$  and A matrix is  $A = \begin{bmatrix} -0.4 & 0 \\ 0.38 & -0.4 \end{bmatrix}$ .

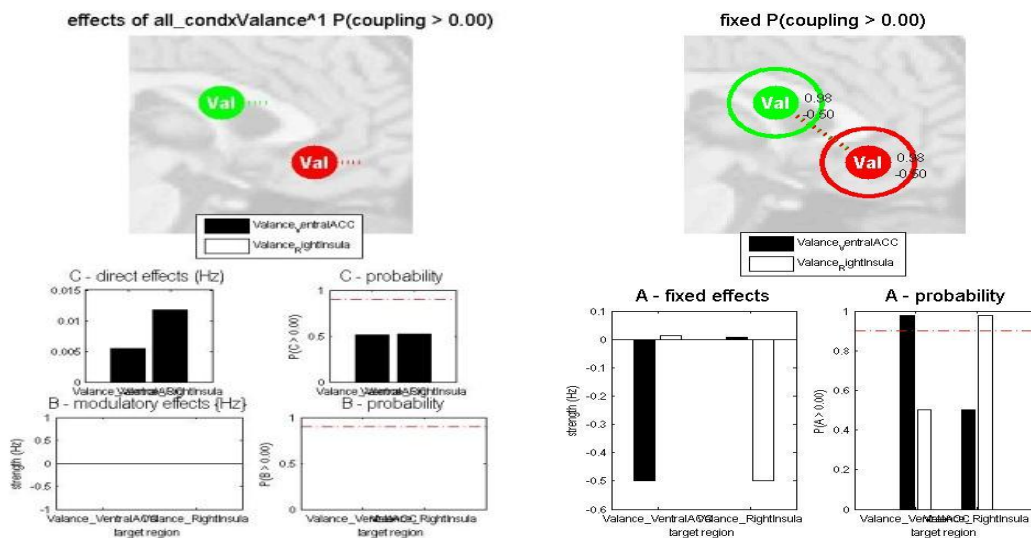


Figure 4.11. Best Model of condition valance: VentralACC and RightInsula

In this condition even without considering any stimulation, the connectivity between two regions is so small. Applying valance to the ROI's in this model will result in a small decrease in connectivity between regions. No modulatory effect is applied. Effect of valance on RightInsula is greater than the effect on VentralACC. C matrix is in the form of  $C = \begin{bmatrix} C_1 \\ C_2 \end{bmatrix} = \begin{bmatrix} 0.006 \\ 0.013 \end{bmatrix}$  and for B matrix its like  $B = \begin{bmatrix} B_{12} \\ B_{21} \end{bmatrix} = \begin{bmatrix} 0 \\ 0 \end{bmatrix}$  and A matrix is  $A = \begin{bmatrix} -0.5 & 0 \\ 0 & -0.5 \end{bmatrix}$ .

For stimulation of valance and its effect on DorsalACC and VentralACC, model6 is selected as best model.

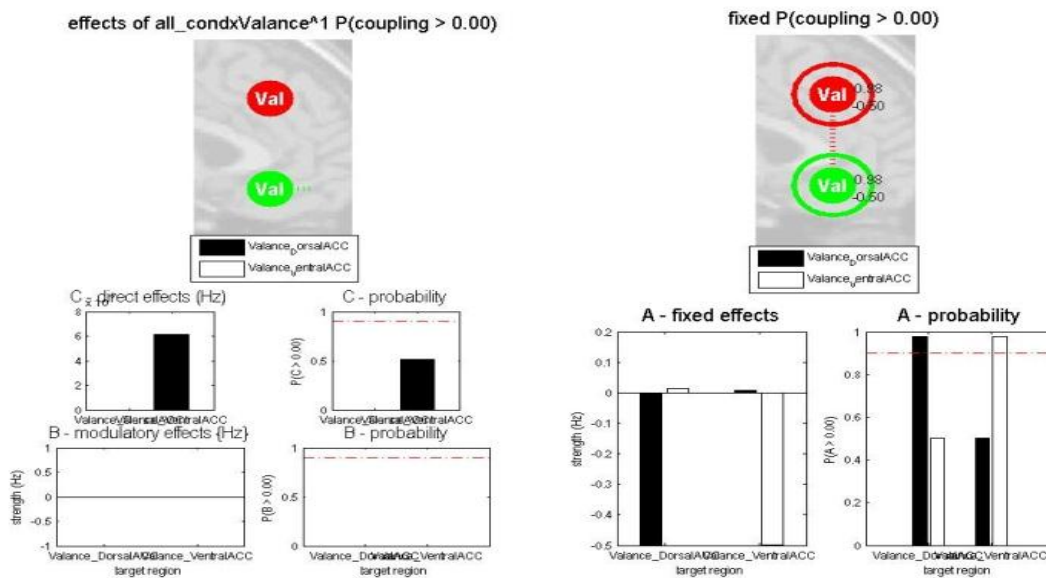


Figure 4.12. Best Model of condition valance: DorsalACC and VentralACC

In the case of no stimulation for this model, there is great intrinsic connection between regions. Applying valance to the region of VentralACC results in a great decrease of connectivity between regions. C matrix is in the form of  $C = \begin{bmatrix} C_1 \\ C_2 \end{bmatrix} = \begin{bmatrix} 0 \\ 0.6 * 10^{-8} \end{bmatrix}$  and for B matrix its like  $B = \begin{bmatrix} B_{12} \\ B_{21} \end{bmatrix} = \begin{bmatrix} 0 \\ 0 \end{bmatrix}$  and A matrix is  $A = \begin{bmatrix} -0.5 & 0 \\ 0 & -0.5 \end{bmatrix}$ .

Probability of error for selected best models are provided for all models of six conditions and included in table 4.1. below.

Table 4.1. Probability of error for all models.

P(e)	Model 1	Model 2	Model 3	Model 4	Model 5	Model 6	Model 7	Model 8	Model 9
Condition 1	0.5	<b>0.2</b>	0.5	0.3	0.5	0.5	0.5	0.3	0.3
Condition 2	0.1	0.5	0.5	0.3	0.1	0.5	<b>0.03</b>	0.3	0.3
Condition 3	0.5	0.5	0.5	0.15	0.5	0.5	<b>0.15</b>	0.15	0.15
Condition 4	0.5	<b>0.05</b>	0.5	0.15	0.5	0.5	0.5	0.05	0.05
Condition 5	0.5	0.5	0.5	0.5	<b>0.2</b>	0.5	0.5	0.5	0.5
Condition 6	0.5	0.5	0.5	0.3	0.5	<b>0.15</b>	0.5	0.3	0.3

In table 3.6 Model NULL is not considered. This model shows the condition of no-stimulation and in this condition only A matrix is considered. This model analyzes only intrinsic connectivity between regions.

Best model selection considers p(e), accuracy and complexity of models then compares these three important parameters for all models shown above and select the best one among sixty models. Selected models for each condition are bolded in table.

#### 4.2 Psychophysiological Interactions Results

In the case of PPI, we choose seven ROI's. These ROI's are named as: DorsalACC, LeftInsula, RightInsula, LeftDLPFC, RightDLPFC, VentralACC and RostralACC. Using these ROI's we design models to analyze connectivity between regions when stimulation applied to these regions. Between all models, only 4 models responded with existence of connectivity between regions and in other models there are not observed existence of connection between regions as a result of stimulation. The main difference of this method and DCM is that in PPI method we can include all three type of stimulation as regressors for our design matrix.

In Model 1, we considered DorsalACC which affected by congruency stimulation and LeftInsula in two conditions which affected by both congruency and valance. Model 2, includes DorsalACC, LeftDLPFC and RightDLPFC. Here in this condition, valance is the only stimulation and we considered LeftDLPFC and RightDLPFC as a single region named DLPFC. Model 3, includes 3 regions of RostralACC which is affected by cong\*valance stimulation, Left and Right DLPFC as a single region DLPFC. Model 6 includes LeftInsula with stimulation of congruency and DLPFC region.

Using General Linear Model, we entered stimulations as our regressors and as we describe in previous chapters, our main purpose here is to deconvolve haemodynamic response with BOLD signal to get neural activity of regions just like DCM.

As the first step we try to extract PPI signals which are the product of psychological and physiological signals of brain. Psychological signals are dependent to stimulations and Physiological signals are depend on brain structure which means in our experiment it depends on our extracted time-series from preprocessing step.

It would be useful if take a look at PPI's of regions and discuss what they really mean. All related figures and descriptions are in Appendix D.

All figures show the PPI term for regions. A graph to show neuronal and haemodynamic response is also seen in each graph. We are sure that there is a response from any of regions to the stimulation. All figures have three graphs. The upper graph shows neuronal and haemodynamic response of region to stimulation. Blue line show BOLD signal and green line shows neuronal. Figure1 shows region of VentralACC and its response to the stimulation valance. In figure2 we have RightInsula while responding to valance. RightDLPFC which is shown in figure3 responds to valance. RostralACC shown in figure4 responds to con\*val. In figure5 we can see LeftInsula responding to valance. LeftInsula in figure6 is different because

it responds to congruency. In figure7 region named LeftDLPFC shows response to the stimulation named valance. Figure8 and 9 shows response of DorsalACC to stimulations valance and congruency.

Now we have PPI which includes interaction term of haemodynamic response and neuronal response. The PPI can be get from looking for a difference between regression slope of ROI1 and activity of ROI2. The slope of ROI1 shows the response of ROI1 to the activity of ROI2.

In our experiment we choose ROI's from group analyses and p-value is 0.05 for our time-series extraction and we have a filter to remove significances lower than 3.9. Range for Z-Score (a rate which shows acceptability of model) for our experiment is (3.9, 4.3) which is a high amount.

We satisfied from 4 models which are able to show effective connectivity between regions in brain. These models are as shown below:

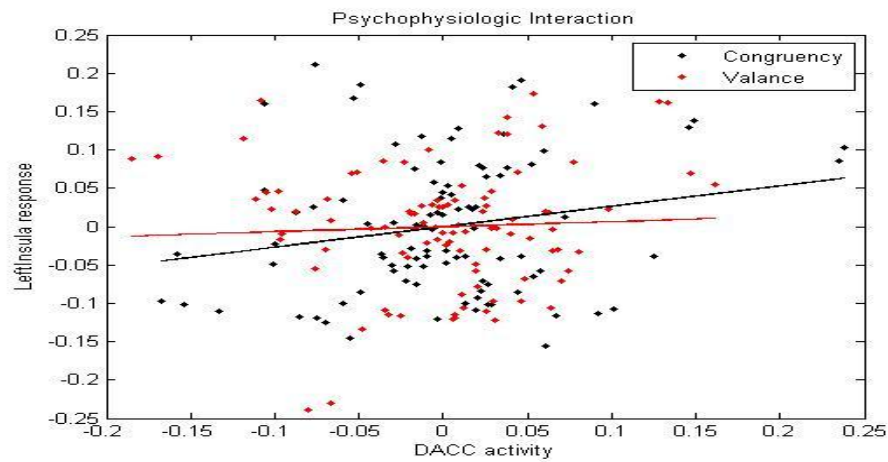


Figure 4.13. PPI of DorsalACC activity and LeftInsula response

Model 1 shows connection between DorsalACC and LeftInsula. Slope of regression which is shown for both regions as their activity and response shows effect of stimulations and activity of one region which results in response from another region. From graph we can see that there is response from LeftInsula to the activity of DorsalACC in both conditions of applying congruency or valance. X and Y axes are in the unit of frequency which both show the power of signal. LeftInsula shows a small response to the activity of DorsalACC when stimulation is valance. This response in attendance of congruency increased when stimulation is congruency. DorsalACC shows activity in case of both congruency and valance.

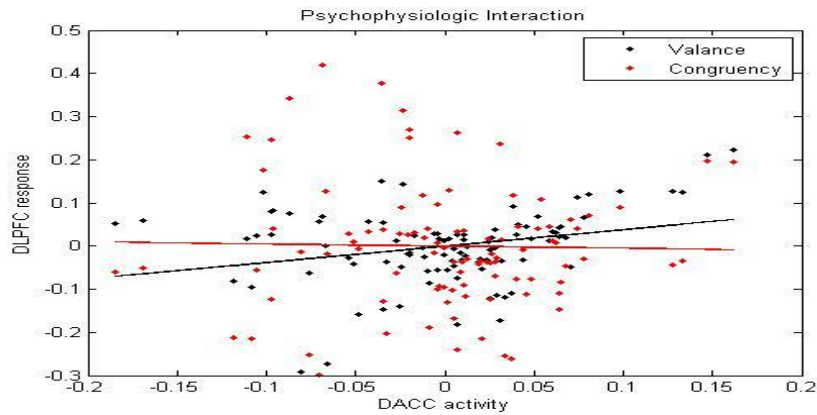


Figure 4.14. PPI of DorsalACC activity and DLPFC response

Model 2 shows connection between DorsalACC and DLPFC. From graph we can see that there is response from LeftInsula to the activity of DorsalACC in both conditions of applying congruency or valance. X and Y axes are in the unit of frequency which both show the power of signal. As we can see response of DLPFC to the activity of DorsalACC when stimulation is congruency is nearly zero while respding rate of DLPFC to the activity of DorsalACC when stimulation is valance is acceptable. DorsalACC shows activity in case of both congruency and valance.

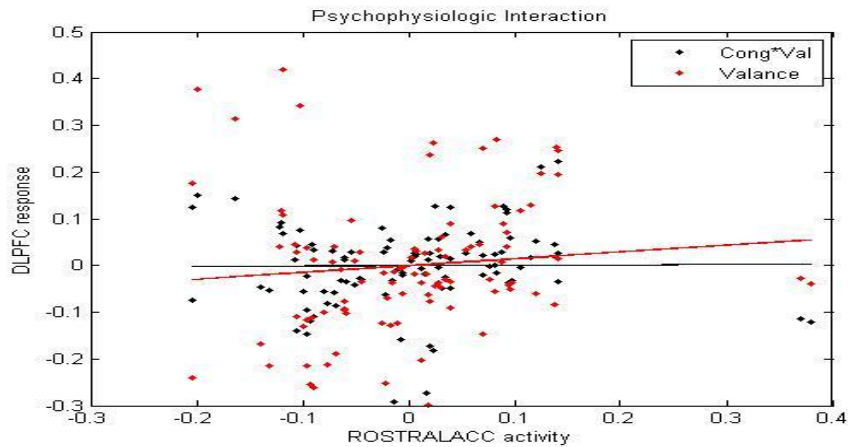


Figure 4.15. PPI of RostralACC activity and DLPFC response.

This model shows activity of RostralACC and response of DLPFC to this activity. In this model the connectivity is low and there is not acceptable changes in responses of DLPFC. Here also, response of DLPFC by applying valance to the activity of RostralACC is more than when the stimulation is cong\*val.

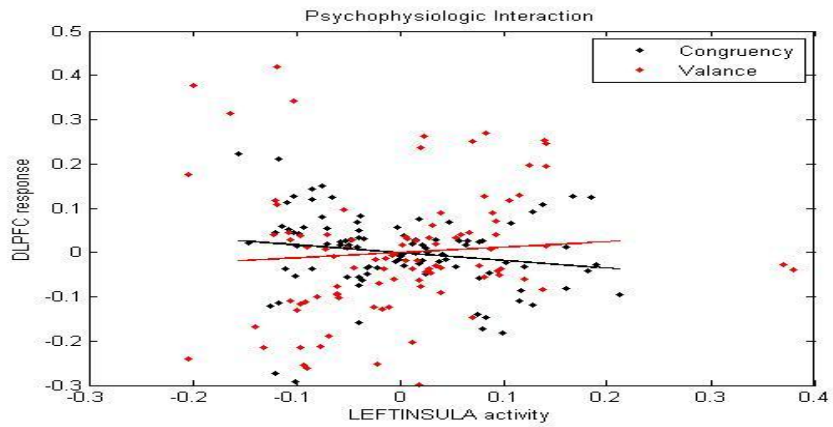


Figure 4.16. PPI of LeftInsula activity and DLPFC response.

In this model, there is response from DLPFC to the activity of LeftInsula in attendance of valance. The interesting issue here is that connectivity between ROI's is reducing when the activity of LeftInsula is increasing and the stimulation is congruency. For more activity from LeftInsula, response from DLPFC reducing.



## CHAPTER 5

### Conclusions

#### 5.1 Conclusion

In this thesis work, effective connectivity is analyzed on a fMRI data. We used two methods of DCM and PPI for our purpose. During data acquisition, 11 subjects were tested using 4 stimulations which are congruency positive, congruency negative, incongruency positive and incongruency negative. We used these stimulations to test the effect of Congruency, Valance and Cong\*Val (combination of both stimulations) on brain regions. 10 different ROIs were created after a group analysis. These ROIs were considered to be connected to each other intrinsically. At the beginning of this study, we assumed that there must be connections between selected ROIs tested them by applying DCM and PPI.

Ten different models were designed for every six pairs of conditions for DCM. Stimulations are considered as inputs which directly affect regions and/or connections between regions. All three parameters of DCM found and applied to all models. Using Bayesian Factors, best model for any condition is selected.

In PPI method seven ROIs are selected and four acceptable models are selected between them and the effect of stimulations on regions are discussed in terms of activity of one region and response of another region when there is one or two of stimulations is available.

Results for DCM are in the form of graphs which are showing parameters of DCM as A, B and C matrices. Any changes in any of these matrices are shown in both graphical and matrix format to ease the comparison of models. Totally, we designed sixty different models for ten ROI's and six situations. One of these models for every situation is stimulus free and means that in this model we don't consider effect of stimuli. Remaining nine models for any six conditions includes stimuli.

For PPI, results are shown in graphs by considering regression slope of activity and responses of two different regions. Changes in slope of regression shows effect of activity of one region over the response of other region.

The results for both methods are as we considered in our hypothesis. The effect of stimulations on ROIs and related connectivity is observed in results of DCM. In most of the designed models, changes in connectivities resulted from effecting stimulations on regions or connections are observed.

In case of PPI, only 4 models were acceptable and the other models were not satisfactory. In these four models, we considered effect of congruency, valance and cong\*val. In two of these four models, there are results that shows reverse effect of stimulation. This means an increase in activity of one region results in decrease in response of another region or connection between regions.

We were able to observe effect of stimulations on regions using DCM method. Applying stimuli to models result in positive or negative connectivity as well. Considering stimuli congruency and ROI's DorsalACC and LeftInsula result in a positive connectivity which means an increase in connection between these two ROI's when stimulus is applied. Results for all models are included in APPENDIX C and selected best models and situation without considering effect of stimuli is considered in chapter 4.

In case of PPI, from mentioned seven different ROI's, we found four suitable models to show changes of activity and response in regions when stimulation is applied. For PPI the psychophysiological interactions for all ROI's are plotted and results are included in APPENDIX D. Results of effective connectivity analysis are included in chapter 4

. From all results which are hold by DCM and PPI after applying stimuli, connectivity between the regions of interest in both of conditions show a similarity between PPI and DCM in some cases. For example consider two ROI's of DorsalACC and DLPFC (right and left), we can see the effect of stimulation on connectivity between ROI's by both DCM and PPI method. In case of DorsalACC and LeftInsula, DCM shows that changes between activity and response as a result of Valance while PPI show this as a result of Congruency. For other three models, results of PPI are similar with results of DCM. This experiment also

proves that DCM is more robust than PPI and the results DCM are more reliable than results obtained by other method.

## **5.2 Future Work**

In this study, Bilinear forward model DCM was used. Our hypothesis was to analyze connectivity between ROI pairs. We did not consider effect of other regions on connections between ROIs. Also, in finding best model, Bayesian factor was selected. As model selection is based on comparison between many models, it is considered as weak point for DCM. Introducing a method which gives more reliable results in model comparison and model selection could be a future work for DCM [46].

## REFERENCES

- [1] K.J. Friston, "Functional and effective connectivity in neuroimaging: a synthesis.," *um. Brain Mapp.*, vol. 2, pp. 56-78, 1994.
- [2] B. Horwitz, M.A. Tagamets, and A.R. McIntosh, "Neural modeling, functional brain imaging, and cognition," *Trends Cogn Sci*, vol. 3, (no. 3), pp. 91-98, Mar 1999.
- [3] K.E. Stephan, J.J. Riera, G. Deco, and B. Horwitz, "The Brain Connectivity Workshops: moving the frontiers of computational systems neuroscience," *Neuroimage*, vol. 42, (no. 1), pp. 1-9, Aug 1 2008.
- [4] K.J. Friston, L. Harrison, and W. Penny, "Dynamic causal modelling," *Neuroimage*, vol. 19, (no. 4), pp. 1273-302, Aug 2003.
- [5] K.E. Stephan, L.M. Harrison, S.J. Kiebel, O. David, W.D. Penny, and K.J. Friston, "Dynamic causal models of neural system dynamics: current state and future extensions," *J Biosci*, vol. 32, (no. 1), pp. 129-44, Jan 2007.
- [6] K.J. Friston, N. Trujillo-Barreto, and J. Daunizeau, "DEM: a variational treatment of dynamic systems," *Neuroimage*, vol. 41, (no. 3), pp. 849-85, Jul 1 2008.
- [7] O. David, S.J. Kiebel, L.M. Harrison, J. Mattout, J.M. Kilner, and K.J. Friston, "Dynamic causal modeling of evoked responses in EEG and MEG," *Neuroimage*, vol. 30, (no. 4), pp. 1255-72, May 1 2006.
- [8] Klaas Enno Stephan, Lars Kasper, Lee M. Harrison, Jean Daunizeau, Hanneke E.M. den Ouden, Michael Breakspear, Karl friston, "Nonlinear dynamic causal models for fMRI", *Neuroimage*, April 2008.
- [9] C. Büchel and K.J. Friston, "Modulation of connectivity in visual pathways by attention: cortical interactions evaluated with structural equation modelling and fMRI," *Cereb Cortex*, vol. 7, (no. 8), pp. 768-78, Dec 1997.
- [10] E. Bullmore, B. Horwitz, G. Honey, M. Brammer, S. Williams, and T. Sharma, "How good is good enough in path analysis of fMRI data?," *Neuroimage*, vol. 11, (no. 4), pp. 289-301, Apr 2000.
- [11] A.R. McIntosh and F. Gonzales-Lima, "Structural equation modelling and its application to network analysis in functional brain imaging," *Hum Brain Mapp*, vol. 2, pp. 2-22, 1994.
- [12] K.J. Friston, C. Buechel, G.R. Fink, J. Morris, E. Rolls, and R.J. Dolan, "Psychophysiological and modulatory interactions in neuroimaging," *Neuroimage*, vol. 6, (no. 3), pp. 218-29, Oct 1997.
- [13] R.B. Buxton, E.C. Wong, and L.R. Frank, "Dynamics of blood flow and oxygenation changes during brain activation: the balloon model," *Magn Reson Med*, vol. 39, (no. 6), pp. 855-64, Jun 1998.

- [14] K.J. Friston, A. Mechelli, R. Turner, and C.J. Price, “Nonlinear responses in fMRI: the Balloon model, Volterra kernels, and other hemodynamics,” *Neuroimage*, vol. 12, (no. 4), pp. 466-77, Oct 2000.
- [15] K.E. Stephan, N. Weiskopf, P.M. Drysdale, P.A. Robinson, and K.J. Friston, “Comparing hemodynamic models with DCM,” *Neuroimage*, vol. 38, (no. 3), pp. 387-401, Nov 15 2007.
- [16] K.J. Friston, “Bayesian estimation of dynamical systems: an application to fMRI,” *Neuroimage*, vol. 16, (no. 2), pp. 513-30, Jun 2002.
- [17] K. Friston, J. Mattout, N. Trujillo-Barreto, J. Ashburner, and W. Penny, “Variational free energy and the Laplace approximation,” *Neuroimage*, vol. 34, (no. 1), pp. 220-34, Jan 1 2007.
- [18] O. David, I. Guillemain, S. Saitet, S. Reyt, C. Deransart, C. Segebarth, and A. Depaulis, “Identifying neural drivers with functional MRI: an electrophysiological validation,” *PLoS Biol*, vol. 6, (no. 12), pp. 2683-97, Dec 23 2008.
- [19] R. Goebel, A. Roebroeck, D.S. Kim, and E. Formisano, “Investigating directed cortical interactions in time-resolved fMRI data using vector autoregressive modeling and Granger causality mapping,” *Magn Reson Imaging*, vol. 21, (no.10), pp. 1251-61, Dec 2003.
- [20] K.E. Stephan, L.M. Harrison, W.D. Penny, and K.J. Friston, “Biophysical models of fMRI responses,” *Curr Opin Neurobiol*, vol. 14, (no. 5), pp. 629-35, Oct 2004.
- [21] W.D. Penny, K.E. Stephan, A. Mechelli, and K.J. Friston, “Modelling functional integration: a comparison of structural equation and dynamic causal models,” *Neuroimage*, vol. 23 Suppl 1, pp. S264-74, 2004.
- [22] M.A. Pitt and I.J. Myung, “When a good fit can be bad,” *Trends Cogn Sci*, vol. 6, (no. 10), pp. 421-425, Oct 1 2002.
- [23] W.D. Penny, K.E. Stephan, A. Mechelli, and K.J. Friston, “Comparing dynamic causal models,” *Neuroimage*, vol. 22, (no. 3), pp. 1157-72, Jul 2004.
- [24] G. Schwarz, “Estimating the dimension of a model.,” *Ann. Stat.*, vol. 6, pp. 461-464, 1978.
- [25] K.E. Stephan, W.D. Penny, J. Daunizeau, R.J. Moran, and K.J. Friston, “Bayesian model selection for group studies,” *Neuroimage*, vol. 46, (no. 4), pp. 1004-17, Jul 15 2009.
- [26] K.E. Stephan, L. Kasper, L.M. Harrison, J. Daunizeau, H.E. den Ouden, M. Breakspear, and K.J. Friston, “Nonlinear dynamic causal models for fMRI,” *Neuroimage*, vol. 42, (no. 2), pp. 649-62, Aug 15 2008.
- [27] Heinz A, Braus DF, Smolka MN, Wrase J, Puls I, Hermann D, Klein S, Grüsser SM, Flor H, Schumann G, Mann K & Büchel C (2004).
- [28] Amygdala-prefrontal coupling depends on a genetic variation of the serotonin transporter *Nature Neuroscience* 8, 20 – 21.

- [29] Boksman K, Theberge J, Williamson P, Drost DJ, Malla A, Densmore M, Takhar J, Pavlosky W, Menon RS, Neufeld RW. (2005)
- [30] A 4.0-T fMRI study of brain connectivity during word fluency in first-episode schizophrenia. *Schizophr Res.* 15:247-63
- [31] Skuse DH, Morris JS, Dolan RJ. (2005) Functional dissociation of amygdala-modulated arousal and cognitive appraisal, in Turner syndrome. *Brain.* 128:2084-96
- [32] Pingel U, Lorenz J, Schoell E, Weiller C, Buchel C. (2006) Mechanisms of placebo analgesia: rACC recruitment of a subcortical antinociceptive network. *Pain* 120:8-15
- [33] K.J.Friston, C.Buechel, G.R.Fink, J.Morris, E.Rolls and R.J.Dolan "Psychophysiological and Modulatory Interactions in Neuroimaging". *Neuroimage* vol. 6, 218-229 (1997), *article number*:NI970291, Feb 19,1997.
- [34] T. Bitan, J.R. Booth, J. Choy, D.D. Burman, D.R. Gitelman, and M.M. Mesulam, "Shifts of effective connectivity within a language network during rhyming and spelling," *J Neurosci*, vol. 25, (no. 22), pp. 5397-403, Jun 1 2005.
- [35] A.P. Smith, K.E. Stephan, M.D. Rugg, and R.J. Dolan, "Task and content modulate amygdala-hippocampal connectivity in emotional retrieval," *Neuron*, vol. 49, (no. 4), pp. 631-8, Feb 16 2006.
- [36] Buechel, C., and Friston, K. J. Assessing modulatory interactions among visual areas using nonlinear structural equation modelling and fMRI. Submitted for publication.
- [37] Buechel, C., Wise, R. S. J., Mummary, C., and Friston, K. J. 1996. Nonlinear regression in parametric activation studies. *NeuroImage* 4:60-66.
- [38] Talairach, J., and Tournoux, P. 1988. *A Co-planar Stereotaxic Atlas of a Human Brain*. Thieme, Stuttgart.
- [39] Gelman, A., Carlin, J.B., Stern, H.S., Rubin, D.B., 1995. Bayesian Data Analysis. Chapman & Hall, Boca Raton.
- [40] Buxton, R.B., Wong, E.C., Frank, L.R., 1998. Dynamics of blood flow and oxygenation changes during brain activation: the Balloon model. *Magn. Reson. Med.* 39, 855-864.
- [41] Friston, K.J., Harrison, L., Penny, W., 2003. Dynamic causal modelling. *NeuroImage* 19 (4), 1273-1302.
- [42] Friston, K.J., Buchel, C., 2000. Attentional modulation of effective connectivity from V2 to V5/MT in humans. *Proc. Natl. Acad. Sci. U. S. A.* 97 (13), 7591-7596.
- [43] Press, W.H., Teukolsky, S.A., Vetterling, W.T., Flannery, B.V.P., 1992. *Numerical Recipes in C*. Cambridge Univ. Press, Cambridge.

- [44] Darren R. Gitelman, William D. Penny, John Ashburner and Karl J. Friston. *Modeling regional and psychophysiological interactions in fMRI: the importance of haemodynamic deconvolution*. Published Dec. 2002 Neuroimage, Elsevier.
- [45] Friston, K.J., Penny, W., Philips, C., Kiebel, S., Hinton, G., Ashburner, J., 2002. Classical and Bayesian inference in neuroimaging; theory. Neuroimage 16(2), 456-483.
- [46] Gabriele Lohmann, Kerstin Erfurth, Karsten Müller, Robert Turner. *Critical comments on dynamic causal modelling*. Published Neuroimage 59 (2012) 2322-2329. Elsevier

## APPENDIX A

### T-TEST

A ***t*-test** is any statistical hypothesis test in which the test statistic follows a Student's *t* distribution if the null hypothesis is supported. It is most commonly applied when the test statistic would follow a normal distribution if the value of a scaling term in the test statistic were known. When the scaling term is unknown and is replaced by an estimate based on the data, the test statistic (under certain conditions) follows a *t* distribution.

Among the most frequently used *t*-tests are:

- A one-sample location test of whether the mean of a normally distributed population has a value specified in a null hypothesis.
- A two sample location test of the null hypothesis that the means of two normally distributed populations are equal. All such tests are usually called ***t*-tests**, though strictly speaking that name should only be used if the variances of the two populations are also assumed to be equal; the form of the test used when this assumption is dropped is sometimes called Welch's *t*-test. These tests are often referred to as "unpaired" or "independent samples" *t*-tests, as they are typically applied when the statistical units underlying the two samples being compared are non-overlapping.
- A test of the null hypothesis that the difference between two responses measured on the same statistical unit has a mean value of zero. For example, suppose we measure the size of a cancer patient's tumor before and after a treatment. If the treatment is effective, we expect the tumor size for many of the patients to be smaller following the treatment. This is often referred to as the "paired" or "repeated measures" *t*-test.
- A test of whether the slope of a regression line differs significantly from 0.

#### Assumptions:

Most *t*-test statistics have the form  $T = Z/s$ , where  $Z$  and  $s$  are functions of the data. Typically,  $Z$  is designed to be sensitive to the alternative hypothesis (i.e. its magnitude tends to be larger when the alternative hypothesis is true), whereas  $s$  is a scaling parameter that allows the distribution of  $T$  to be determined.

As an example, in the one-sample *t*-test  $Z = X/\delta/\sqrt{n}$ , where  $X$  is the sample mean of the data,  $n$  is the sample size, and  $\delta$  is the population standard deviation of the data;  $s$  in the one-sample *t*-test is  $\delta^\wedge$ , where  $\delta^\wedge$  is the sample standard deviation.

The assumptions underlying a *t*-test are that

- $Z$  follows a standard normal distribution under the null hypothesis
- $s^2$  follows a  $\chi^2$  distribution with  $p$  degrees of freedom under the null hypothesis, where  $p$  is a positive constant
- $Z$  and  $s$  are independent.

In a specific type of  $t$ -test, these conditions are consequences of the population being studied, and of the way in which the data are sampled. For example, in the  $t$ -test comparing the means of two independent samples, the following assumptions should be met:

- Each of the two populations being compared should follow a normal distribution. This can be tested using a normality test, such as the Shapiro-Wilk or Kolmogorov–Smirnov test, or it can be assessed graphically using a normal quantile plot.
- If using Student's original definition of the  $t$ -test, the two populations being compared should have the same variance (testable using F test, Levene's test, Bartlett's test, or the Brown–Forsythe test; or assessable graphically using a Q-Q plot). If the sample sizes in the two groups being compared are equal, Student's original  $t$ -test is highly robust to the presence of unequal variances. Welch's  $t$ -test is insensitive to equality of the variances regardless of whether the sample sizes are similar.
- The data used to carry out the test should be sampled independently from the two populations being compared. This is in general not testable from the data, but if the data are known to be dependently sampled (i.e. if they were sampled in clusters), then the classical  $t$ -tests discussed here may give misleading results.

### **Paired and Unpaired two-sample $t$ -tests:**

Two-sample  $t$ -tests for a difference in mean involve independent samples, paired samples and overlapping samples. Paired  $t$ -tests are a form of blocking, and have greater power than unpaired tests when the paired units are similar with respect to "noise factors" that are independent of membership in the two groups being compared. In a different context, paired  $t$ -tests can be used to reduce the effects of confounding factors in an observational study.

### **Independent samples**

The independent samples  $t$ -test is used when two separate sets of independent and identically distributed samples are obtained, one from each of the two populations being compared. For example, suppose we are evaluating the effect of a medical treatment, and we enroll 100 subjects into our study, then randomize 50 subjects to the treatment group and 50 subjects to the control group. In this case, we have two independent samples and would use the unpaired form of the  $t$ -test. The randomization is not essential here—if we contacted 100 people by phone and obtained each person's age and gender, and then used a two-sample  $t$ -test to see whether the mean ages differ by gender, this would also be an independent samples  $t$ -test, even though the data are observational.

### **Paired samples**

Paired samples  $t$ -tests typically consist of a sample of matched pairs of similar units, or one group of units that has been tested twice (a "repeated measures"  $t$ -test).

A typical example of the repeated measures  $t$ -test would be where subjects are tested prior to a treatment, say for high blood pressure, and the same subjects are tested again after treatment with a blood-pressure lowering medication. By comparing the same patient's numbers before and after treatment, we are effectively using each patient as their own control. That way the correct rejection of the null hypothesis (here: of no difference made by the treatment) can become much more likely, with statistical power increasing simply because the random between-patient variation has now been eliminated. Note however that an increase of statistical power comes at a price: more tests are required, each subject having to be tested twice. Because half of the sample now depends on the other half, the paired version of Student's  $t$ -test has only ' $n/2 - 1$ ' degrees of freedom (with ' $n$ ' being the total number of observations). Pairs become individual test units, and the sample has to be doubled to achieve the same number of degrees of freedom.

A paired samples  $t$ -test based on a "matched-pairs sample" results from an unpaired sample that is subsequently used to form a paired sample, by using additional variables that were measured along with the variable of interest. The matching is carried out by identifying pairs of values consisting of one observation from each of the two samples, where the pair is similar in terms of other measured variables. This approach is sometimes used in observational studies to reduce or eliminate the effects of confounding factors.

Paired samples  $t$ -tests are often referred to as "dependent samples  $t$ -tests" (as are  $t$ -tests on overlapping samples).

**Calculations:**

Explicit expressions that can be used to carry out various  $t$ -tests are given below. In each case, the formula for a test statistic that either exactly follows or closely approximates a  $t$ -distribution under the null hypothesis is given. Also, the appropriate degrees of freedom are given in each case. Each of these statistics can be used to carry out either a one-tailed test or a two-tailed test.

Once a  $t$  value is determined, a  $p$ -value can be found using a table of values from Student's  $t$ -distribution. If the calculated  $p$ -value is below the threshold chosen for statistical significance (usually the 0.10, the 0.05, or 0.01 level), then the null hypothesis is rejected in favor of the alternative hypothesis.

**One-sample  $t$ -test**

In testing the null hypothesis that the population mean is equal to a specified value  $\mu_0$ , one uses the statistic

$$t = \frac{\bar{x} - \mu_0}{s/\sqrt{n}}$$

where  $\bar{x}$  is the sample mean,  $s$  is the sample standard deviation of the sample and  $n$  is the sample size. The degrees of freedom used in this test is  $n - 1$ .

**Slope of a regression line**

Suppose one is fitting the model

$$Y_i = \alpha + \beta x_i + \varepsilon_i$$

where  $x_i, i = 1, \dots, n$  are known,  $\alpha$  and  $\beta$  are unknown, and  $\varepsilon_i$  are independent identically normally distributed random errors with expected value 0 and unknown variance  $\sigma^2$ , and  $Y_i, i = 1, \dots, n$  are observed. It is desired to test the null hypothesis that the slope  $\beta$  is equal to some specified value  $\beta_0$  (often taken to be 0, in which case the hypothesis is that  $x$  and  $y$  are unrelated).

Let

$$\hat{\alpha}, \hat{\beta} = \text{least-squares estimators}$$

$$SE_{\hat{\alpha}}, SE_{\hat{\beta}} = \text{the standard errors of least-squares estimators}$$

Then

$$t_{score} = \frac{\hat{\beta} - \beta_0}{SE_{\hat{\beta}}}$$

has a  $t$ -distribution with  $n - 2$  degrees of freedom if the null hypothesis is true. The standard

$$\text{error of the slope coefficient } SE_{\hat{\beta}} = \frac{\sqrt{\frac{1}{n-2} \sum_{i=1}^n (Y_i - \hat{y}_i)^2}}{\sqrt{\sum_{i=1}^n (x_i - \bar{x})^2}}$$

can be written in terms of the residuals. Let  $\hat{\varepsilon}_i = Y_i - \hat{y}_i = Y_i - (\hat{\alpha} + \hat{\beta}x_i)$  = residuals = estimated errors

$$SSR = \sum_{i=1}^n \hat{\varepsilon}_i^2 = \text{sum of squares of residuals}$$

Then  $t$ -score is given by:

$$t_{scores} = \frac{(\hat{\beta} - \beta_0)\sqrt{n-2}}{\sqrt{SSR}/\sqrt{\sum_{i=1}^n (x_i - \bar{x})^2}}$$

## APPENDIX B

### STATISTICAL REGRESSION ANALYSIS AND GENERAL LINEAR MODEL

In statistics, **regression analysis** is a statistical technique for estimating the relationships among variables. It includes many techniques for modeling and analyzing several variables, when the focus is on the relationship between a dependent variable and one or more independent variables. More specifically, regression analysis helps one understand how the typical value of the dependent variable changes when any one of the independent variables is varied, while the other independent variables are held fixed. Most commonly, regression analysis estimates the conditional expectation of the dependent variable given the independent variables — that is, the average value of the dependent variable when the independent variables are fixed. Less commonly other location parameter of the conditional distribution of the dependent variable given the independent variables. In all cases, the estimation target is a function of the independent variables called the **regression function**. In regression analysis, it is also of interest to characterize the variation of the dependent variable around the regression function, which can be described by a probability distribution.

Regression analysis is widely used for prediction and forecasting, where its use has substantial overlap with the field of machine learning. Regression analysis is also used to understand which among the independent variables are related to the dependent variable, and to explore the forms of these relationships. In restricted circumstances, regression analysis can be used to infer causal relationships between the independent and dependent variables. However this can lead to illusions or false relationships, so caution is advisable: See correlation does not imply causation.

A large body of techniques for carrying out regression analysis has been developed. Familiar methods such as linear regression and ordinary least squares regression are parametric, in that the regression function is defined in terms of a finite number of unknown parameters that are estimated from the data. Nonparametric regression refers to techniques that allow the regression function to lie in a specified set of functions, which may be infinite-dimensional.

The performance of regression analysis methods in practice depends on the form of the data generating process, and how it relates to the regression approach being used. Since the true form of the data-generating process is generally not known, regression analysis often depends to some extent on making assumptions about this process. These assumptions are sometimes testable if a large amount of data is available. Regression models for prediction are often useful even when the assumptions are moderately violated, although they may not perform optimally. However, in many applications, especially with small effects or questions of causality based on observational data, regression methods give misleading results.

#### Regression Models

Regression models involve the following variables:

- The **unknown parameters**, denoted as  $\beta$ , which may represent a scalar or a vector.
- The **independent variables**,  $X$ .
- The **dependent variable**,  $Y$ .

In various fields of application, different terminologies are used in place of dependent and independent variables.

A regression model relates  $Y$  to a function of  $X$  and  $\beta$ .

$$Y \approx f(\mathbf{X}, \boldsymbol{\beta})$$

The approximation is usually formalized as  $E(Y | \mathbf{X}) = f(\mathbf{X}, \boldsymbol{\beta})$ . To carry out regression analysis, the form of the function  $f$  must be specified. Sometimes the form of this function is based on knowledge about the relationship between  $Y$  and  $\mathbf{X}$  that does not rely on the data. If no such knowledge is available, a flexible or convenient form for  $f$  is chosen.

Assume now that the vector of unknown parameters  $\boldsymbol{\beta}$  is of length  $k$ . In order to perform a regression analysis the user must provide information about the dependent variable  $Y$ :

- If  $N$  data points of the form  $(Y, \mathbf{X})$  are observed, where  $N < k$ , most classical approaches to regression analysis cannot be performed: since the system of equations defining the regression model is underdetermined, there is not enough data to recover  $\boldsymbol{\beta}$ .
- If exactly  $N = k$  data points are observed, and the function  $f$  is linear, the equations  $Y = f(\mathbf{X}, \boldsymbol{\beta})$  can be solved exactly rather than approximately. This reduces to solving a set of  $N$  equations with  $N$  unknowns (the elements of  $\boldsymbol{\beta}$ ), which has a unique solution as long as the  $\mathbf{X}$  are linearly independent. If  $f$  is nonlinear, a solution may not exist, or many solutions may exist.
- The most common situation is where  $N > k$  data points are observed. In this case, there is enough information in the data to estimate a unique value for  $\boldsymbol{\beta}$  that best fits the data in some sense, and the regression model when applied to the data can be viewed as an over determined system in  $\boldsymbol{\beta}$ .

In the last case, the regression analysis provides the tools for:

1. Finding a solution for unknown parameters  $\boldsymbol{\beta}$  that will, for example, minimize the distance between the measured and predicted values of the dependent variable  $Y$  (also known as method of least squares).
2. Under certain statistical assumptions, the regression analysis uses the surplus of information to provide statistical information about the unknown parameters  $\boldsymbol{\beta}$  and predicted values of the dependent variable  $Y$ .

#### **Necessary number of independent measurements**

Consider a regression model which has three unknown parameters,  $\beta_0$ ,  $\beta_1$ , and  $\beta_2$ . Suppose an experimenter performs 10 measurements all at exactly the same value of independent variable vector  $\mathbf{X}$  (which contains the independent variables  $X_1$ ,  $X_2$ , and  $X_3$ ). In this case, regression analysis fails to give a unique set of estimated values for the three unknown parameters; the experimenter did not provide enough information. The best one can do is to estimate the average value and the standard deviation of the dependent variable  $Y$ . Similarly, measuring at two different values of  $\mathbf{X}$  would give enough data for a regression with two unknowns, but not for three or more unknowns.

If the experimenter had performed measurements at three different values of the independent variable vector  $\mathbf{X}$ , then regression analysis would provide a unique set of estimates for the three unknown parameters in  $\boldsymbol{\beta}$ .

In the case of general linear regression, the above statement is equivalent to the requirement that matrix  $\mathbf{X}^T \mathbf{X}$  is invertible.

#### **Statistical assumptions**

When the number of measurements,  $N$ , is larger than the number of unknown parameters,  $k$ , and the measurement errors  $\epsilon_i$  are normally distributed then *the excess of information* contained in  $(N - k)$  measurements is used to make statistical predictions about the unknown parameters. This excess of information is referred to as the degrees of freedom of the regression.

#### **Assumptions:**

Classical assumptions for regression analysis include:

- The sample is representative of the population for the inference prediction.
- The error is a random variable with a mean of zero conditional on the explanatory variables.
- The independent variables are measured with no error. (Note: If this is not so, modeling may be done instead using errors-in-variables model techniques).
- The predictors are linearly independent, i.e. it is not possible to express any predictor as a linear combination of the others.
- The errors are uncorrelated, that is, the variance–covariance matrix of the errors is diagonal and each non-zero element is the variance of the error.
- The variance of the error is constant across observations (homoscedasticity). (Note: If not, weighted least squares or other methods might instead be used).

These are sufficient conditions for the least-squares estimator to possess desirable properties; in particular, these assumptions imply that the parameter estimates will be unbiased, consistent, and efficient in the class of linear unbiased estimators. It is important to note that actual data rarely satisfies the assumptions. That is, the method is used even though the assumptions are not true. Variation from the assumptions can sometimes be used as a measure of how far the model is from being useful. Many of these assumptions may be relaxed in more advanced treatments. Reports of statistical analyses usually include analyses of tests on the sample data and methodology for the fit and usefulness of the model.

### Linear Regression:

In linear regression, the model specification is that the dependent variable,  $y_i$  is a linear combination of the *parameters* (but need not be linear in the *independent variables*). For example, in simple linear regression for modeling  $n$  data points there is one independent variable:  $x_i$ , and two parameters,  $\beta_0$  and  $\beta_1$ :

straight line: 
$$y_i = \beta_0 + \beta_1 x_i + \varepsilon_i \quad i = 1, \dots, n.$$

(In multiple linear regression, there are several independent variables or functions of independent variables.)

Adding a term in  $x_i^2$  to the preceding regression gives:

parabola: 
$$y_i = \beta_0 + \beta_1 x_i + \beta_2 x_i^2 + \varepsilon_i \quad i = 1, \dots, n.$$

This is still linear regression; although the expression on the right hand side is quadratic in the independent variable  $x_i$ , it is linear in the parameters  $\beta_0$ ,  $\beta_1$  and  $\beta_2$ .

In both cases,  $\varepsilon_i$  is an error term and the subscript  $i$  indexes a particular observation. Given a random sample from the population, we estimate the population parameters and obtain the sample linear regression model:

$$y_i = \hat{\beta}_0 + \hat{\beta}_1 x_i$$

The residual  $e_i = y_i - \hat{y}_i$  is the difference between the value of the dependent variable predicted by the model,  $\hat{y}_i$ , and the true value of the dependent variable,  $y_i$ . One method of estimation is ordinary least squares. This method obtains parameter estimates that minimize the sum of squared residuals, SSE, also sometimes denoted RSS:

$$SSE = \sum_{i=1}^N e_i^2$$

Minimization of this function results in a set of normal equations, a set of simultaneous linear equations in the parameters, which are solved to yield the parameter estimators,  $\hat{\beta}_0, \hat{\beta}_1$ .

In the case of simple regression, the formulas for the least squares estimates are ,

$$\hat{\beta}_1 = \frac{\sum(x_i - \bar{x})(y_i - \bar{y})}{\sum(x_i - \bar{x})^2} \text{ and } \hat{\beta}_0 = \bar{y} - \hat{\beta}_1 \bar{x}$$

where  $\bar{x}$  is the mean (average) of the  $x$  values and  $\bar{y}$  is the mean of the  $y$  values. See simple linear regression for a derivation of these formulas and a numerical example. Under the assumption that the population error term has a constant variance, the estimate of that variance is given by:

$$\widehat{\sigma_\varepsilon^2} = \frac{SSE}{N - 2}$$

This is called the mean square error (MSE) of the regression. The standard errors of the parameter estimates are given by

$$\sigma_{\beta_0} = \widehat{\sigma_\varepsilon} \sqrt{\frac{1}{N} + \frac{\bar{x}^2}{\sum(x_i - \bar{x})^2}}$$

$$\sigma_{\beta_1} = \widehat{\sigma_\varepsilon} \sqrt{\frac{1}{\sum(x_i - \bar{x})^2}}$$

Under the further assumption that the population error term is normally distributed, the researcher can use these estimated standard errors to create confidence intervals and conduct hypothesis tests about the population parameters.

**General Linear Model:**

In the more general multiple regression model, there are  $p$  independent variables:

$$y_i = \beta_1 x_{i1} + \beta_2 x_{i2} + \dots + \varepsilon_i$$

where  $x_{ij}$  is the  $i^{\text{th}}$  observation on the  $j^{\text{th}}$  independent variable, and where the first independent variable takes the value 1 for all  $i$  (so  $\beta$  is the regression intercept).

The least squares parameter estimates are obtained from  $p$  normal equations. The residual can be written as

$$\varepsilon_i = y_i - \beta_1 x_{i1} + \beta_2 x_{i2} + \dots$$

The **normal equations** are:

$$\sum_{i=1}^n \sum_{k=1}^p X_{ij} X_{ik} \widehat{\beta}_k = \sum_{i=1}^n X_{ij} y_i, \quad j=1, \dots, p.$$

In matrix notation, the normal equations are written as  $(X^T X) \hat{\beta} = X^T Y$

where the  $ij$  element of  $X$  is  $x_{ij}$ , the  $i$  element of the column vector  $Y$  is  $y_i$ , and the  $j$  element of  $\hat{\beta}$  is  $\hat{\beta}_j$ .

Thus  $X$  is  $n \times p$ ,  $Y$  is  $n \times 1$ , and  $\hat{\beta}$  is  $p \times 1$ . The solution is  $\hat{\beta} = (X^T X)^{-1} X^T Y$

## APPENDIX C

### DCM RESULTS

In this step, we will consider remaining nine models for six situations. In all these models, we included stimulation in model. Models are based on the details given in chapter 4.

4.2.1 **Congruency : Dorsal ACC and LeftInsula:** We will consider remaining 9 models.

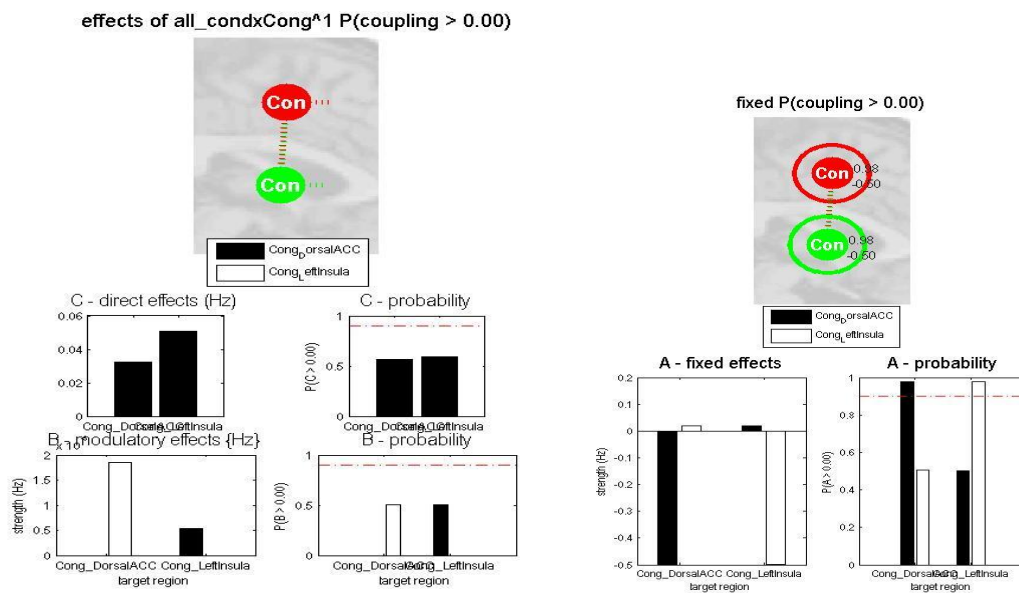


Figure C1: Model 1

In this model as seen in graphs, there is a change in fixed effects in ROI's. Considering this model without applying any stimulations, we can see the effect of congruency on fixed connection, which there is a small increase in connectivity between ROI's after applying Congruency. As we can see from B and C matrices which I illustrate them, we can see the effect of congruency on LeftInsula is greater than its effect on DorsalACC. In a similar way, effect of congruency on connection from DorsalACC toward LeftInsula is greater than reverse connection.

This model shows a small increase in positive direction in connectivity.

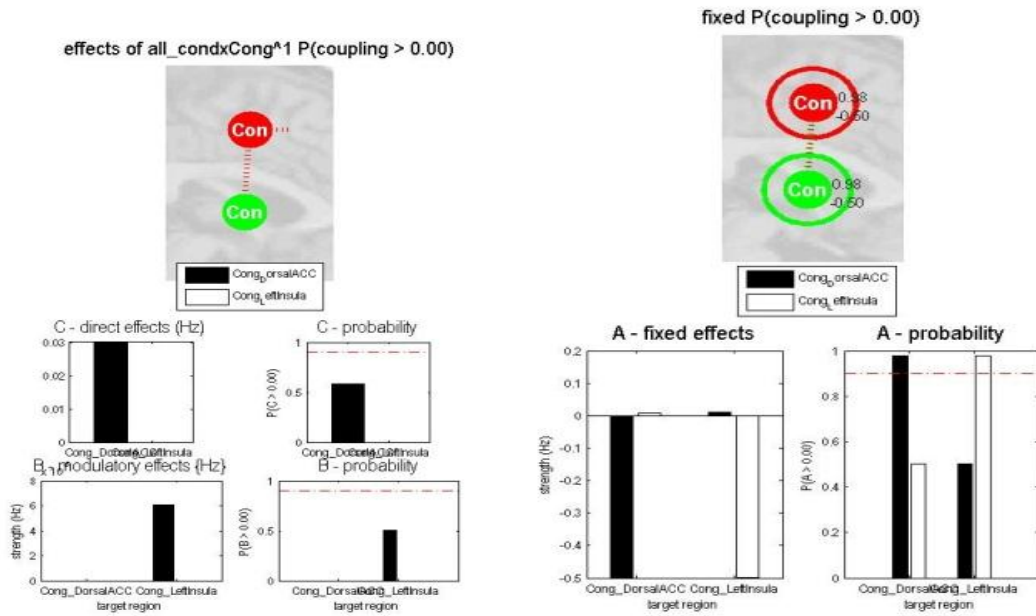


Figure C2: Model 2

In this model, there is nearly zero connection between ROI's. Direct effect of congruency on DorsalACC is small (0.03 Hz) and also we have a small effect of congruency on connection from DorsalACC toward LeftInsula .

In this model also there is a small increase in activity in positive direction.

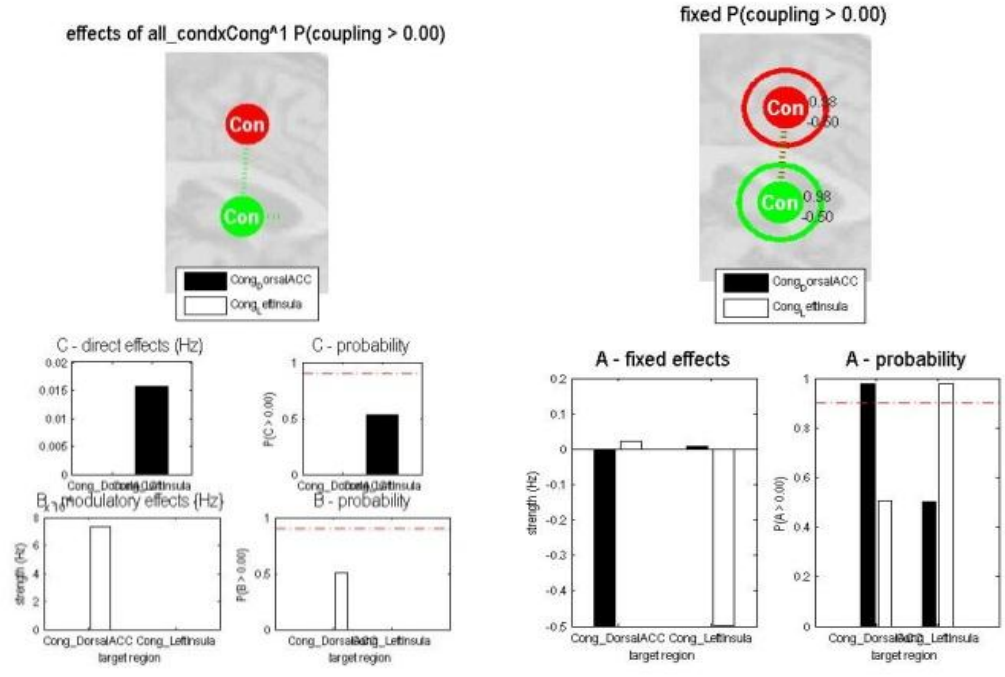


Figure C3: Model 3

This model, like model 3 shows small changes but the probability of this model is so smaller than the threshold.

Figure C4: Model 4

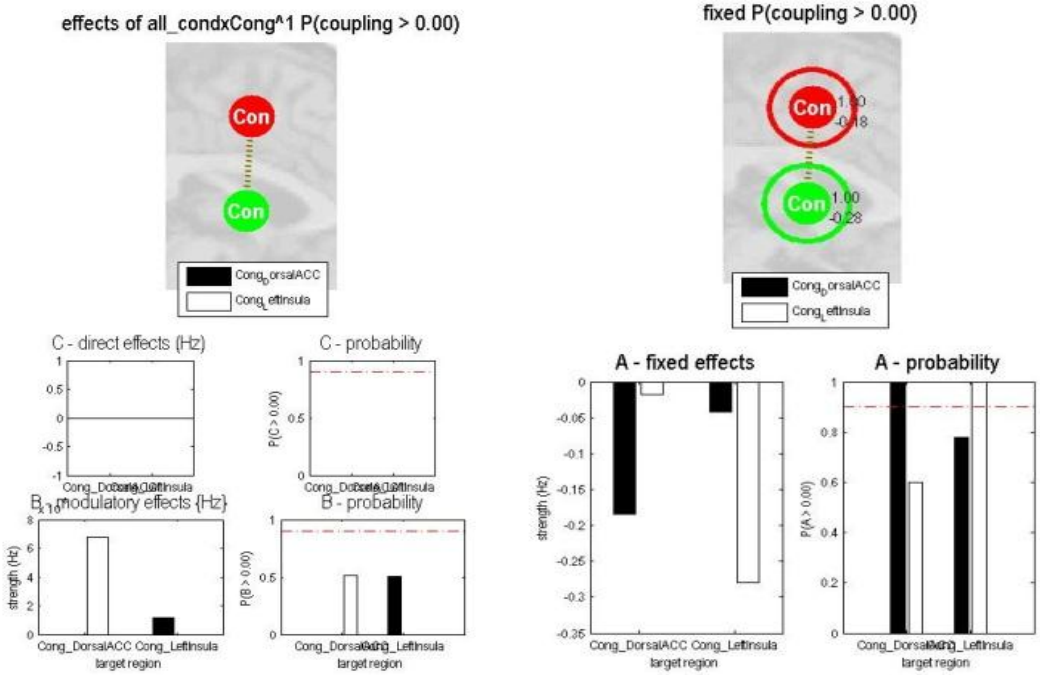


Figure C4: Model 4

In model above, we can see considering connection between two regions without applying stimuli directly on regions, there is not any change in activity and connectivity.

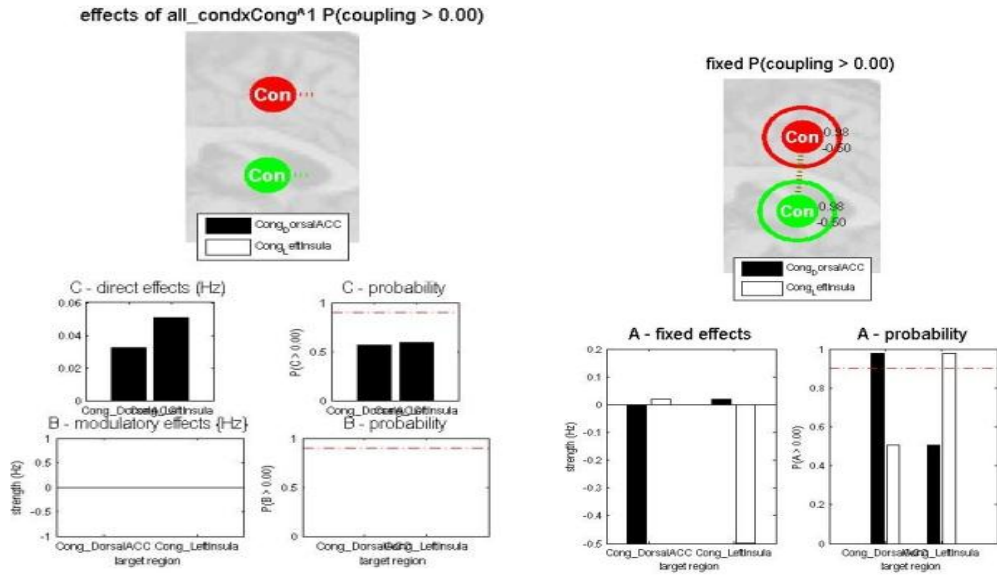


Figure C5: Model 5

This model is like model 3 and 4. Here also the probability of choosing such a model is low. We don't see any B matrix in this model. Effect of congruency on LeftInsula is greater than DorsalACC.

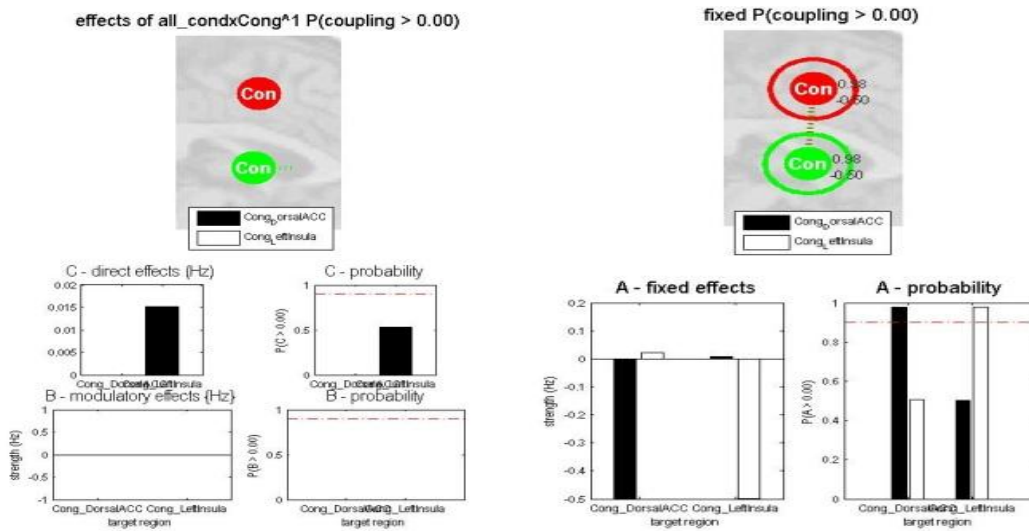


Figure C6: Model 6

As it's clear from graphs, this model, like previous models, could not change connectivity. In such models the connection nearly disappears.

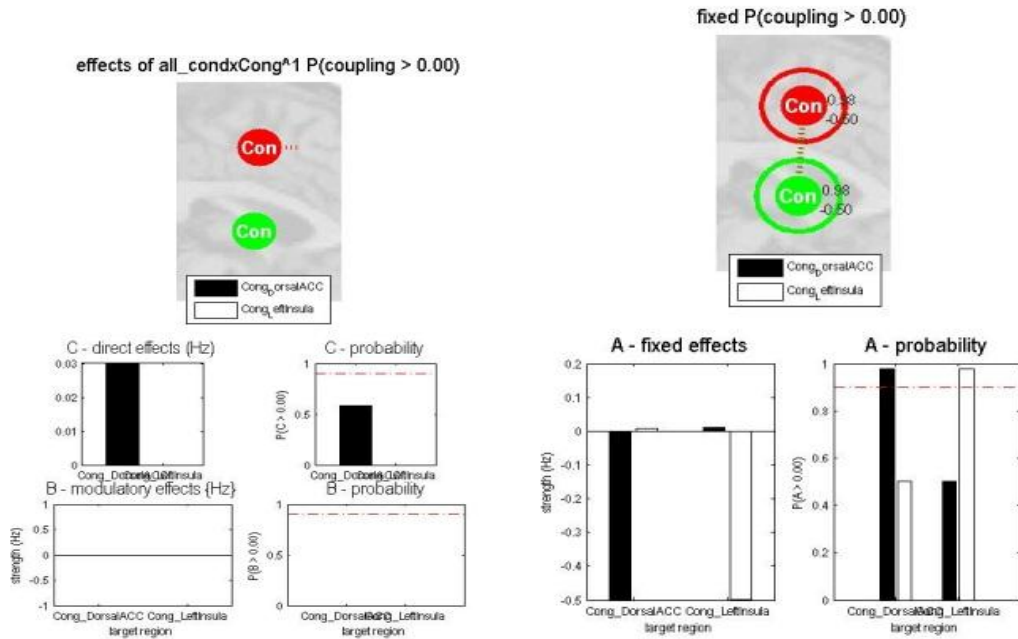


Figure C7: Model 7

In model above the only difference with model6 is increasing in effect of stimulation on DorsalACC.

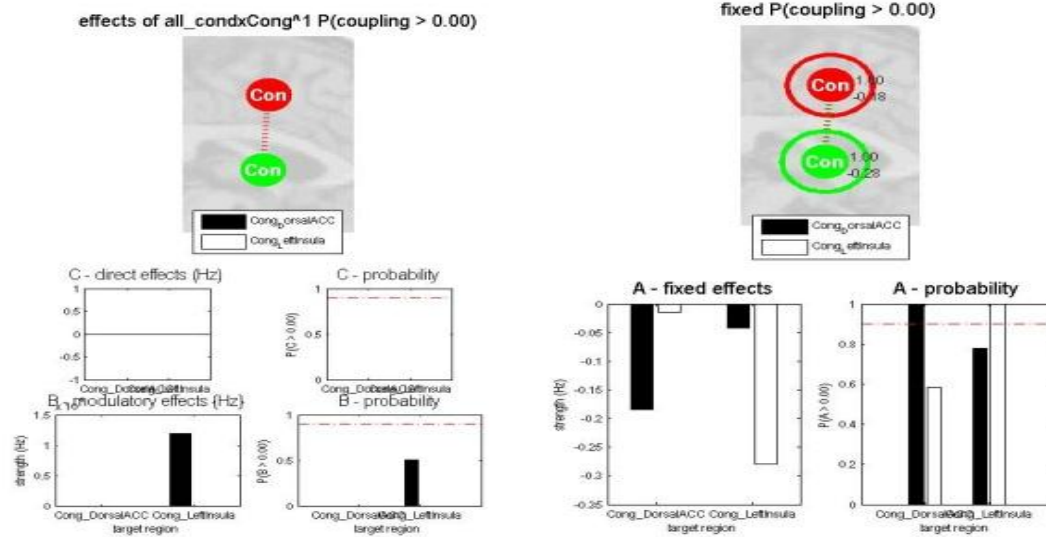


Figure C8: Model 8

This model does not have any effect on connection and as we see there is an acceptable probability to have an increase in connection from LeftInsula towards DorsalACC.

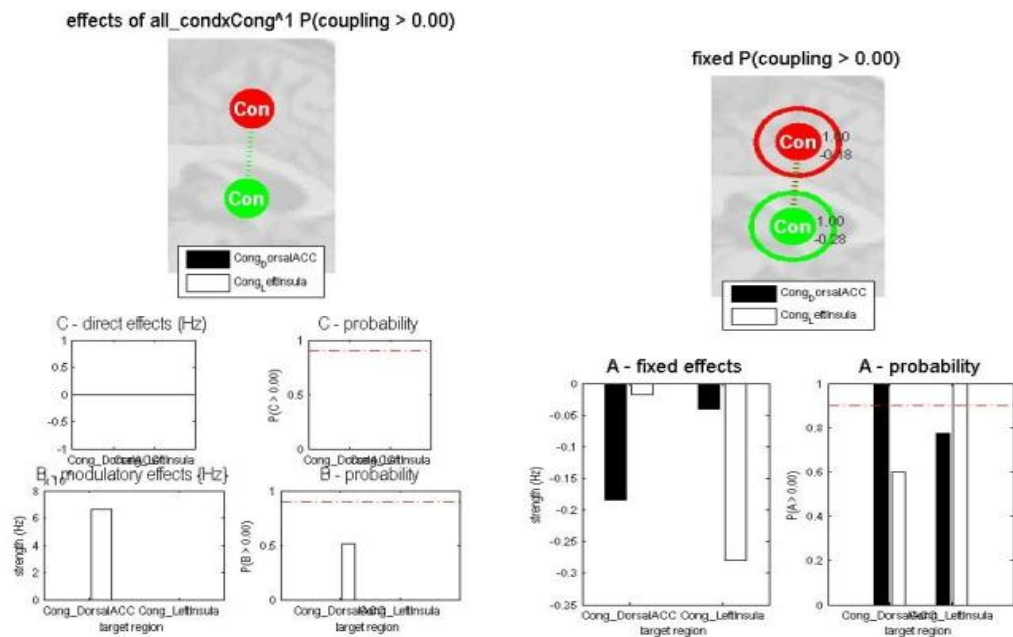


Figure C9: Model 9

There is not so much difference between model 8 and 9.

The graphs above were all the possible models for analyzing congruency in regions DorsalACC and LeftInsula.

In the same way, I did analyze other situations and 9 models for any situation.

#### 4.2.2 Congruency\*Valance: RostralACC and VentralACC

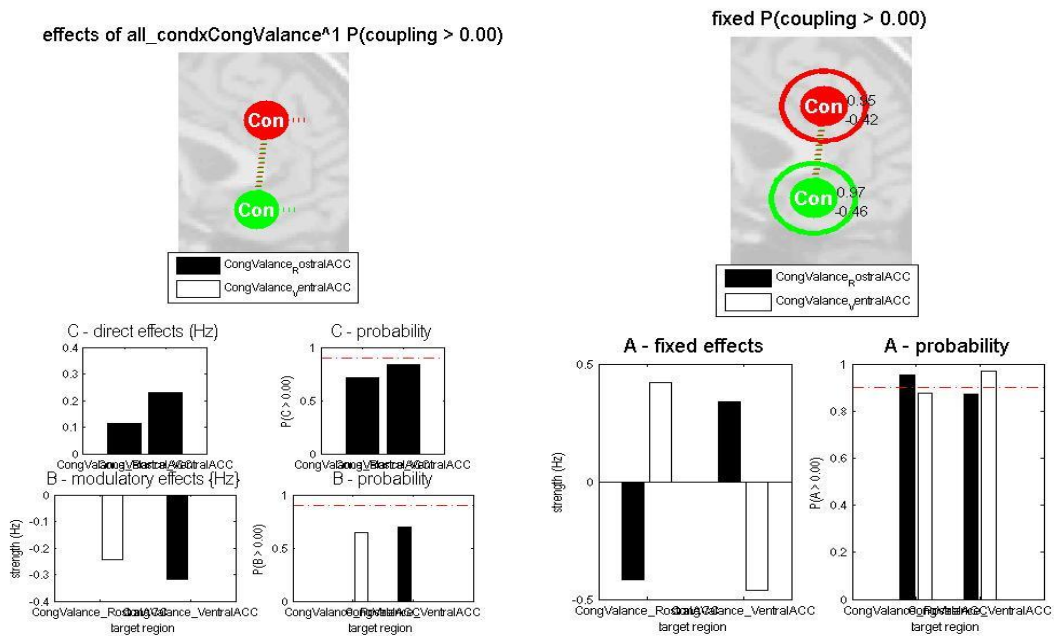


Figure C10: Model 1

This is a model which shows applying stimuli directly on both regions and connections, will results in a decrease in effective connectivity. Effect of stimulation on connections is in a negative direction. This means that for example by effecting connection from RostralACC to VentralACC. The probability of reducing connectivity by this model is high enough to be acceptable.

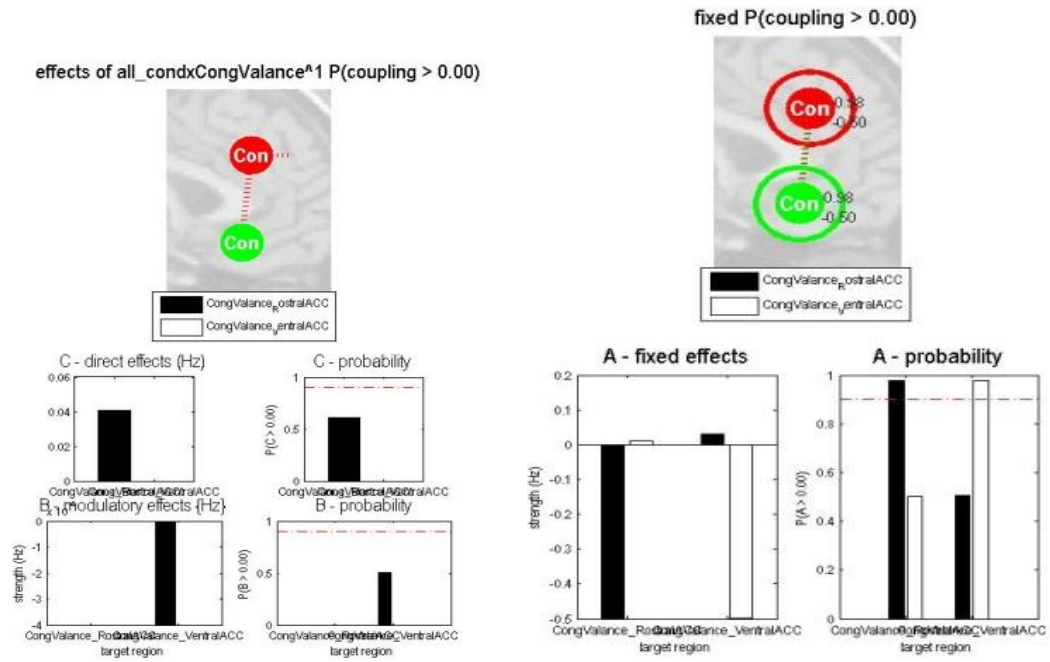


Figure C11: *Model 2*

By this model we can see great decrease in connectivity but the probability of this model is low.

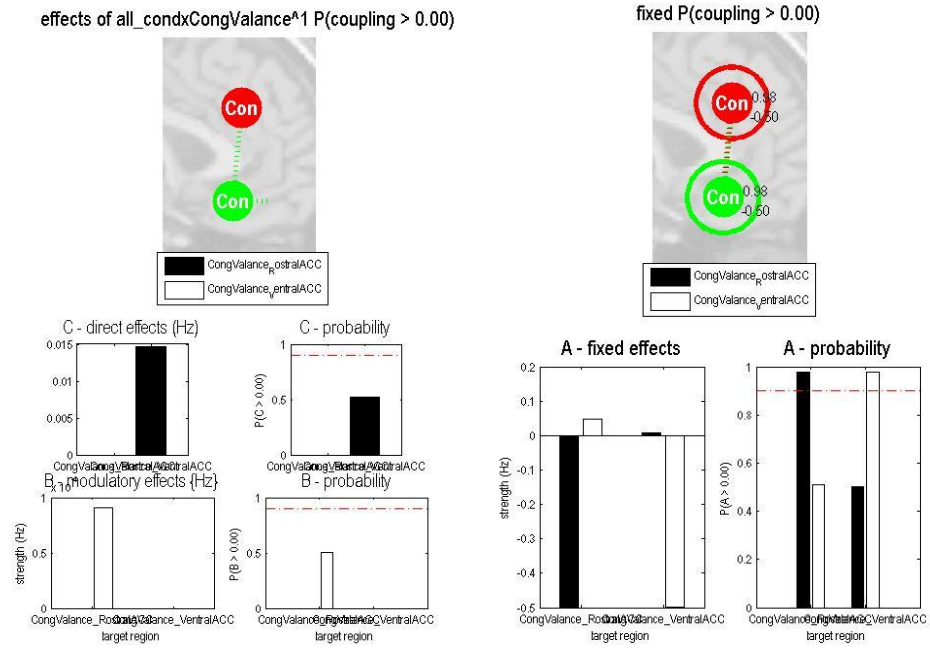


Figure C12: Model 3

This model like previous model has a low probability but in this model we also see a great increase in connectivity. Direct effects on regions and connections are very small.

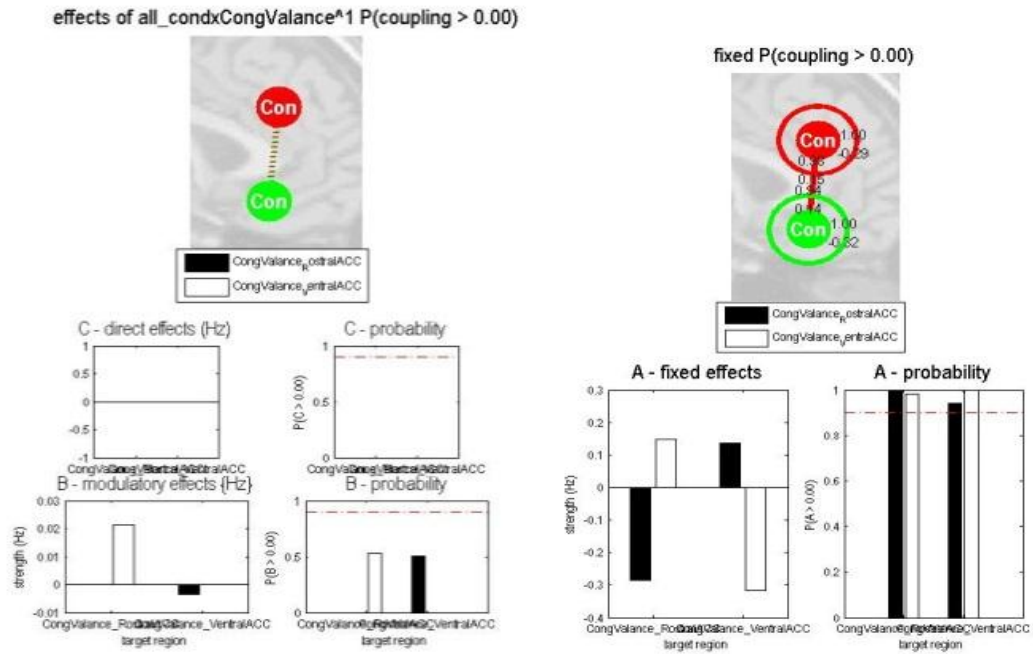


Figure C13: Model 4

This model as seen does not have effect on connectivity and can illustrate our model. Probability of B is small.

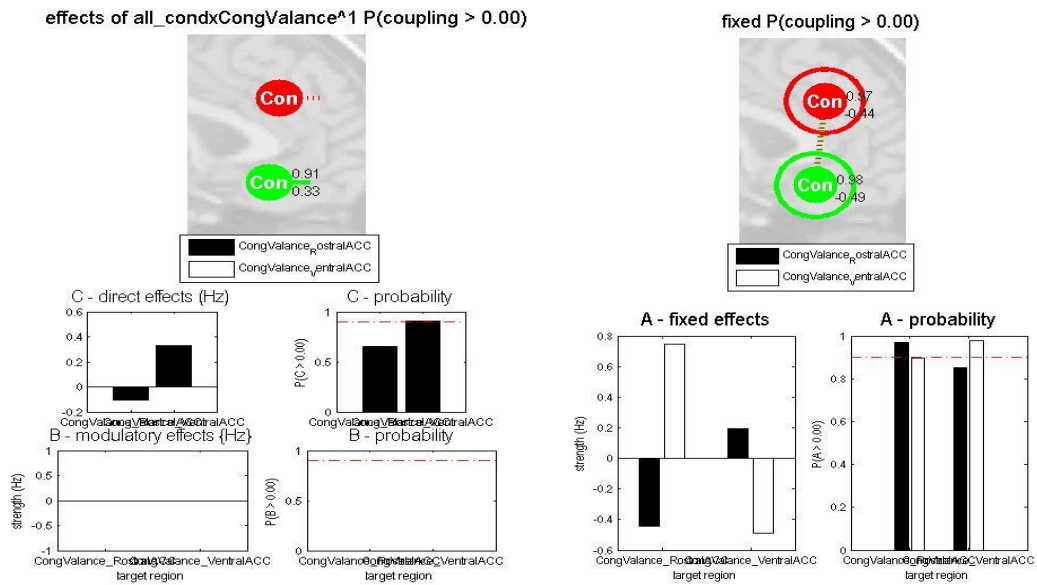


Figure C14: Model 5

This could be another model which is so close to the situation of testing intrinsic connectivity. Applying stimuli on only regions can increase connection between regions in the direction from RostralACC towards VentralACC.

Probability of applying stimuli directly on VentralACC is almost 90% and is very possible.

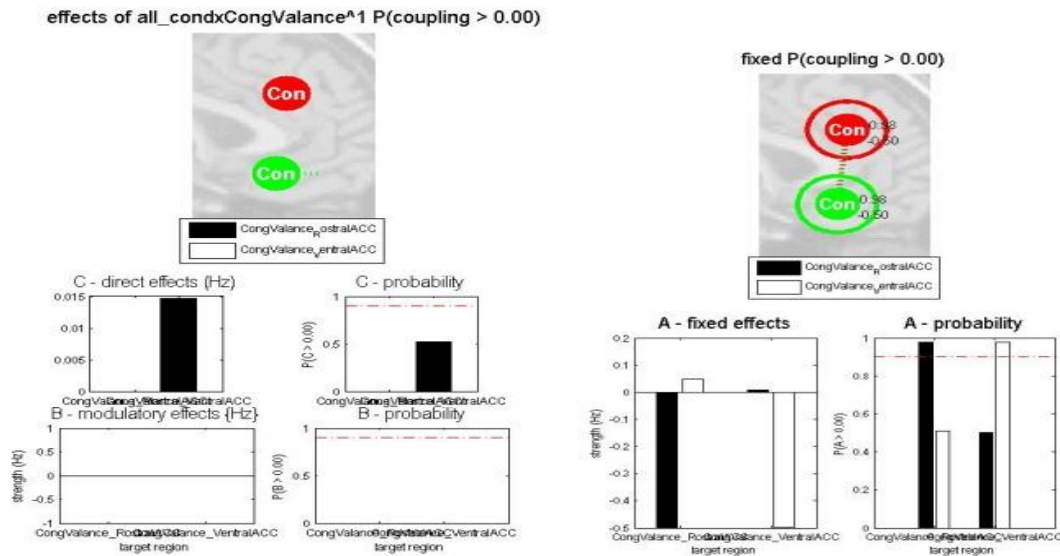


Figure C15: Model 6

This model shows decrease in connectivity. C here takes small parameters and the probability of this model is low.

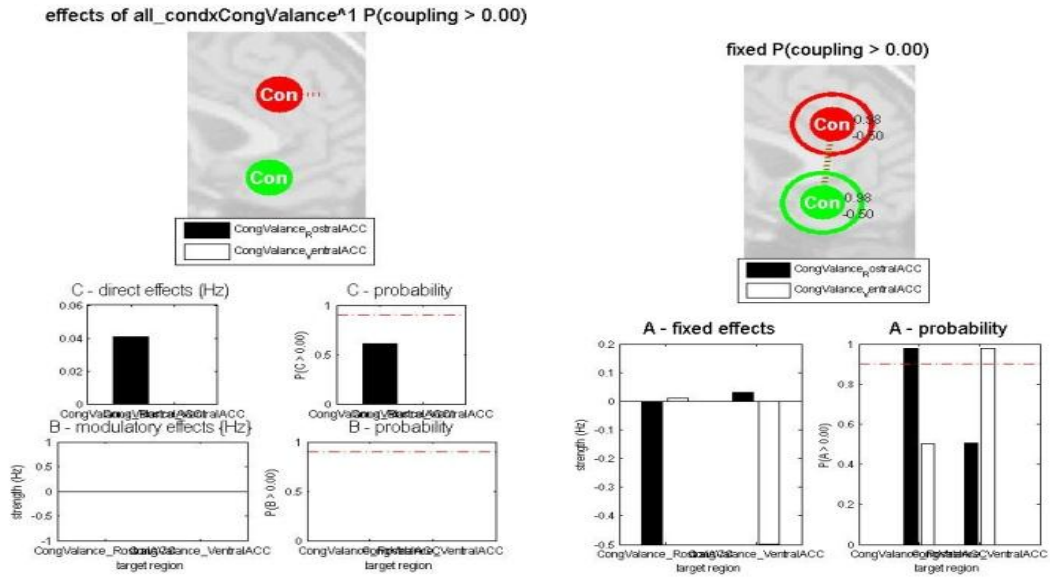


Figure C16: Model 7

This model is so similar to model 6. The probability of happening this condition is low.

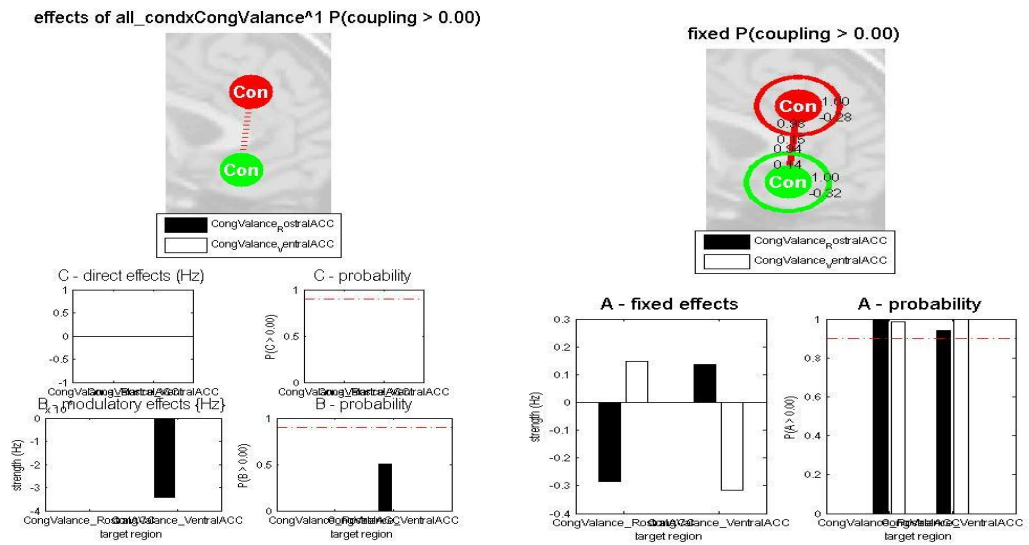


Figure C17: Model 8

In this model we don't see any acceptable changes by applying stimuli directly to connection but as it's obvious there is a high probability of choosing this model. Effect of B here is negative and means that connection from RostralACC to VentralACC decreases in power so we are sure that in this condition there is an increase in connection in reverse direction.

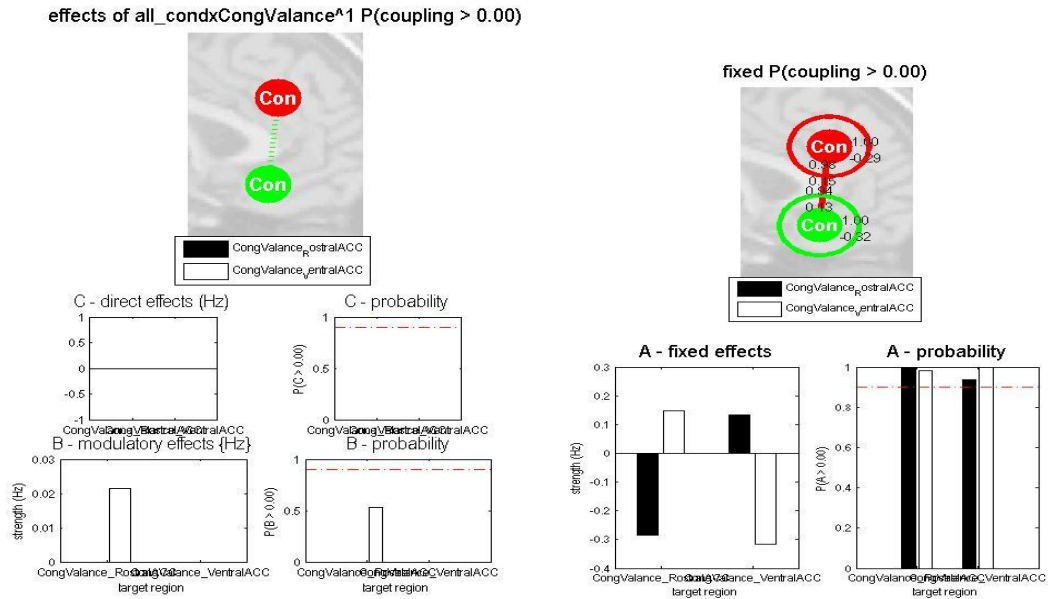


Figure C18: Model 9

This model is also like previous model, shows almost no changes but we can see an small changes in connection from VentralACC to RostralACC here.

#### 4.2.3 Valance: DorsalACC and LeftDLPFC

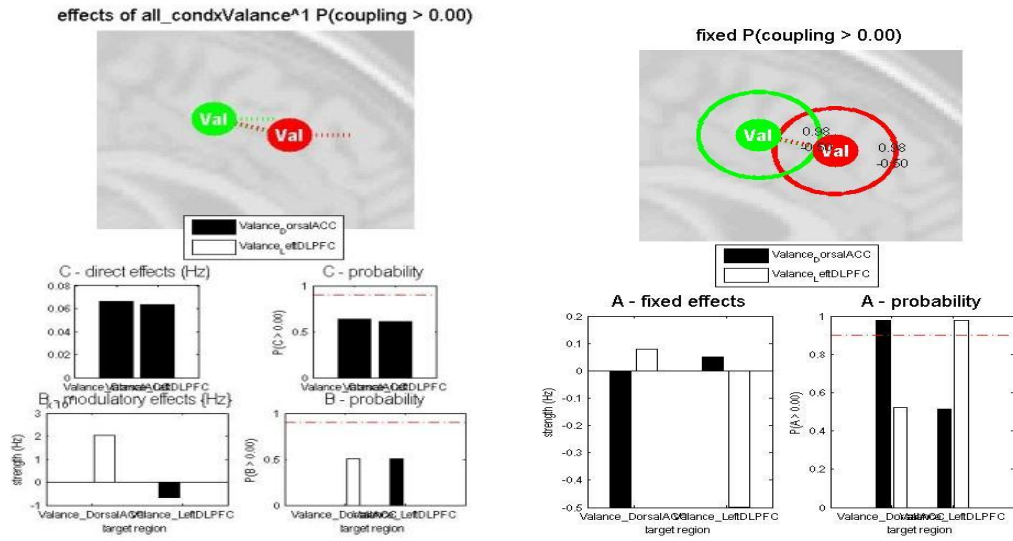


Figure C19: *Model 1*

In the first model, we can see an increase in negative direction for self-connectivity in DorsalACC but there is no change in connectivity. The only issue is an increase in probability of happening such a model. Direct effect of stimuli on both regions and connections is small.

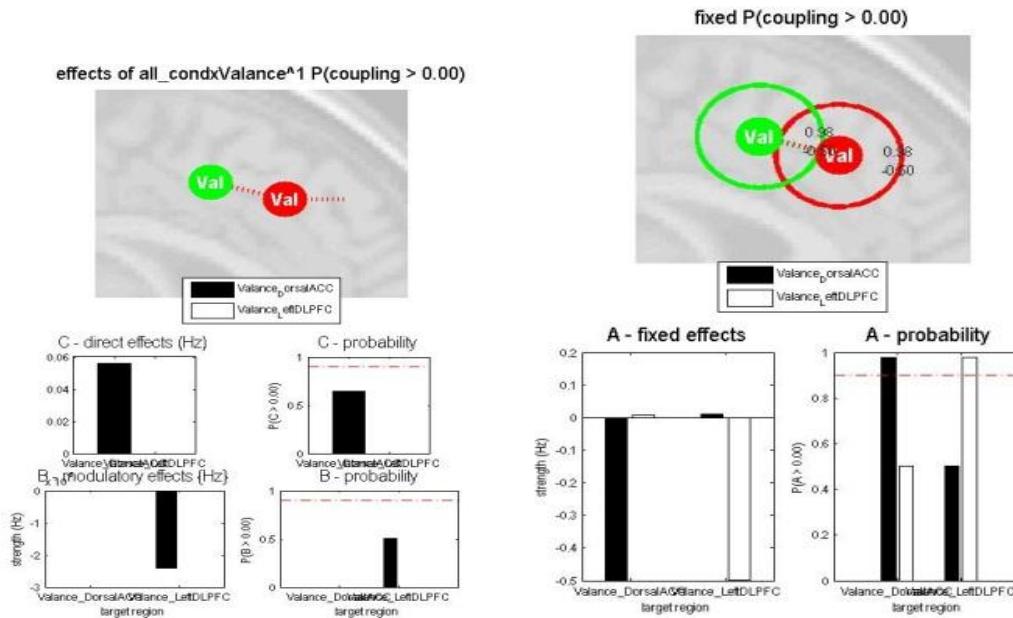


Figure C20: *Model 2*

There is a decrease in connectivity by using this condition. Reverse effect of stimuli on connection between regions is observable. Probability of this model is low.

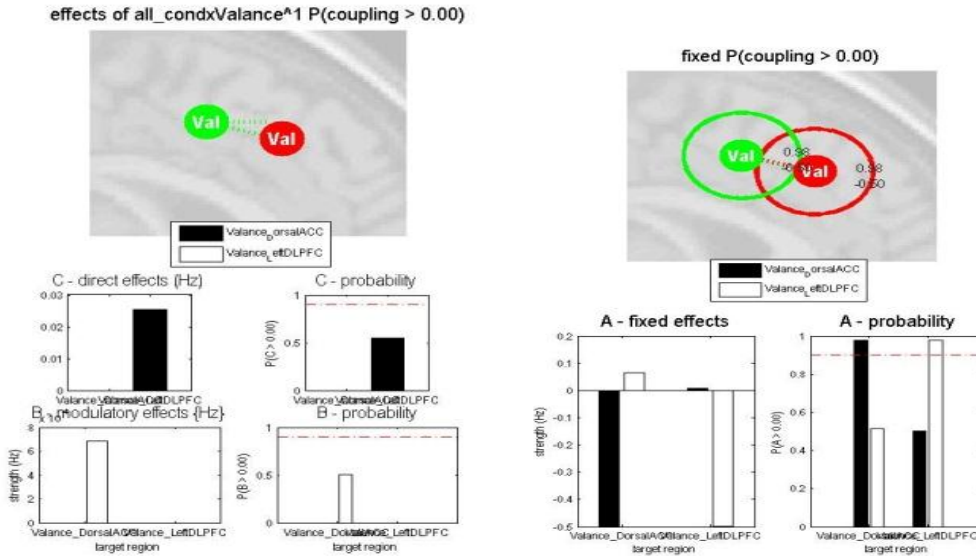


Figure C21: Model 3

In model 3, the connection from DorsalACC to LeftDLFPC seems to be unchanged but we can see decrease in reverse connection by applying stimuli to region LeftDLFPC and connection from this region towards DorsalACC.

Probability of this model is also very low.

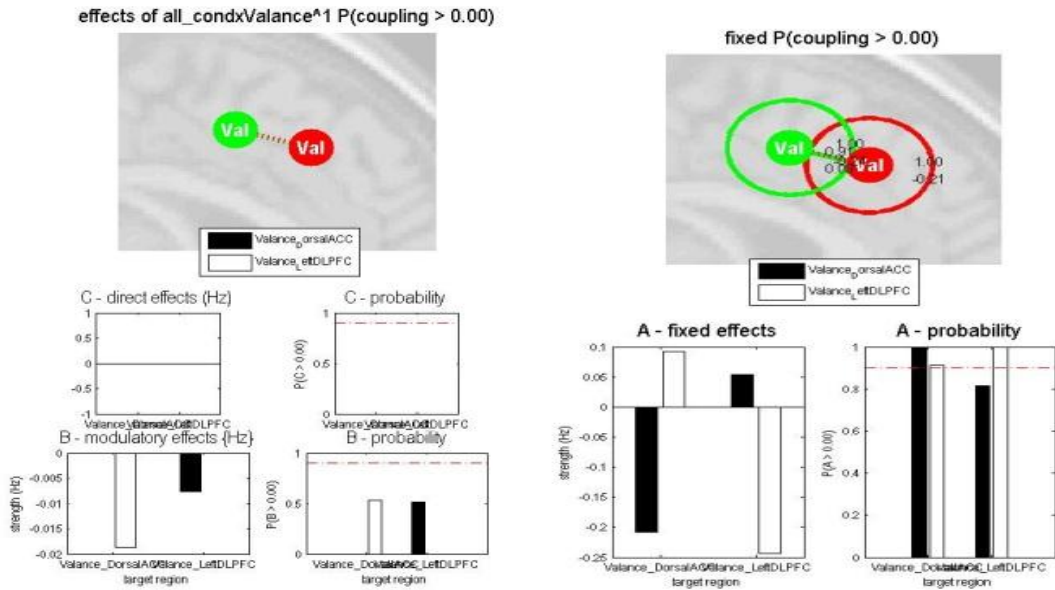


Figure C22: *Model 4*

This model looks like the model without any stimulation if we look at connectivities. There is a reverse increase in connections between regions. By applying valance to connection from DorsalACC to LeftDLFFC, we can see an increase connection but in negative direction which means by applying this stimuli, there will be decrease in the connection in forward direction and an increase in reverse direction.

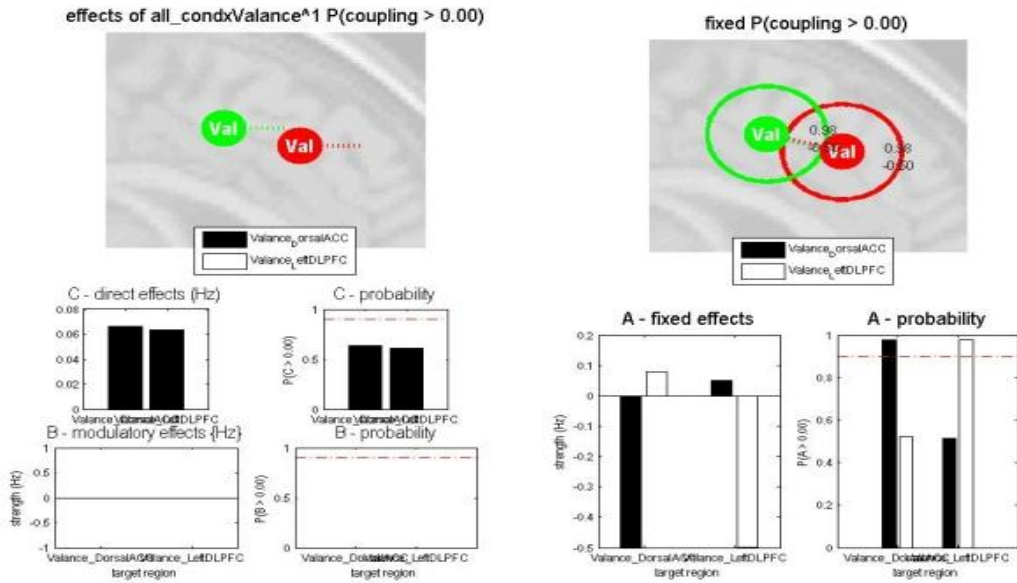


Figure C23: Model 5

This model shows an increase in self connectivities of regions and almost no change in effective connectivity.  
 Direct effect of valance on these two regions is very small in amount so that it just results in an increase in self-connectivity.

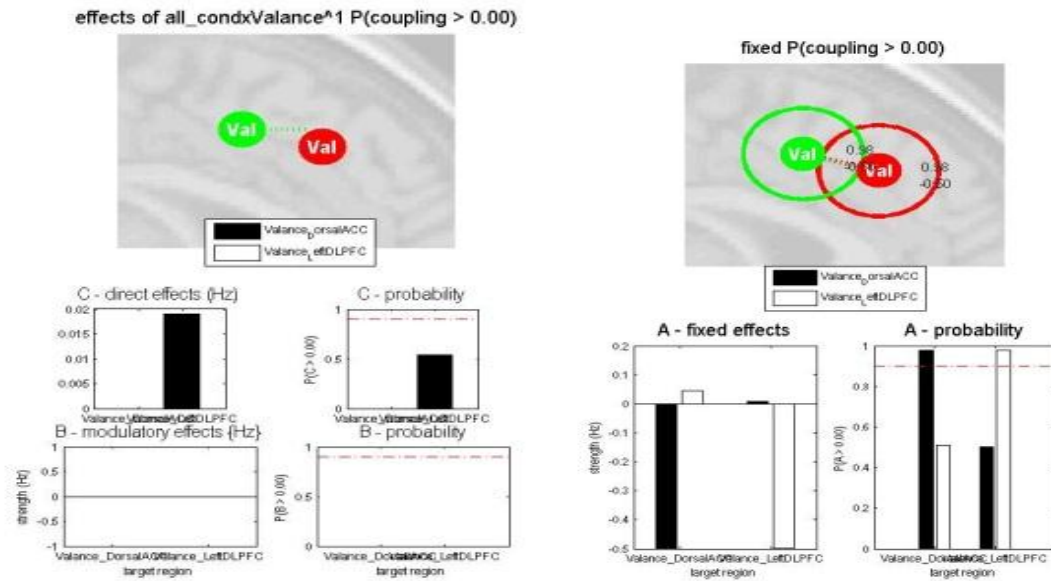


Figure C24: Model 6

In this model we have direct effect on LeftDLPFC and as it's obvious from graphs there is a great increase in self connectivity and decrease in effective connectivity between regions.

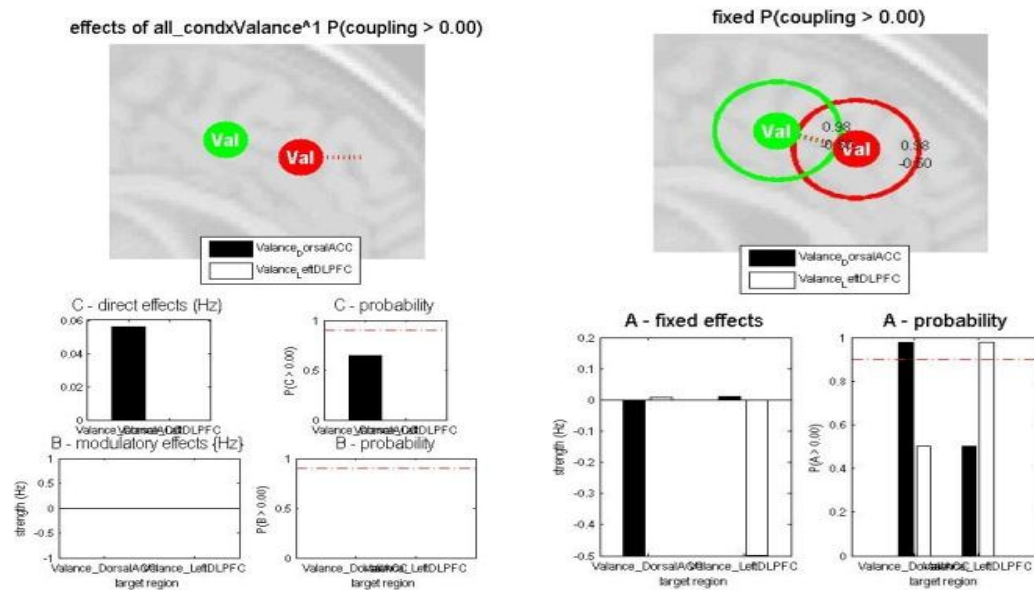


Figure C25: Model 7

Effective connectivity in this model between regions is already zero and there is a small effect of valance on DorsalACC. Probability is also so small.

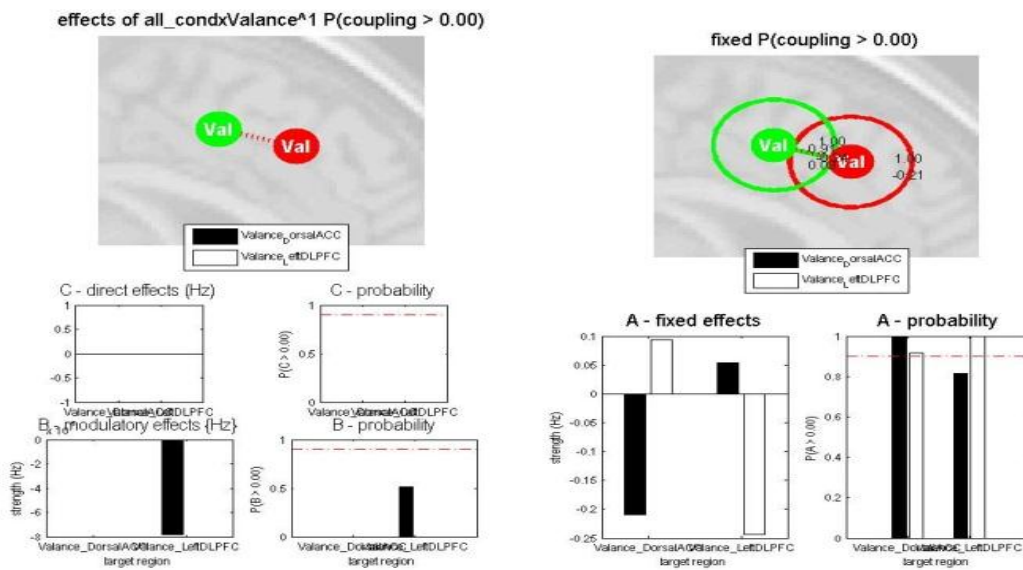


Figure C26: Model 8

Applying valance to the connection from DorsalACC towards LeftDLPFC is not able to change connectivity in a positive or negative direction. There is also a great decrease in amount of connection from LeftDLPFC to DorsalACC. The probability for this model is also high.

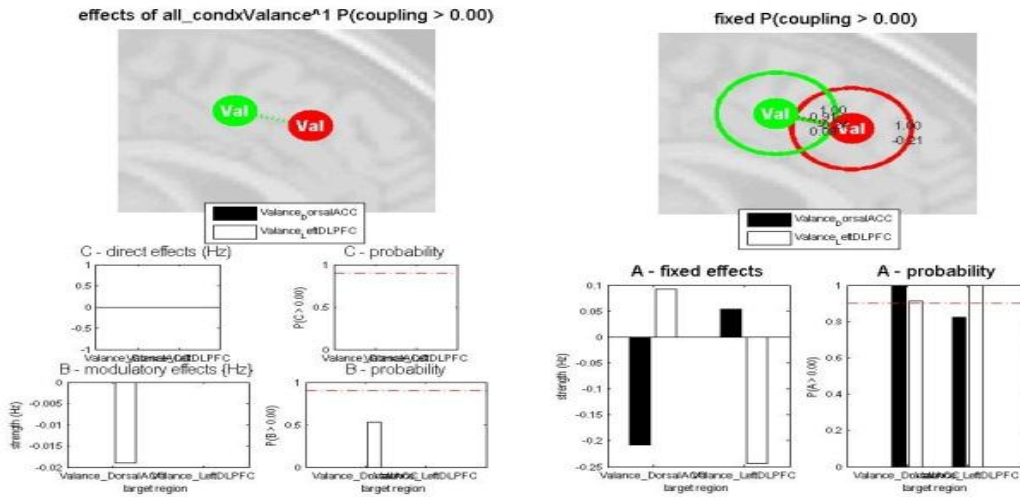


Figure C27: Model 9

This model is so similar to the previous model discussed. The only difference is in entrance of stimulation which in this model it enters to the connection of leftDLFFC to DorsalACC in negative direction. The reverse connection will be positive.

#### 4.2.4 Valance: DorsalACC and RightDLFFC

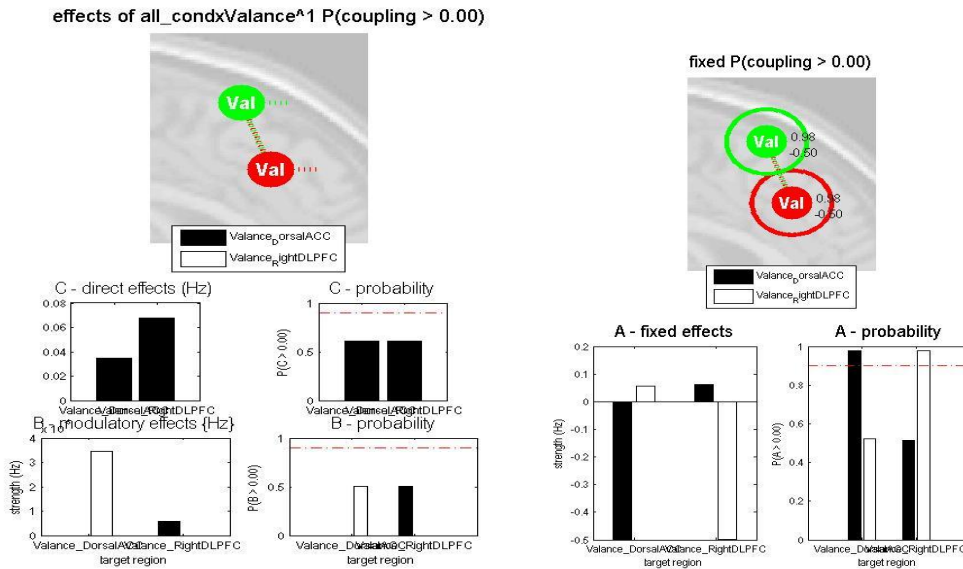


Figure C28: Model 1

Considering this model we see great differences in both regions. Changes in self connectivity and effective connectivity. Direct effects of valance on regions and connections are almost zero. The probability of such a model is very low.

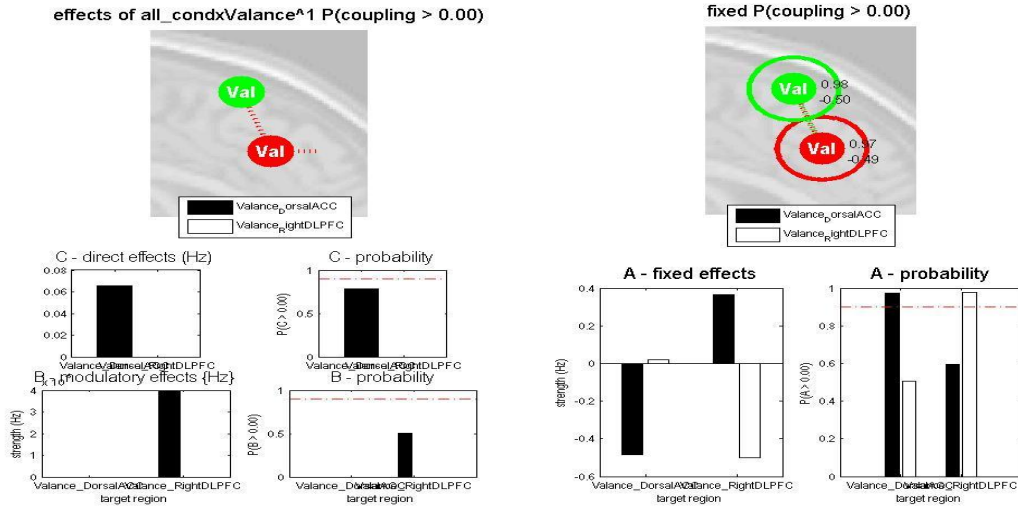


Figure C29: Model 2

Effective connectivity from DorsalACC to RightDLPFC decreased by applying stimuli while we observe an increase of the effective connectivity in reverse direction. Probability of effecting stimuli directly on region is high but direct effect of stimuli on connections is not considerable.

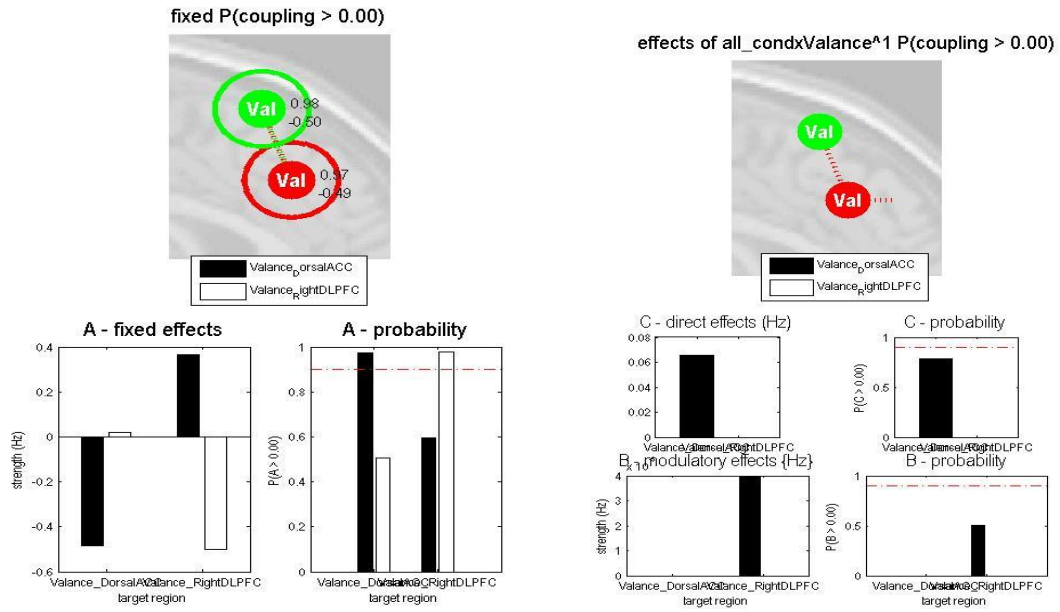


Figure C30: Model 3

Applying stimulation to the RightDLPFC increases the effective connectivity from RightDLPFC to DorsalACC but decreases connectivity in reverse direction. There is also a small amount of direct effect on region and connection between regions.

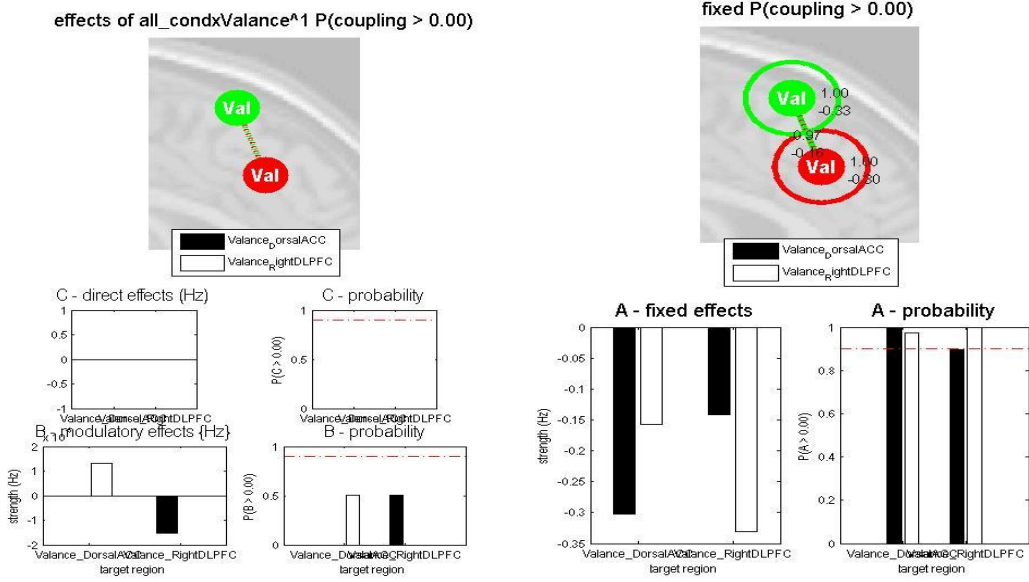


Figure C31: Model 4

This model does not have any effect on effective connectivity between these two regions because as we can see the effect of valance on connections is not high and it is an amount near zero.

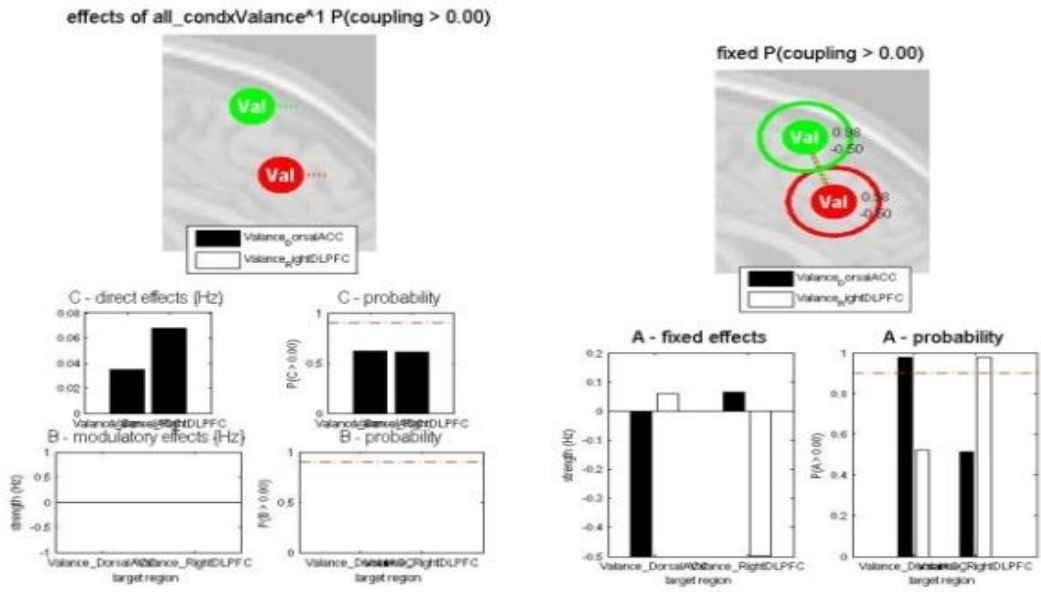


Figure C32: Model 5

A change in effective connectivity is observable in this model. A great self-connection in both regions is seen. Effect of valance in this condition on both effective connectivities is almost same.

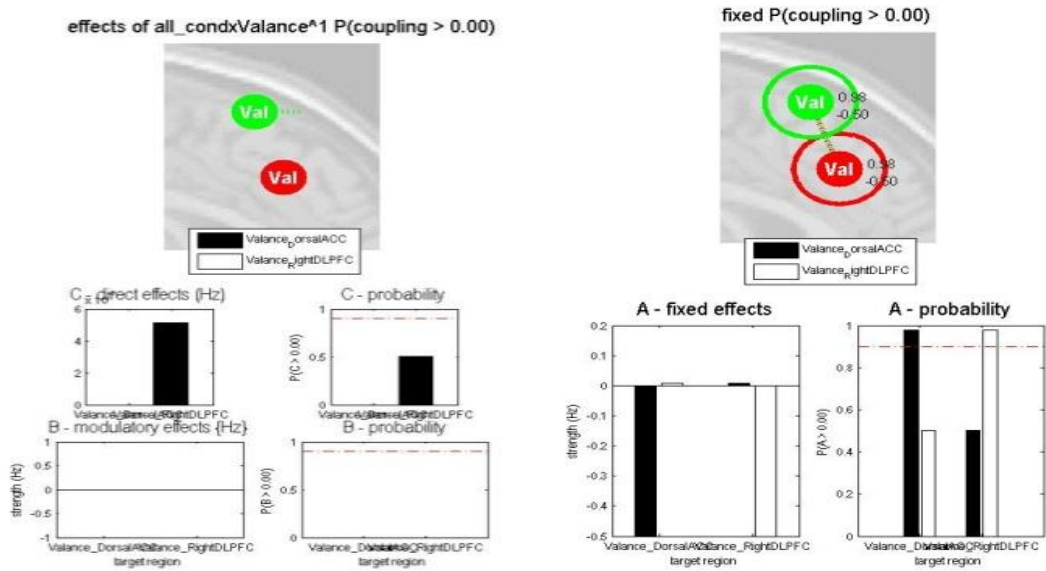


Figure C33: Model 6

Applying stimulation only on RightDLFFC results in a decrease of connectivity for both regions. Effective connectivity is almost zero for this model.

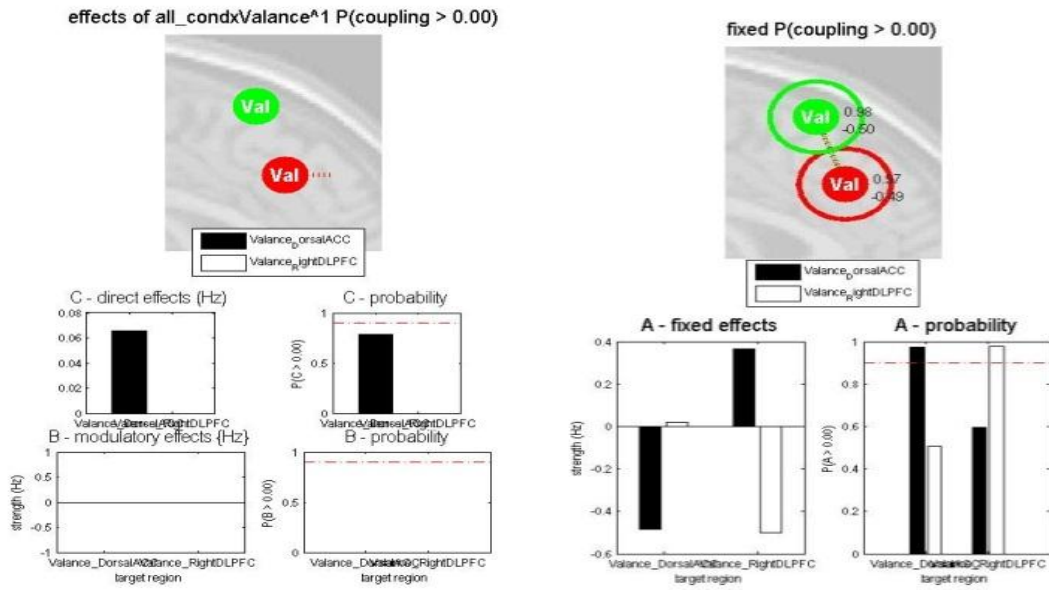


Figure C34: Model 7

Increase in self-connectivity of DorsalACC and decrease in effective connectivity from DorsalACC to RightDLPFC is observable while there is a great increase in connectivity from RightDLPFC to DorsalACC is shown in graphics.

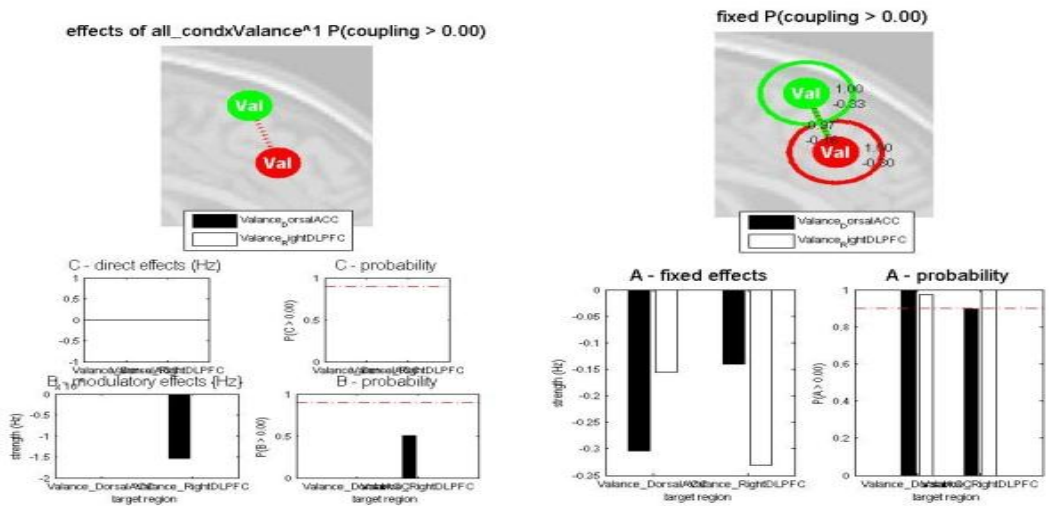


Figure C35: Model 8

This model is so close to the condition that no stimulation was applied. So stimulation applied on connection from DorsalACC to RightDLPFC does not effect model.

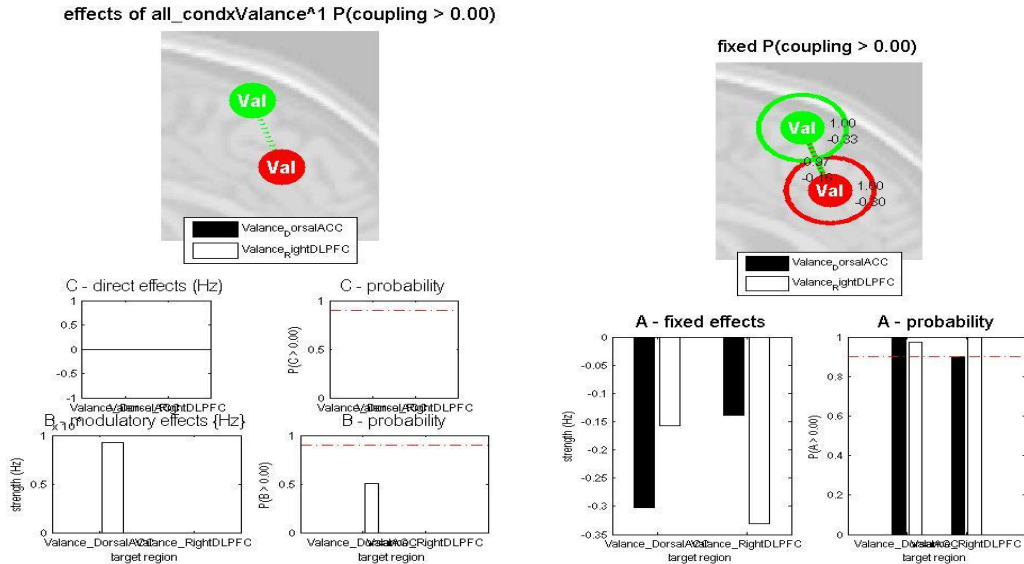


Figure C36: Model 9

Like previous model we can't see any difference here by applying valance directly to connection.

#### 4.2.5 Valance: VentralACC and RightInsula

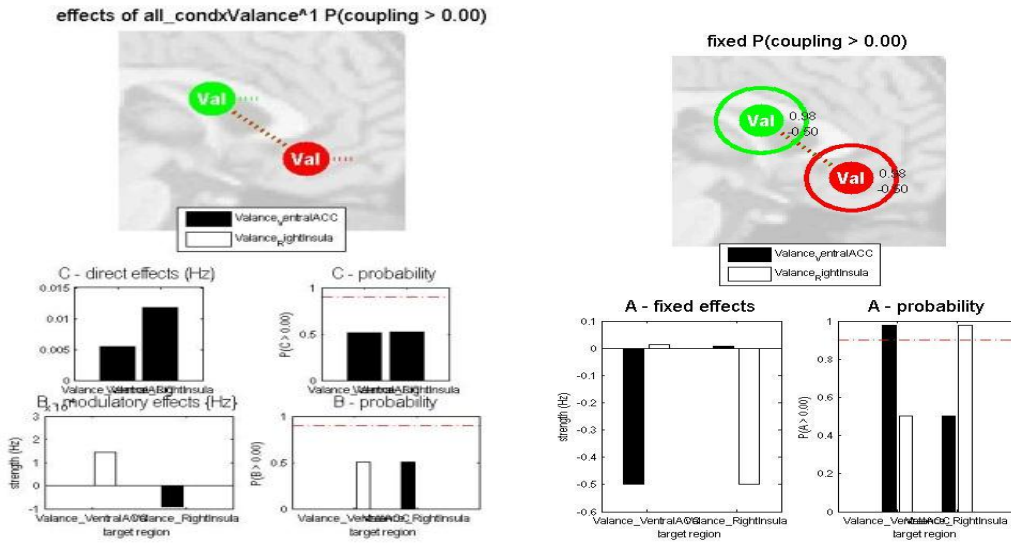


Figure C37: Model 1

There are not observable changes in connectivity in this model. Small amounts of B and C matrices are shown in graphs.

This model is almost the same as model 1 and we can't see any changes in effective connectivity except increase in self-connectivities.

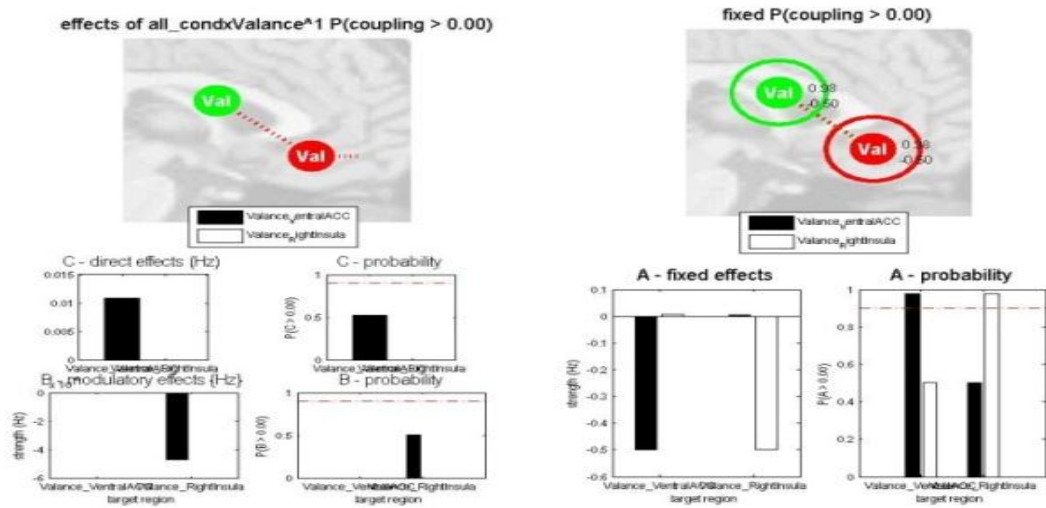


Figure C38: Model 2

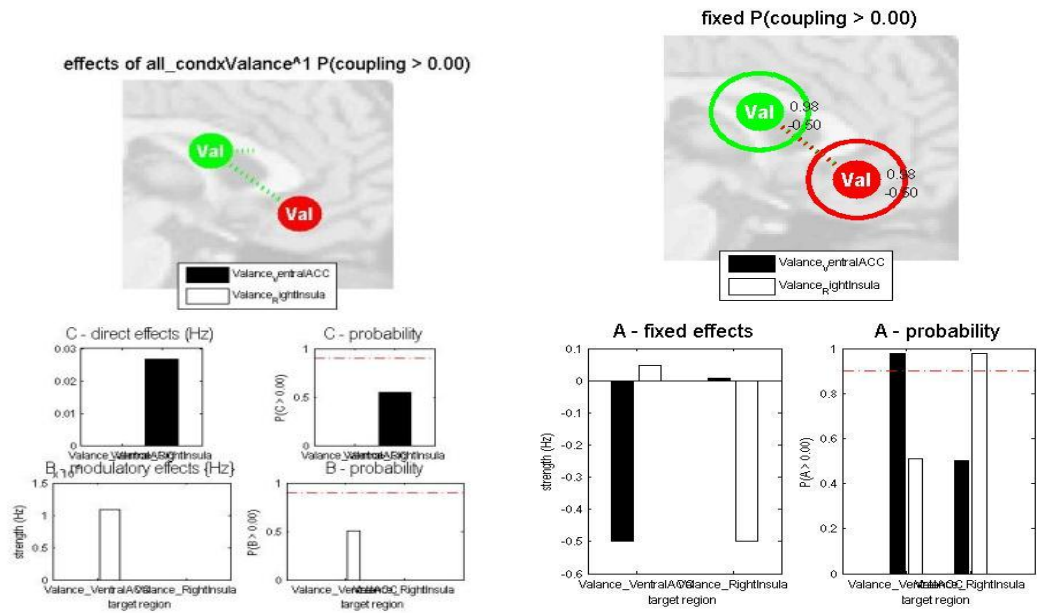


Figure C39: Model 3

This model is also not able to decrease or increase connectivity. Here, self-connections have an increase.

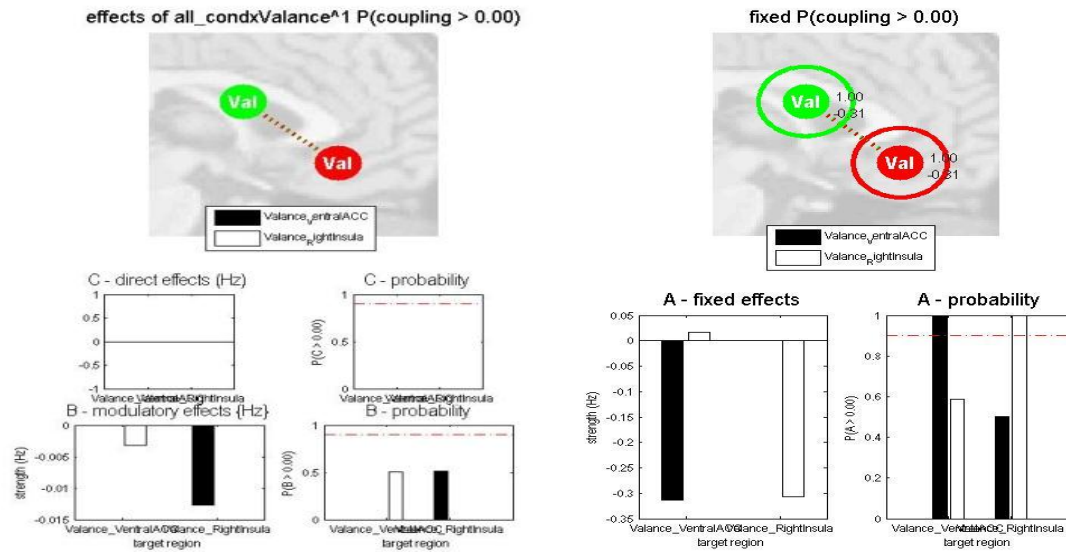


Figure C40: Model 4

Model 4 is same as two previous models discussed above.

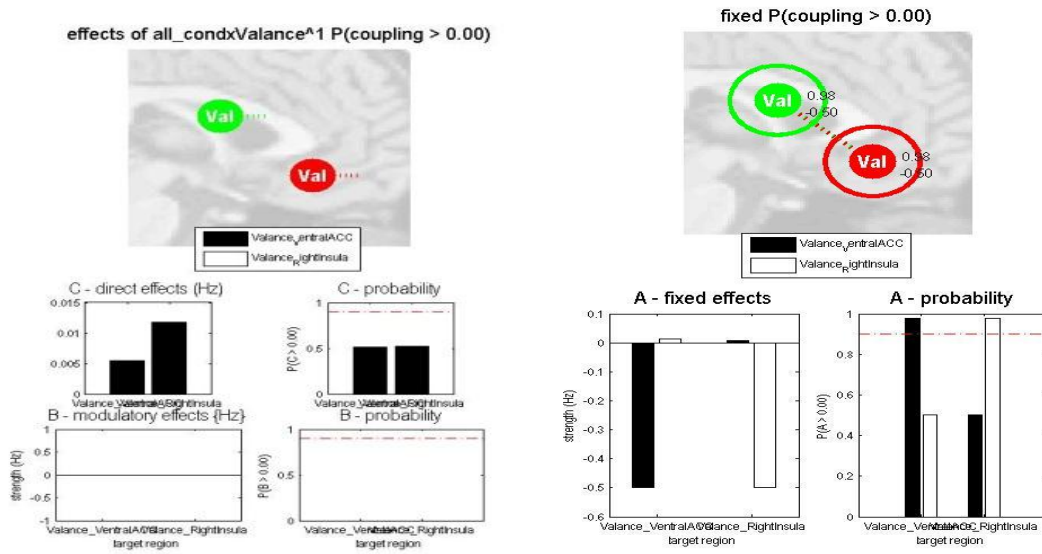


Figure C41: Model 5

Effective connectivity for this model is also zero and we can't see any connection between regions for this model except self-connection.

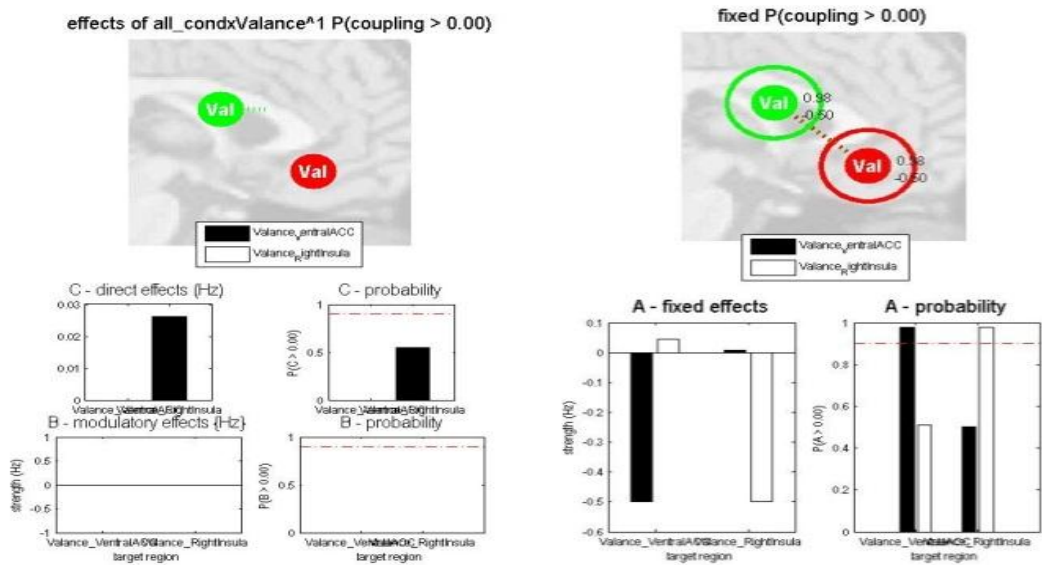


Figure C42: Model 6

Applying valance directly to the RightInsula does not effect effective connectivity between regions. The probability of this model is very low.

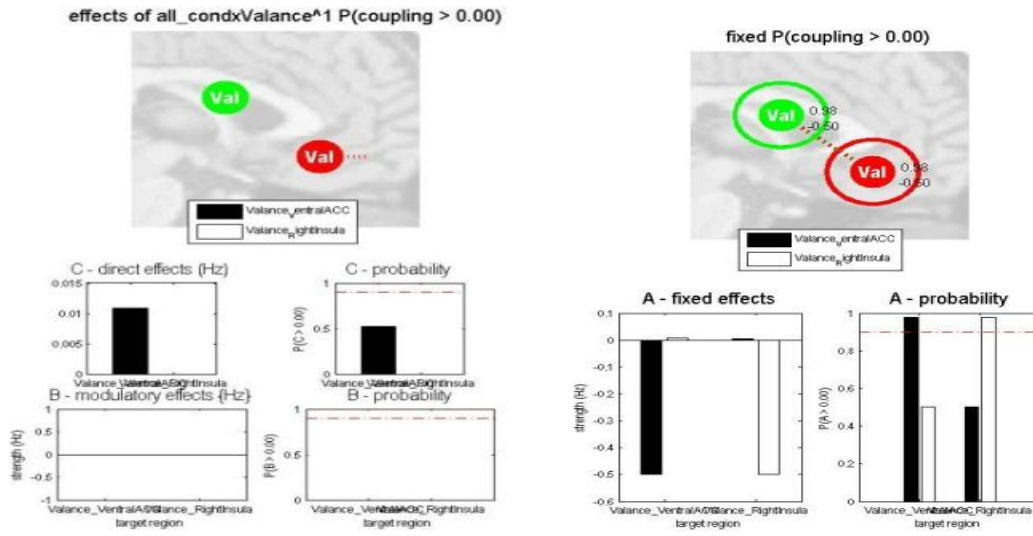


Figure C43: Model 7

This model separates two regions completely so that the connectivity in this condition is zero.

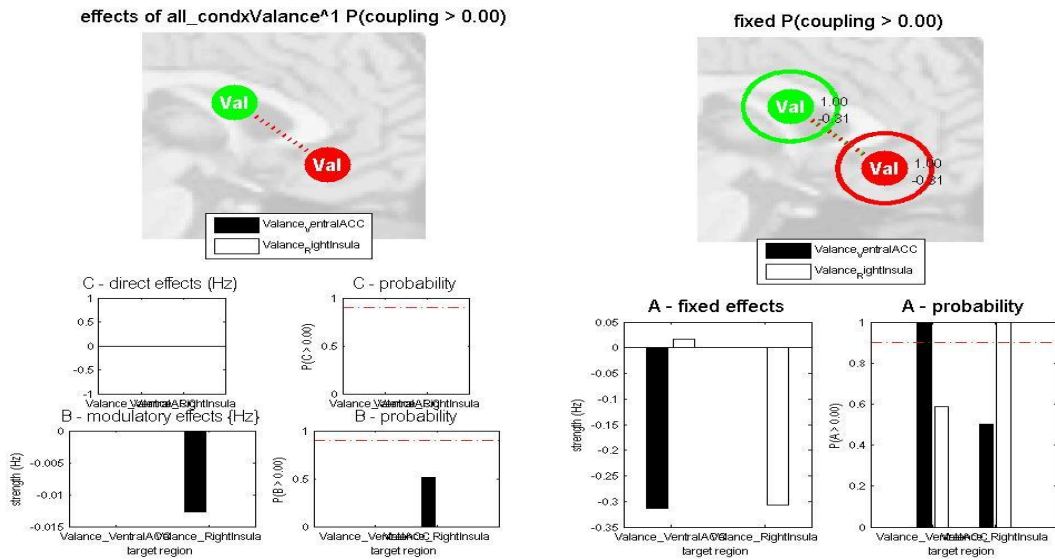


Figure C44: Model 8

In this model we see a small connectivity from VentralACC to RightInsula is observed. This is not true for reverse connection.

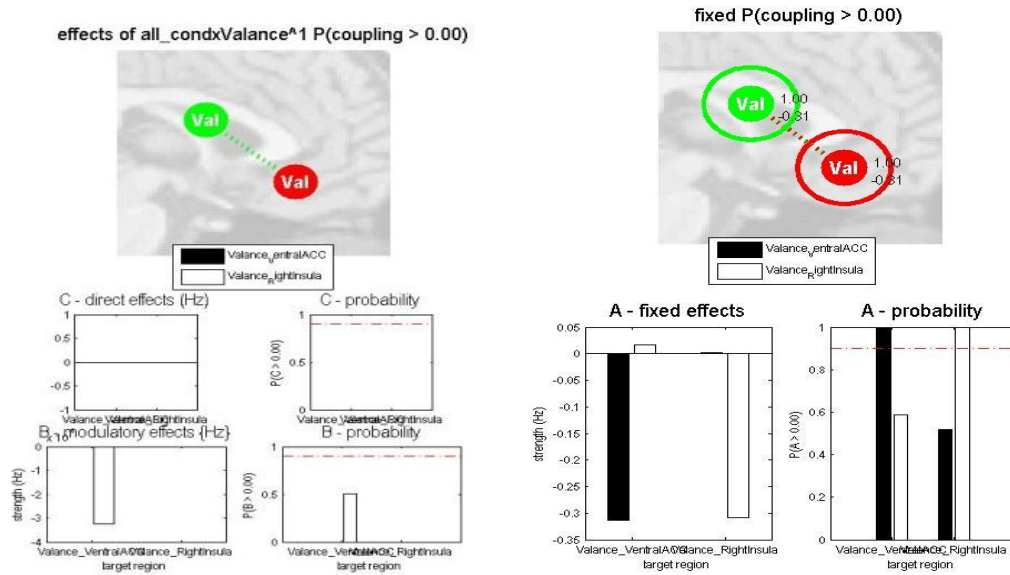


Figure C45: Model 9

This model can't apply changes to effective connectivity between two regions also. Changes in parameters of B matrix of this model and previous model is interesting.

#### 4.2.6 Valance: DorsalACC and VentralACC

This model applies a great decrease in effective connectivity between regions. As its obvious from graphs, the connectivity between regions becomes zero.

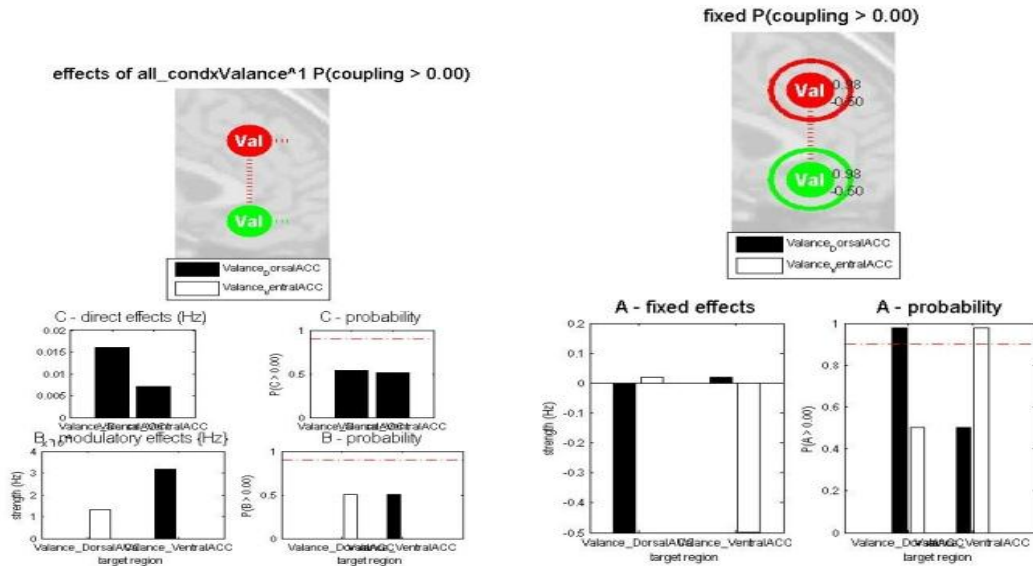


Figure C46: Model 1

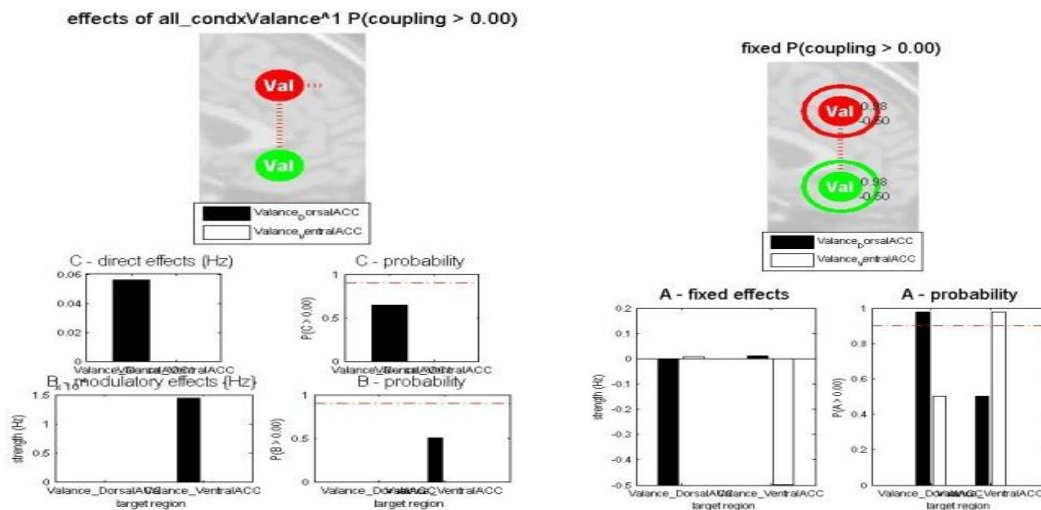


Figure C47: Model 2

Like model 1, this model also shows a decrease in connectivity. Direct effect of valance on VentralACC is very small.

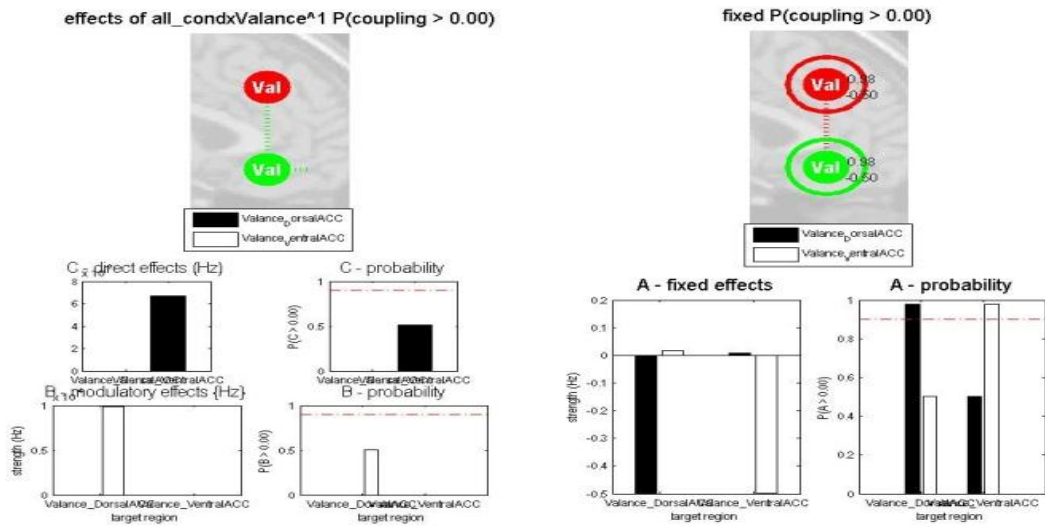


Figure C48: Model 3

Here, we can see that direct effect of valance on VentralACC and connection from this region to DorsalACC will result in a decrease of connectivity between regions and as it's clear from graphs VentralACC did not affected by valance.

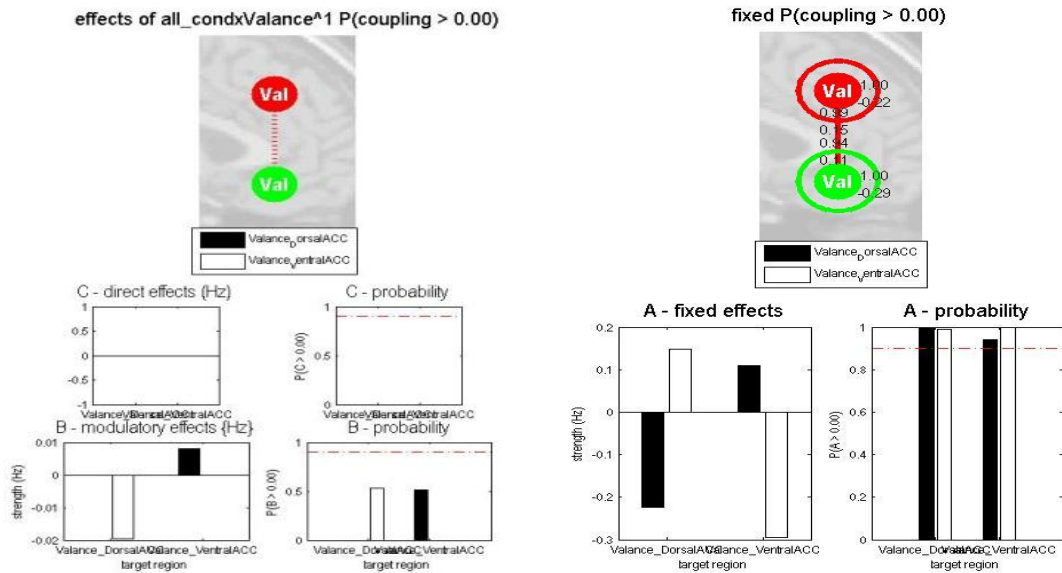


Figure C49: Model 4

Applying valance only on connections did not change connectivity. There is just a small effect on connections could be seen from graphs.

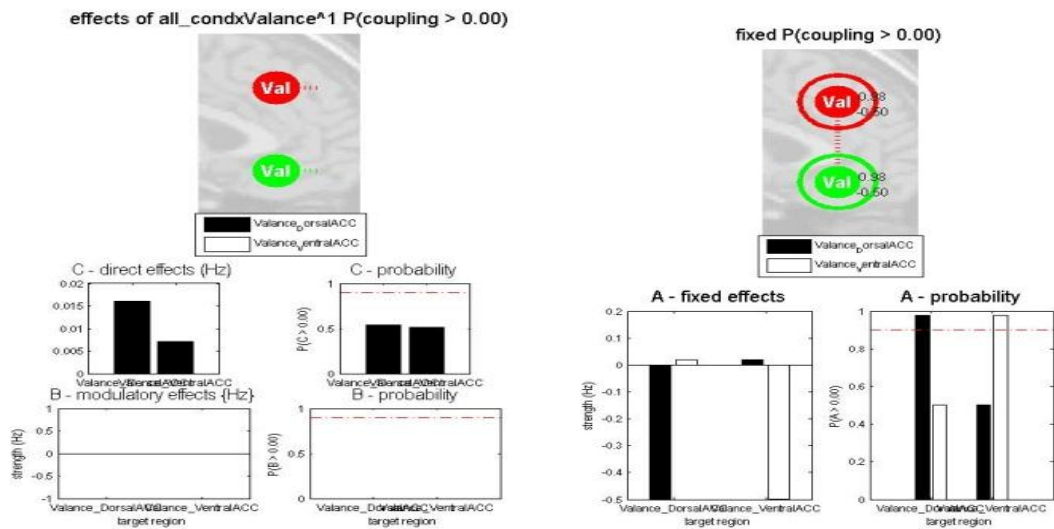


Figure C50: Model 5

Applying valance only on regions results in a decrease of connectivity. Valance has greater effect on DorsalACC than VentralACC.

Even an small effect of valance on VentralACC will be enough to result in a decrease in connectivity between regions as its obvious from graphics below.

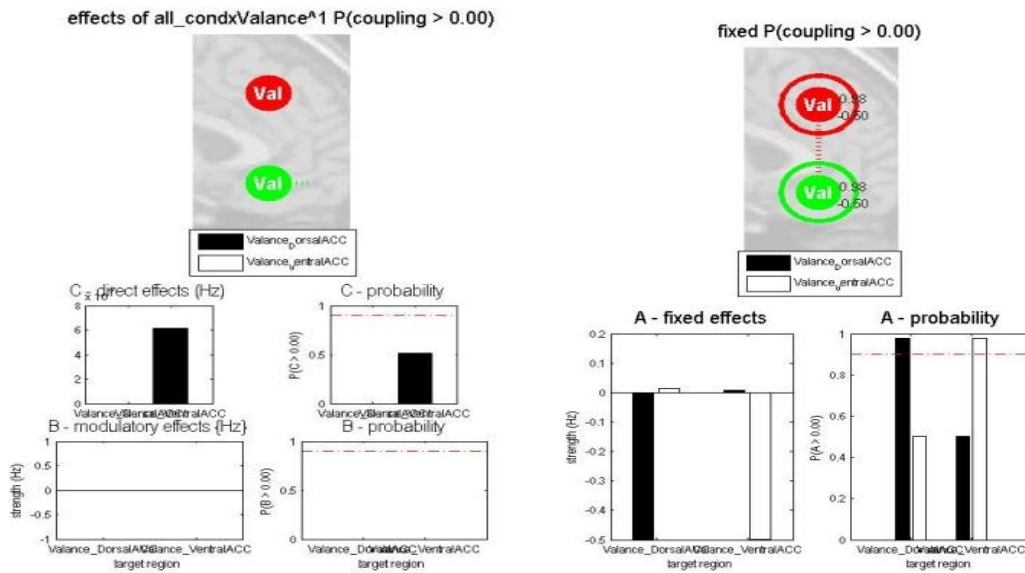


Figure C51: Model 6

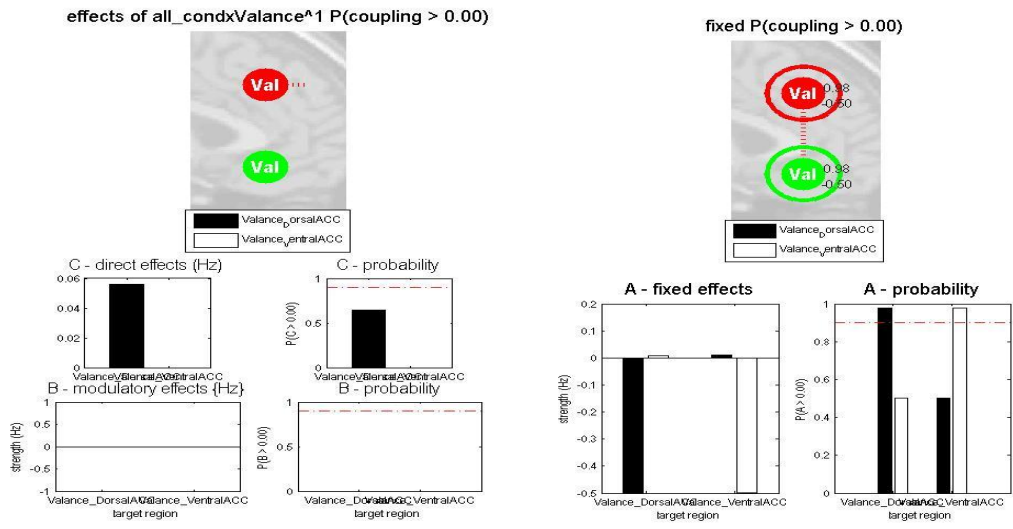


Figure C52: Model 7

Like model 6, any effect on DorsalACC results in a decrease in effective connectivity between regions.

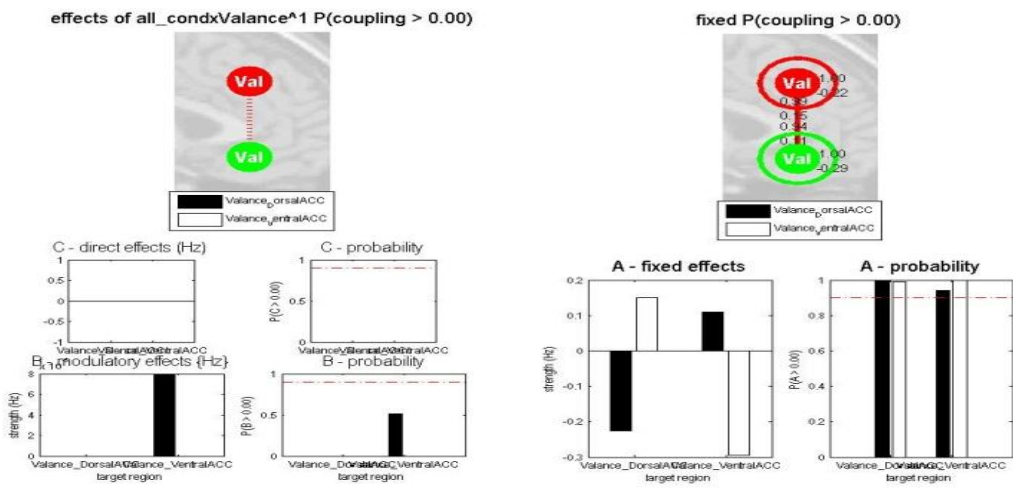


Figure C53: Model 8

Applying valance to the connection from DorsalACC to VentralACC does not have any effect to

connectivity between these two regions. Almost by looking to the B matrix, we can say this connections does not effect by stimulation.

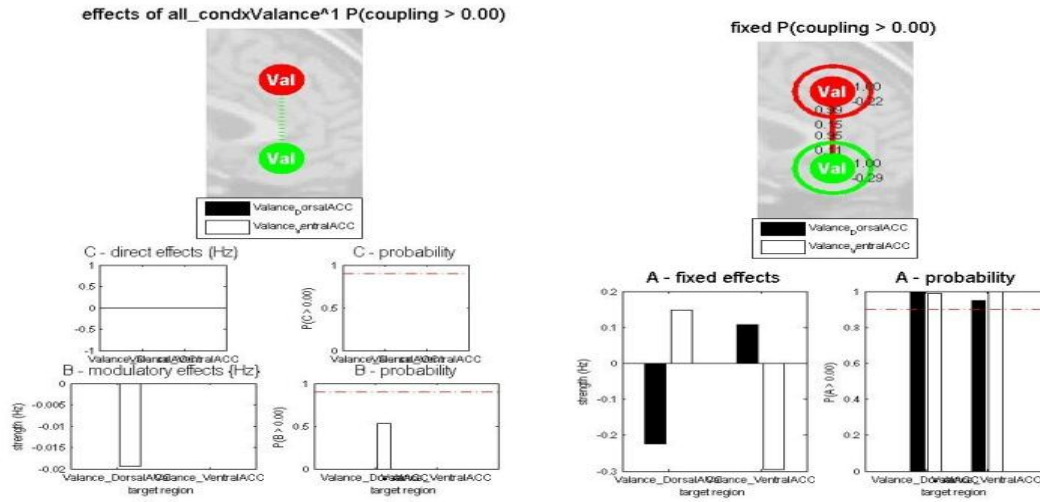


Figure C54: Model 9

This model is also like model 8, can't show any change in connectivity by applying valance to the connection from VentralACC to DorsalACC.

## **APPENDIX D**

### **PPI RESULTS**

We considered nine different regions in brain for PPI method. In all these regions, we found haemodynamic and neuronal responses. The results are shown in graphs. Psychophysiological responses also depicted using graphs and are included in figures. PPI for any of regions mentioned, are achieved and illustrated in graphs. Below we give all graphs mentioned.

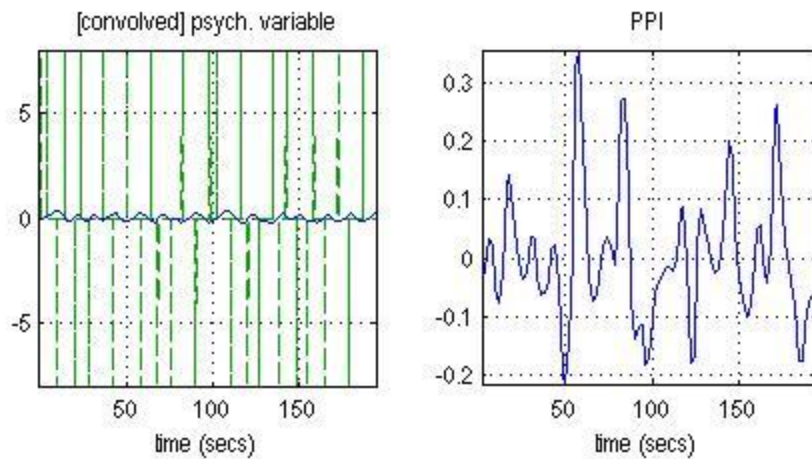
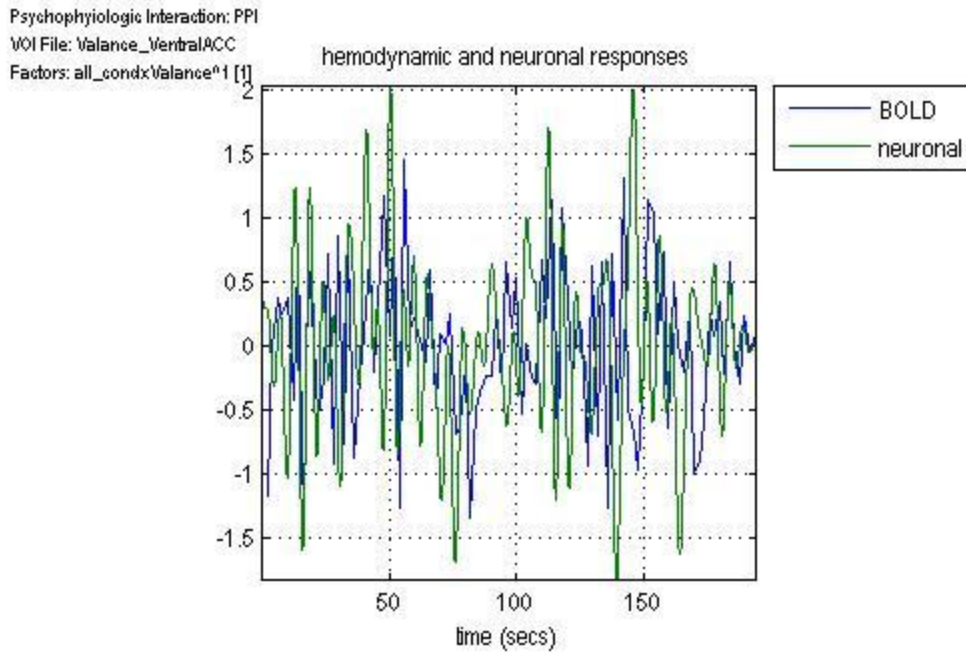


Figure C55. Hemodynamic and neuronal responses for the region VentralACC when stimulation of valance affects that region. Bottom-left graph shows convolution of hemodynamic and neural response for VentralACC. Graph in bottom-right shows psychophysiological response of region VentralACC to the stimulation of Valance.

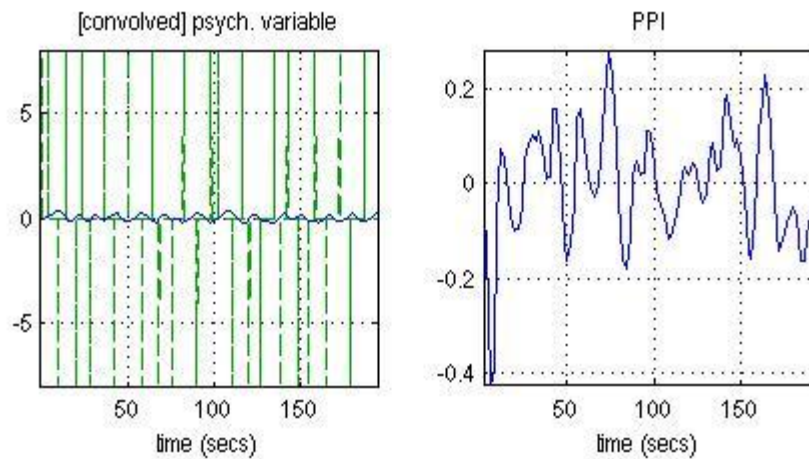
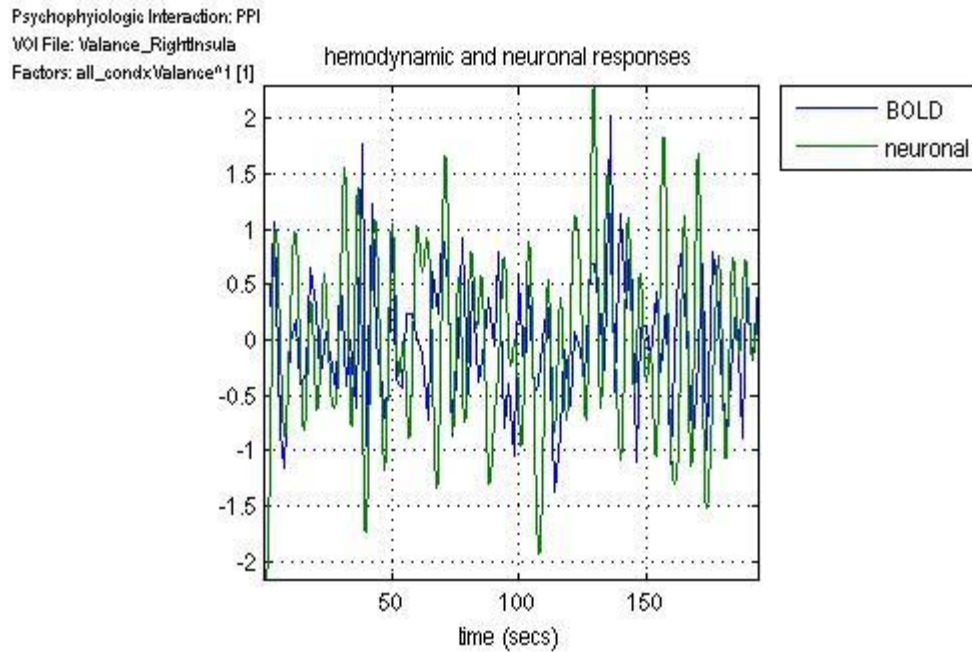


Figure C56. Hemodynamic and neuronal responses for the region RightInsula when stimulation of valance affects that region. Bottom-left graph shows convolution of hemodynamic and neural response for RightInsula. Graph in bottom-right shows psychophysiological response of region RightInsula to the stimulation of Valance.

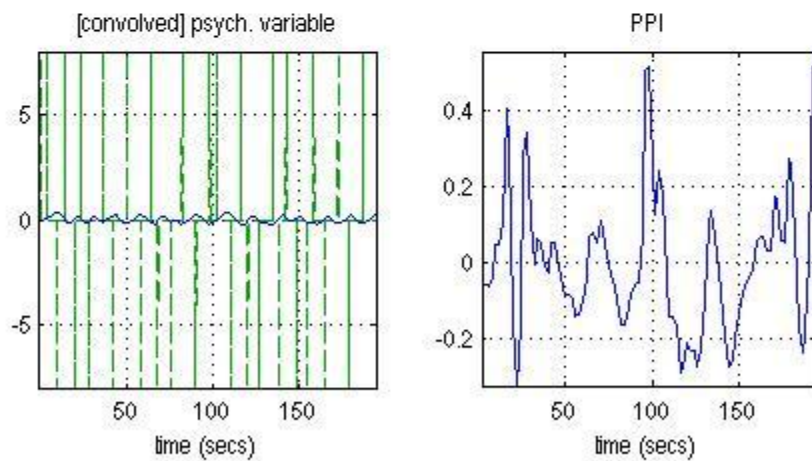
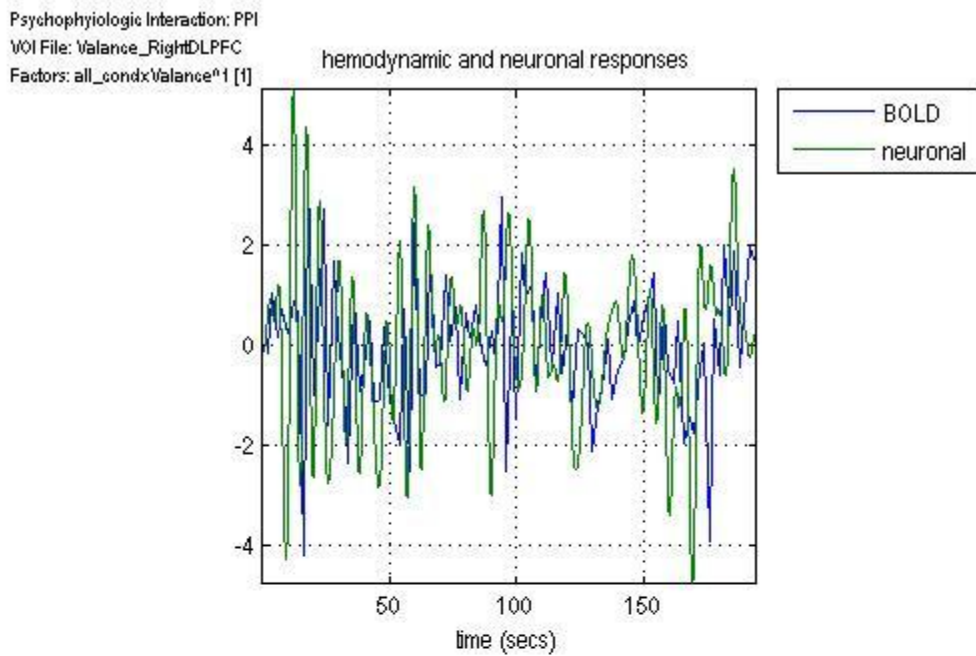


Figure C57. Hemodynamic and neuronal responses for the region RightDLPFC when stimulation of valance affects that region. Bottom-left graph shows convolution of hemodynamic and neural response for RightDLPFC. Graph in bottom-right shows psychophysiological response of region RightDLPFC to the stimulation of Valance.

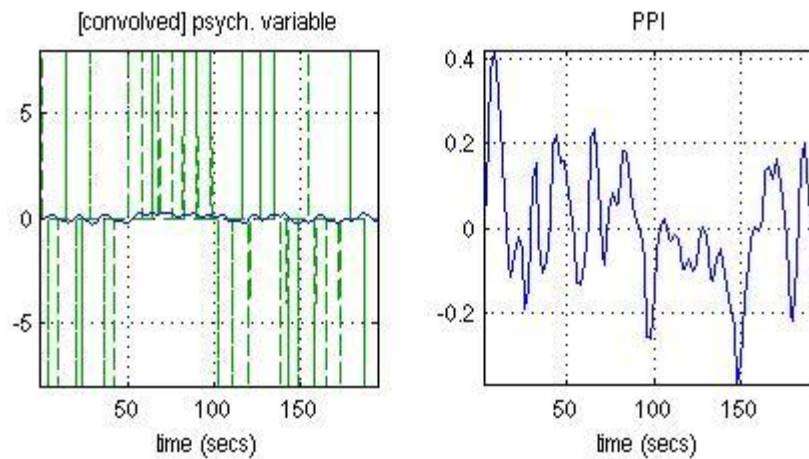
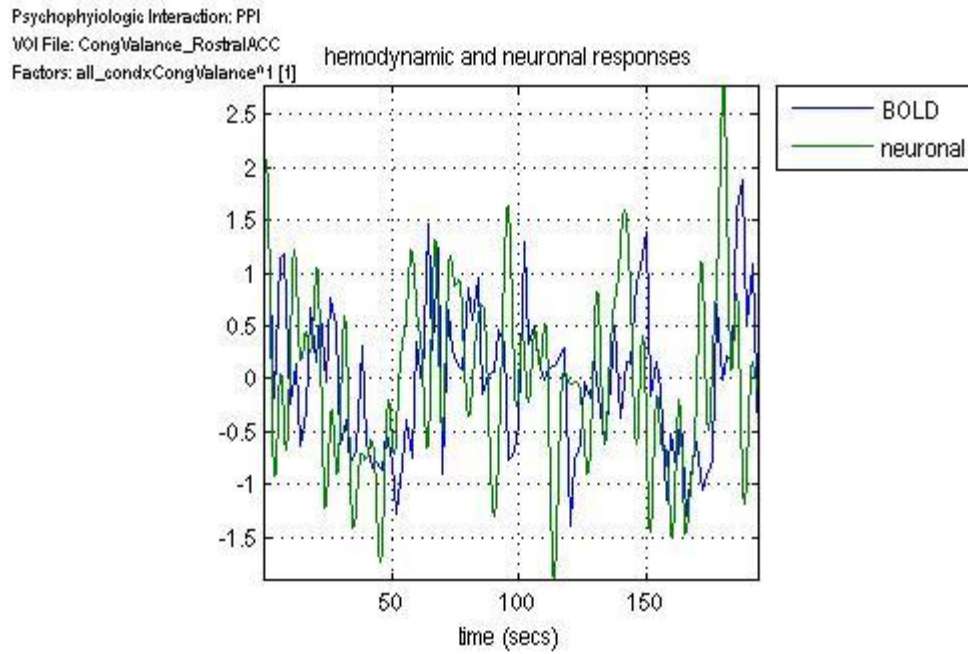


Figure C58. Hemodynamic and neuronal responses for the region RostralACC when stimulation of cong\*val affects that region. Bottom-left graph shows convolution of hemodynamic and neural response for RostralACC. Graph in bottom-right shows psychophysiological response of region RostralACC to the stimulation of cong\*val.

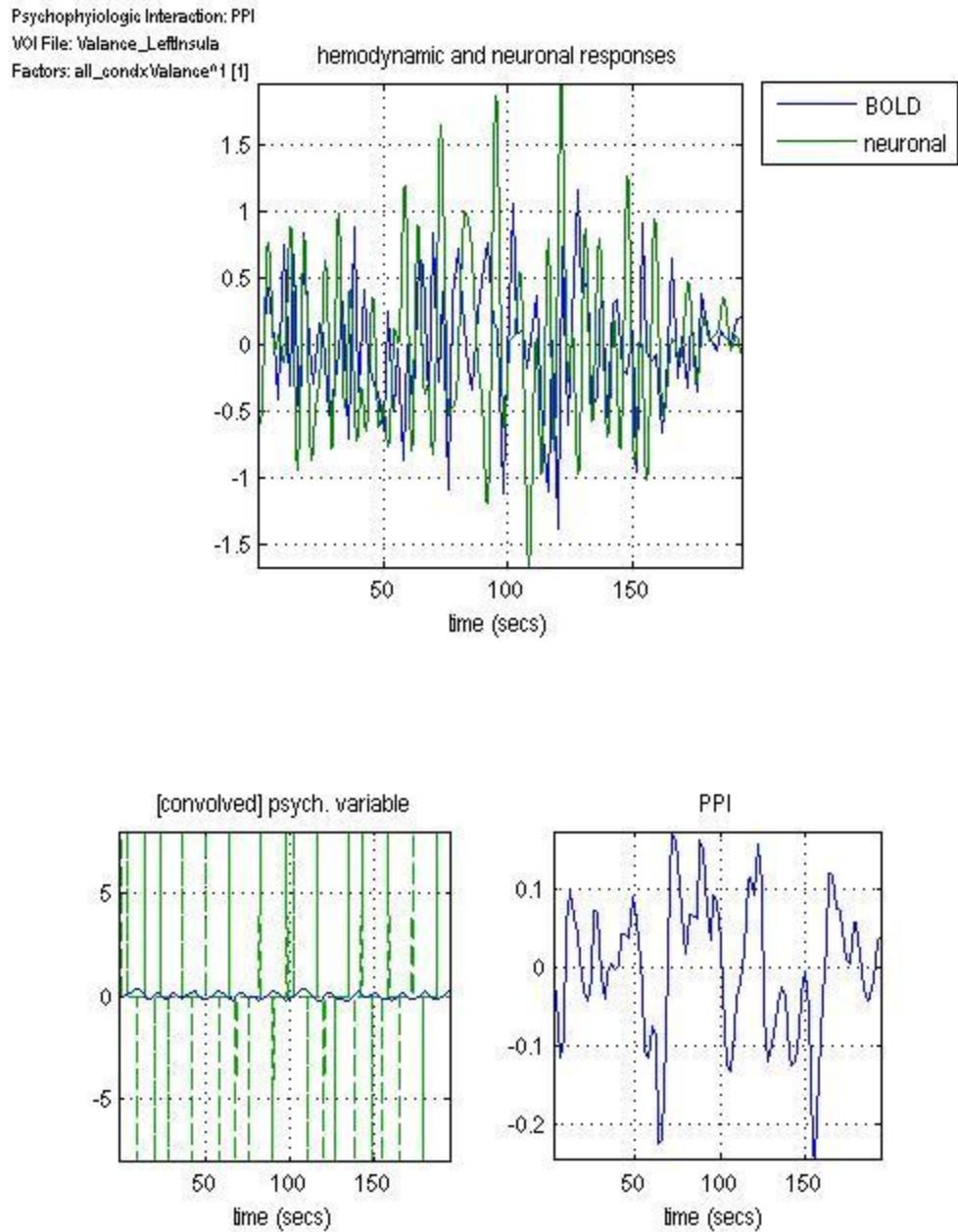


Figure C59. Hemodynamic and neuronal responses for the region LeftInsula when stimulation of valance affects that region. Bottom-left graph shows convolution of hemodynamic and neural response for LeftInsula. Graph in bottom-right shows psychophysiological response of region LeftInsula to the stimulation of Valance.

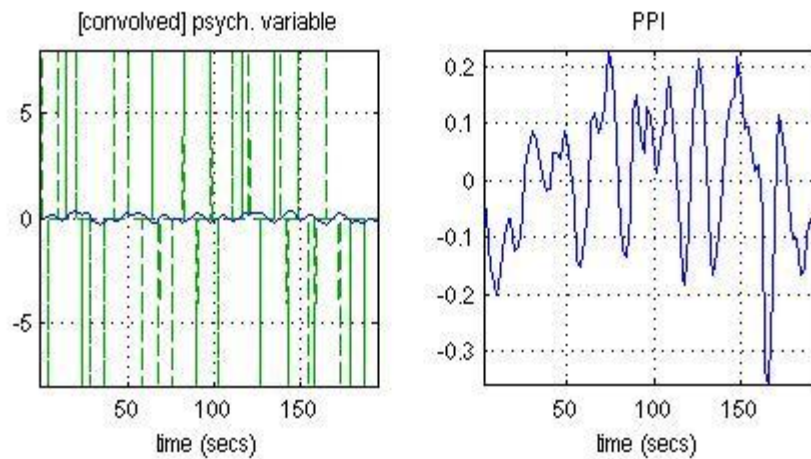
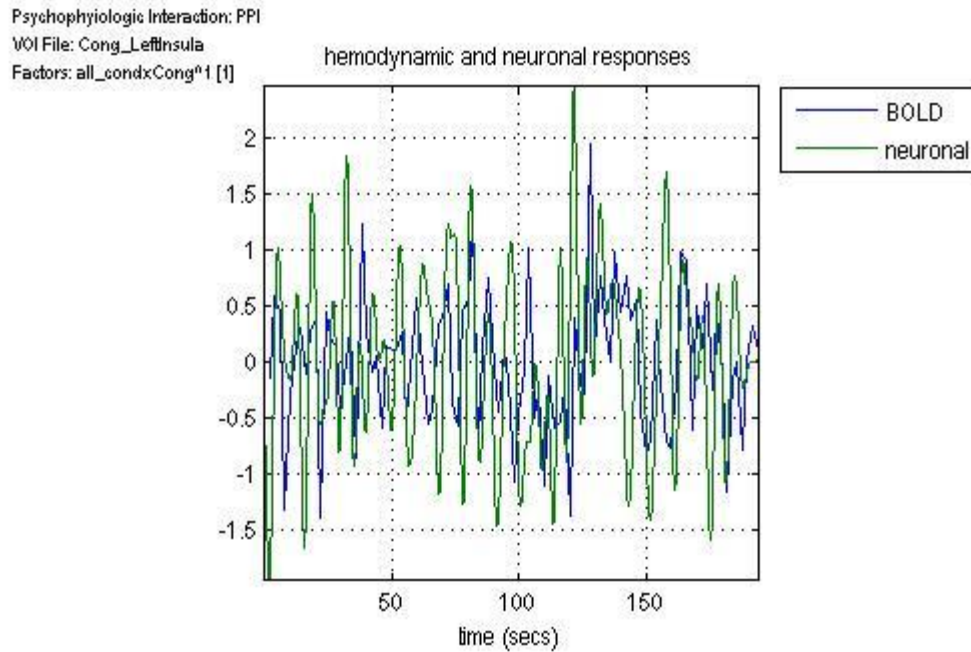


Figure C60. Hemodynamic and neuronal responses for the region LeftInsula when stimulation of affects that region. Bottom-left graph shows convolution of hemodynamic and neuronal response for LeftInsula. Graph in bottom-right shows psychophysiological response of region LeftInsula to the stimulation of Congruency.

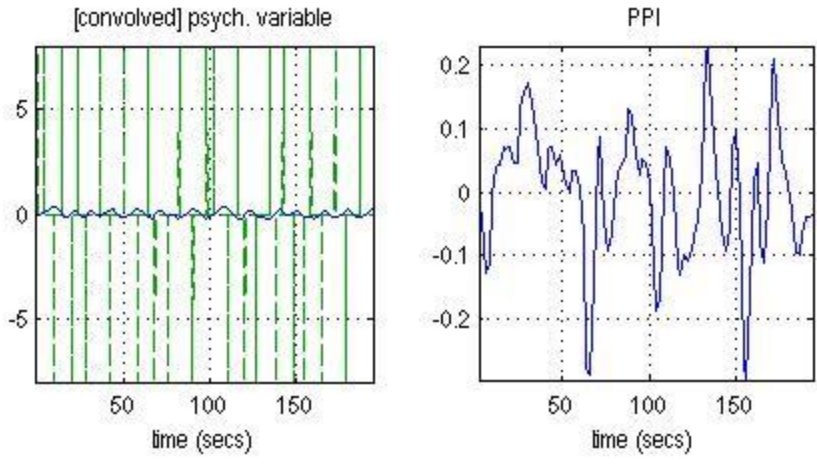
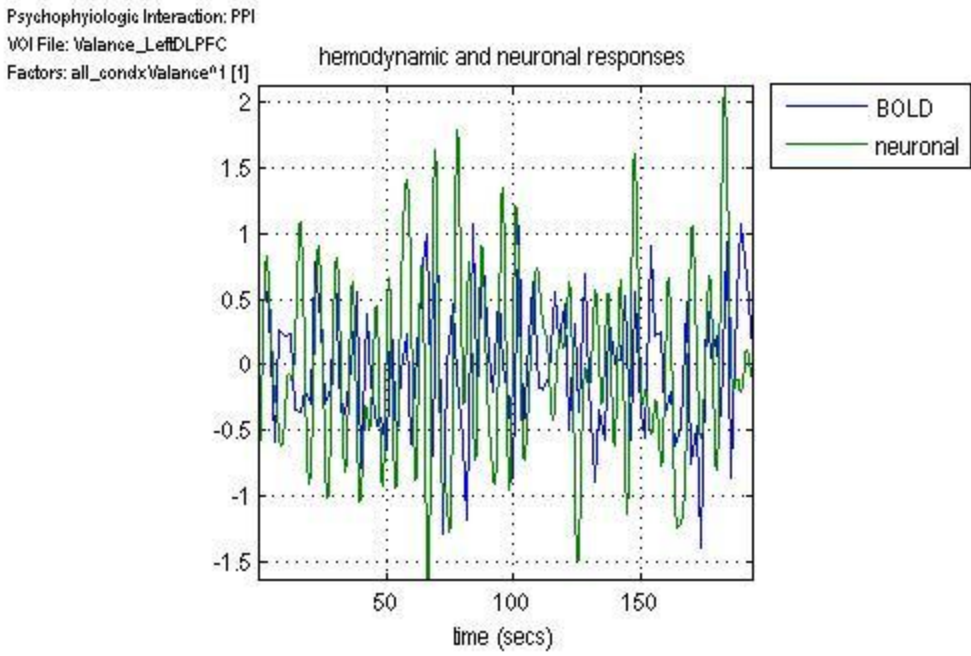


Figure C61. Hemodynamic and neuronal responses for the region LeftDLPFC when stimulation of valance affects that region. Bottom-left graph shows convolution of hemodynamic and neural response for LeftDLPFC. Graph in bottom-right shows psychophysiological response of region LeftDLPFC to the stimulation of Valance.

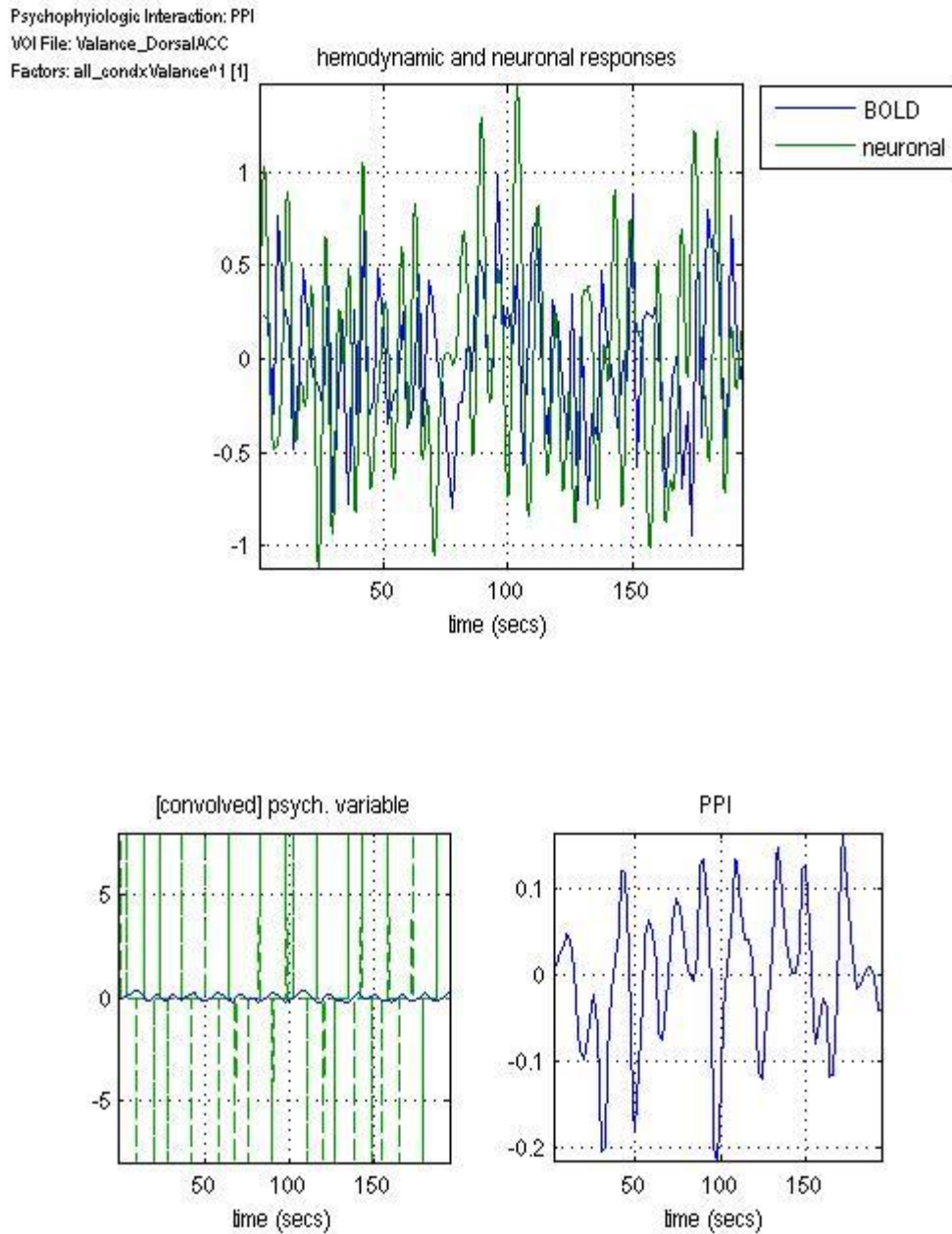


Figure C62. Hemodynamic and neuronal responses for the region DorsalACC when stimulation of valance affects that region. Bottom-left graph shows convolution of hemodynamic and neural response for DorsalACC. Graph in bottom-right shows psychophysiological response of region DorsalACC to the stimulation of Valance.

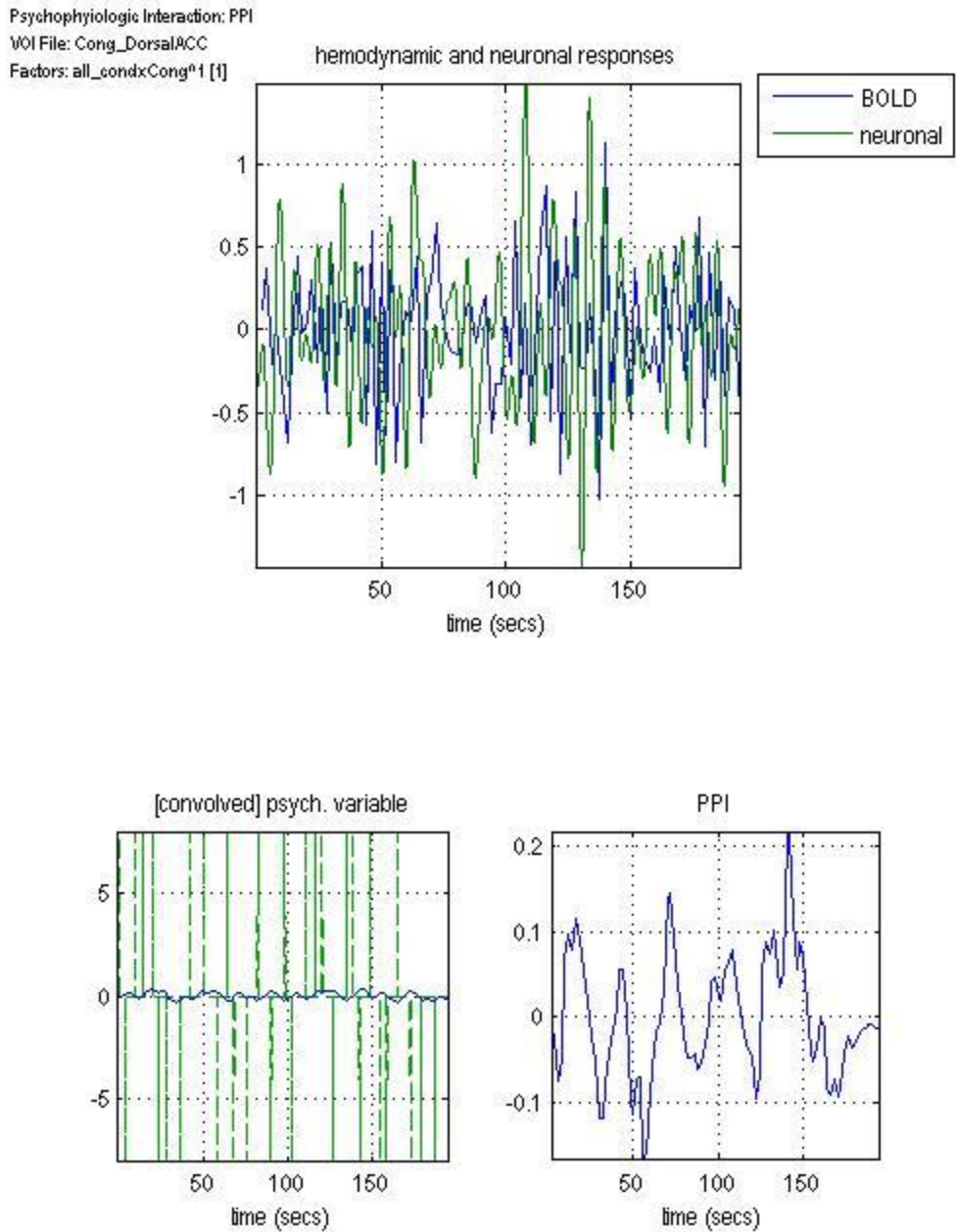


Figure C63. Hemodynamic and neuronal responses for the region DorsalACC when stimulation of congruency affects that region. Bottom-left graph shows convolution of hemodynamic and neural response for DorsalACC. Graph in bottom-right shows psychophysiological response of region DorsalACC to the stimulation of Congruency.